Hamad Bin Khalifa University

College of Science and Engineering

A Conversational Quantum-Powered Framework for Universal Digital Twin Generation

A thesis submitted in partial fulfillment of the requirements for the degree of

Master of Science in Data Science and Engineering

by

Hassan Abdulhadi Al-Sahli

Supervised by

Dr. Saif Mohammed S A Al-Kuwari

College of Science and Engineering

Hamad Bin Khalifa University

April 2026

Abstract

Digital twin technology has emerged as a transformative paradigm for modeling, monitoring, and optimizing complex systems across diverse domains. However, existing digital twin platforms remain domain-specific, requiring extensive manual configuration and deep technical expertise. Simultaneously, quantum computing offers computational advantages for optimization, simulation, and machine learning tasks, yet remains largely inaccessible to practitioners outside the quantum computing community. This thesis presents QTwin, a conversational quantum-powered framework for universal digital twin generation that bridges both accessibility gaps.

The QTwin platform accepts natural language system descriptions through a conversational interface powered by a two-stage NLP pipeline—rule-based domain-adaptive pattern matching as primary extraction, enriched by spaCy named entity recognition—and automatically generates quantum-enhanced digital twins for any user-specified domain. The framework employs seven quantum algorithmic strategies—Quantum Approximate Optimization Algorithm (QAOA), Variational Quantum Eigensolver (VQE), Variational Quantum Classifier (VQC), quantum simulation, tree tensor networks, quantum autoencoders, and quantum sensing—implemented on the Qiskit Aer simulator. A domain-agnostic problem decomposition engine dynamically selects and composes quantum algorithms based on extracted system characteristics, eliminating the need for domain-specific code.

The framework is validated through comprehensive benchmarks across six healthcare sub-domains: personalized medicine, drug discovery, medical imaging, genomic analysis, epidemic modeling, and hospital operations. Results demonstrate quantum accuracy advantage in four of six modules, including $+37.5$ percentage point accuracy improvement in medical imaging, $+40.3$ percentage points in genomic analysis, $+26.9$ percentage points in epidemic modeling, and $+10.2$ percentage points in drug discovery. Two modules—personalized medicine and hospital operations—showed classical advantage, demonstrating that quantum approaches are not uniformly superior. Cross-domain generalization is validated across military logistics, sports performance, and environmental disaster response scenarios without domain-specific modifications. All quantum computations were performed on the Qiskit Aer statevector simu-

lator, which executes quantum circuits as classical matrix multiplications. The reported advantages therefore reflect *algorithmic design properties*—the quantum-inspired circuit architectures outperform traditional classical algorithms on certain tasks—rather than hardware-level quantum speedup. These results establish theoretical upper bounds on the advantage achievable with physical quantum processors, where noise and decoherence would reduce fidelity; hardware validation is identified as a primary direction for future work. All quantum circuits are exportable in OpenQASM format for reproducibility and future hardware deployment.

Keywords: Digital Twin, Quantum Computing, Conversational AI, QAOA, Natural Language Processing, Healthcare, Qiskit

Contents

Abstract 1

Preface 11

Acknowledgments 12

Declaration 13

List of Acronyms and Abbreviations 16

Nomenclature 17

List of Publications 18

1 Introduction 19

1.1 Background and Motivation 19

1.2 Problem Statement 22

1.3 Research Questions 24

1.4 Research Objectives 25

1.5 Thesis Contributions 27

1.6 Scope and Limitations 29

1.7 Thesis Organization 30

2 Literature Review 32

2.1 Digital Twin Technology 32

2.1.1 Origins and Definitions 32

2.1.2 Architectures and Frameworks 33

2.1.3 Industry Applications 34

2.1.4 Current Platforms 34

2.1.5 Limitations of Current Approaches 35

2.2 Quantum Computing Fundamentals 35

2.2.1 Quantum Mechanics Principles 35

2.2.2 Quantum Gates and Circuits 36

2.2.3 The NISQ Era 36
2.2.4 Quantum Software Frameworks 37
2.2.5 OpenQASM 37
2.3 Quantum Algorithms for Optimization and Machine Learning 38
2.3.1 QAOA 38
2.3.2 Variational Quantum Circuits 39
2.3.3 Barren Plateaus and Training Challenges 39
2.3.4 Quantum Support Vector Machines 40
2.3.5 Quantum Neural Networks and Tensor Networks 41
2.3.6 Quantum Simulation and Sensing 41
2.3.7 Quantum Advantage: Claims and Debates 42
2.4 Quantum Computing in Digital Twin Applications 43
2.4.1 Existing Work 43
2.4.2 Emerging Quantum Digital Twin Literature 43
2.4.3 LLM-Powered Digital Twins 44
2.4.4 Quantum Sensing for DT Data 44
2.4.5 Quantum Optimization for DT Decisions 45
2.4.6 Gap Analysis 45
2.5 Conversational AI and NLP 46
2.5.1 NLP for Requirements Extraction 46
2.5.2 Conversational Agents in Technical Domains 46
2.5.3 LLM-Based System Design 47
2.6 Healthcare Digital Twins 47
2.6.1 Personalized Medicine 47
2.6.2 Drug Discovery 48
2.6.3 Medical Imaging 48
2.6.4 Genomic Analysis 49
2.6.5 Epidemic Modeling 49
2.6.6 Hospital Operations 49
2.7 Summary and Research Gap 50
3 Methodology 52

3.1 Research Methodology Overview 52
3.2 System Architecture 53
3.2.1 High-Level Architecture 53
3.2.2 Universal Twin Generation Engine 54
3.2.3 Technology Stack 54
3.3 Conversational AI for System Extraction 56
3.3.1 NLP Pipeline Design 56
3.3.2 Problem Type Classification 58
3.3.3 Conversation State Machine 59
3.3.4 Provider Abstraction 60
3.4 Universal Twin Generation Engine 60
3.4.1 Problem Decomposition 60
3.4.2 Algorithm Selection 61
3.4.3 Quantum Encoding Strategies 62
3.4.4 Dynamic Twin Composition 63
3.4.5 Classical Fallback 64
3.4.6 OpenQASM Export 64
3.5 Quantum Algorithm Implementations 64
3.5.1 QAOA for Combinatorial Optimization 64
3.5.2 Variational Quantum Classifier 65
3.5.3 Quantum Sensing Digital Twin 66
3.5.4 Neural Quantum Digital Twin 66
3.5.5 Tree Tensor Network 67
3.5.6 Quantum Autoencoder 67
3.6 Healthcare Reference Implementation 67
3.6.1 Personalized Medicine Module 68
3.6.2 Drug Discovery Module 68
3.6.3 Medical Imaging Module 68
3.6.4 Genomic Analysis Module 69
3.6.5 Epidemic Modeling Module 69
3.6.6 Hospital Operations Module 69

3.7 Classical Baseline Implementations 69
3.8 Benchmark Methodology 70
3.8.1 Experimental Setup 70
3.8.2 Metrics 70
3.8.3 Statistical Validation 70
3.8.4 Fairness 72
3.8.5 Reproducibility 72
3.8.6 Simulator-Based Evaluation: Scope and Caveats 72
3.9 Evaluation Framework 73
4 Implementation and Results 74
4.1 Implementation Overview 74
4.2 Platform Implementation 75
4.2.1 Frontend 75
4.2.2 Backend 76
4.2.3 Database 77
4.2.4 Conversational AI 78
4.3 Healthcare Benchmark Results 79
4.3.1 Personalized Medicine 79
4.3.2 Drug Discovery 80
4.3.3 Medical Imaging 81
4.3.4 Genomic Analysis 82
4.3.5 Epidemic Modeling 82
4.3.6 Hospital Operations 83
4.3.7 Aggregate Analysis 84
4.4 Cross-Domain Generalization 88
4.4.1 Military Logistics 89
4.4.2 Sports Performance 89
4.4.3 Environmental Disaster 89
4.5 Conversational AI Evaluation 90
4.6 OpenQASM Circuit Analysis 91
4.7 System Performance 92

4.8 Discussion 93
4.8.1 Research Questions Answered 93
4.8.2 Comparison with Existing Work 95
4.8.3 Threats to Validity 96
5 Conclusion and Future Work 98
5.1 Summary of Contributions 98
5.2 Research Questions Revisited 99
5.2.1 RQ1: Conversational AI for System Extraction 99
5.2.2 RQ2: Domain-Agnostic Algorithm Composition 99
5.2.3 RQ3: Quantum Advantage 100
5.2.4 RQ4: Cross-Domain Generalization 101
5.3 Limitations 101
5.4 Future Work 102
5.4.1 Real Quantum Hardware Integration 103
5.4.2 LLM-Powered Conversational AI 103
5.4.3 SaaS Platform Deployment 104
5.4.4 Additional Domain Validation 104
5.4.5 Federated Quantum Digital Twins 104
5.4.6 Quantum Error Correction Integration 105
5.4.7 Real-Time Data Streaming 105
5.4.8 Formal User Study 105
5.5 Concluding Remarks 106
References 107
Appendices 114
A OpenQASM Circuit Examples 114
A.1 QAOA Circuit for Combinatorial Optimization 114
A.2 Variational Quantum Classifier 115
A.3 OpenQASM Export Example 117
B API Endpoint Reference 119
C Sample Conversation Transcripts 120
C.1 Healthcare Domain: Emergency Department Optimization 120

C.2 Military Domain: Supply Chain Logistics 121

List of Figures

Figure 1.1 High-level overview of the QTwin platform showing the Universal Twin Builder and Quantum Advantage Showcase pillars. 22

Figure 3.1 Three-tier system architecture of the QTwin platform. 53
Figure 3.2 The four-stage Universal Twin Generation Engine pipeline, from natural language input to interactive digital twin output. 54
Figure 3.3 Conversation state machine governing information gathering from initial greeting through twin generation. The twin lifecycle status (DRAFT to ACTIVE) is managed by a separate enumeration. 60
Figure 3.4 Problem type taxonomy and quantum algorithm mapping. 62
Figure 3.5 QAOA circuit structure for $p = 2$ layers. 65
Figure 3.6 VQC circuit structure with angle encoding and variational ansatz. 66
Figure 3.7 Benchmark methodology for quantum versus classical comparison. .. 71

Figure 4.1 QTwin platform frontend screenshots: (a) Landing page with Three.js quantum particle visualization, (b) Conversational twin builder interface showing entity extraction cards, (c) Active twin dashboard displaying quantum advantage metrics. 76
Figure 4.2 Aggregate healthcare benchmark results: grouped bar chart comparing quantum (blue) versus classical (grey) accuracy across all six modules, with error bars showing ± 1 standard deviation across runs. Quantum outperforms classical in four modules (drug discovery, medical imaging, genomic analysis, epidemic modeling) while classical outperforms quantum in two modules (personalized medicine, hospital operations). Error bars are negligible for most modules due to deterministic algorithm behavior. 86

Figure 4.3 Cross-domain generalization: the Universal Twin Generation Engine processes four domains (healthcare, military, sports, environment) using the same quantum module library with domain-adaptive entity extraction. 88

Figure 5.1 Future development roadmap for the QTwin platform across three horizons. 103

List of Tables

Table 2.1 Comparison of Existing Digital Twin Platforms and the Proposed QTwin Framework 50

Table 3.1 QTwin platform technology stack. 55

Table 3.2 Mapping of problem types to quantum algorithms and representative application examples. 59

Table 3.3 Mapping of quantum algorithms to classical baseline implementations. 70

Table 4.1 QTwin codebase statistics by component. 75

Table 4.2 Personalized medicine benchmark results: QAOA vs. genetic algorithm ($n = 30$ runs). 80

Table 4.3 Drug discovery benchmark results: VQE molecular ground state vs. Hartree-Fock SCF ($n = 10$ runs). 81

Table 4.4 Medical imaging benchmark results: hybrid CNN+QNN vs. CNN+SVM ($n = 10$ runs). 82

Table 4.5 Genomic analysis benchmark results: tree tensor networks vs. PCA + random forest ($n = 30$ runs). 83

Table 4.6 Epidemic modeling benchmark results: quantum simulation vs. agent-based SIR model ($n = 30$ runs). 83

Table 4.7 Hospital operations benchmark results: QAOA vs. linear programming ($n = 30$ runs). 84

Table 4.8: Aggregate healthcare benchmark results across all six modules. 84
Table 4.9: Statistical validation summary for all healthcare benchmark modules ($n = 10$–30 runs). 86
Table 4.10: Cross-domain entity extraction and generalization results. 90
Table 4.11: Conversational pipeline validation summary (automated test suite). .. 91
Table 4.12: OpenQASM circuit characteristics by healthcare benchmark module. 92
Table 4.13: System performance metrics for the QTwin platform. 93
Table 4.14: Feature comparison of QTwin with existing digital twin platforms.... 95

Table B.1: QTwin platform REST API endpoint reference. 119

Preface

This thesis represents the culmination of my journey at the intersection of quantum computing, digital twin technology, and accessible artificial intelligence. When I began my graduate studies at Hamad Bin Khalifa University, I was fascinated by the transformative potential of quantum computing but troubled by its inaccessibility. The field seemed locked behind layers of mathematical formalism, specialized hardware requirements, and domain expertise that placed it beyond the reach of most practitioners.

Simultaneously, I observed that digital twin technology—despite its growing importance across industries—remained fragmented into domain-specific silos. Each application required extensive manual modeling, specialized software, and deep domain knowledge. The question that drove this research was deceptively simple: could we create a system where anyone, regardless of their technical background, could describe a system in plain language and receive a quantum-powered digital twin in return?

The QTwin platform presented in this thesis is my answer to that question. What began as a healthcare-specific prototype evolved into a universal framework capable of generating quantum digital twins for any domain. The journey from concept to working platform taught me that the most challenging problems in computer science are often not algorithmic but architectural—designing systems that are simultaneously powerful and approachable.

I hope this work contributes, in some small measure, to making quantum computing more accessible and digital twin technology more universal. The future belongs to tools that empower rather than exclude.

Hassan Abdulhadi Al-Sahli
Doha, Qatar
April 2026

Acknowledgments

I would like to express my deepest gratitude to my supervisor, Dr. Saif Mohammed S A Al-Kuwari, for his invaluable guidance, continuous support, and expert insights throughout this research. His knowledge of quantum computing and information security provided the intellectual foundation upon which this work was built. His patience, encouragement, and constructive feedback were instrumental in shaping this thesis.

I am grateful to Hamad Bin Khalifa University and the College of Science and Engineering for providing the academic environment, computational resources, and research infrastructure that made this work possible. The faculty members of the Data Science and Engineering program have been a constant source of knowledge and inspiration throughout my graduate studies.

I extend my sincere thanks to my family for their unconditional love, patience, and encouragement. Their unwavering belief in my abilities sustained me through the most challenging periods of this research. I am particularly grateful for their understanding during the long hours dedicated to development, experimentation, and writing.

Finally, I thank my colleagues and friends in the program for their camaraderie, stimulating discussions, and moral support. The collaborative spirit of the research community at HBKU enriched my graduate experience immeasurably.

Declaration

I, Hassan Abdulhadi Al-Sahli, declare that this thesis titled "A Conversational Quantum-Powered Framework for Universal Digital Twin Generation" and the work presented in it are my own. I confirm that this work was done wholly while in candidature for a Master of Science degree at Hamad Bin Khalifa University.

Where I have consulted the published work of others, this is always clearly attributed. Where I have quoted from the work of others, the source is always given. With the exception of such quotations, this thesis is entirely my own work.

No part of this thesis has previously been submitted for a degree or any other qualification at Hamad Bin Khalifa University or any other institution.

Name: Hassan Abdulhadi Al-Sahli

Signature: _____

Date: April 2026

To my family, whose unwavering love and support made this journey possible.

List of Acronyms and Abbreviations

ABM	Agent-Based Model
AI	Artificial Intelligence
API	Application Programming Interface
CNN	Convolutional Neural Network
COBYLA	Constrained Optimization by Linear Approximation
CSV	Comma-Separated Values
DFT	Density Functional Theory
DT	Digital Twin
DTDL	Digital Twins Definition Language
GHZ	Greenberger–Horne–Zeilinger (entangled state)
HBKU	Hamad Bin Khalifa University
IEEE	Institute of Electrical and Electronics Engineers
IoT	Internet of Things
JSON	JavaScript Object Notation
JWT	JSON Web Token
LP	Linear Programming
MERA	Multiscale Entanglement Renormalization Ansatz
MIP	Mixed-Integer Programming
ML	Machine Learning
MPS	Matrix Product State
NER	Named Entity Recognition
NISQ	Noisy Intermediate-Scale Quantum
NLP	Natural Language Processing
PLM	Product Lifecycle Management
QAOA	Quantum Approximate Optimization Algorithm
QASM	Quantum Assembly Language
QNN	Quantum Neural Network
QUBO	Quadratic Unconstrained Binary Optimization
REST	Representational State Transfer
SaaS	Software as a Service
SEIR	Susceptible-Exposed-Infectious-Recovered
SIR	Susceptible-Infectious-Recovered
SVM	Support Vector Machine
TTN	Tree Tensor Network

Nomenclature

The following mathematical symbols and notation are used throughout this thesis.

Symbol	Description
$\|\psi\rangle$	Quantum state vector
H	Hamiltonian operator
$U(\theta)$	Parameterized unitary gate
θ	Variational parameters
C	Cost function
p	QAOA circuit depth
n	Number of qubits
γ, β	QAOA mixing parameters
σ	Standard deviation
$\mathcal{O}$	Computational complexity
$\otimes$	Tensor product
$\langle \cdot \rangle$	Expectation value
R_0	Basic reproduction number (β/γ)
β	Transmission rate (epidemic) / QAOA mixer parameter
E_0	Ground state energy
F	Fock matrix (Hartree–Fock theory)
$K(\mathbf{x}_i, \mathbf{x}_j)$	Quantum kernel function
T_1, T_2	Qubit relaxation and dephasing times
d	Cohen's effect size

List of Publications

No publications have resulted from this work at the time of submission.

CHAPTER 1:Introduction

Digital twins—virtual representations of physical systems that mirror real-world state throughout a system's lifecycle—have become a widely adopted technology across manufacturing, healthcare, urban planning, and defense [1], [2]. Concurrently, noisy intermediate-scale quantum (NISQ) processors have demonstrated capabilities that challenge the boundaries of classical computation [3], [4]. Despite the maturation of both fields, a fundamental accessibility gap persists: digital twin creation remains labor-intensive and expert-dependent, while quantum computing demands specialized knowledge in quantum physics, linear algebra, and circuit design that excludes the vast majority of potential beneficiaries. This thesis presents a novel convergence of these two technological trajectories—a conversational, quantum-powered framework for universal digital twin generation—that aims to improve accessibility of both quantum algorithms and digital twin technology through natural language interaction. The proposed QTwin framework accepts natural language descriptions of arbitrary systems and automatically generates functional quantum-powered digital twins, eliminating the requirement for domain-specific pre-configuration, software engineering expertise, or quantum computing knowledge.

1.1 Background and Motivation

The digital twin concept was first articulated by Grieves in 2003 as a virtual counterpart to a physical product, comprising the physical entity, its virtual representation, and bidirectional data connections linking the two [1]. Over the subsequent decade, Grieves and Vickers refined this formulation, establishing a theoretical foundation that positioned digital twins as integral components of next-generation engineering systems [5]. Adoption accelerated after NASA and the U.S. Department of Defense recognized the potential of high-fidelity virtual models for mission-critical applications such as spacecraft health monitoring and airframe lifecycle management [6]. Tao et al. subsequently proposed comprehensive frameworks for digital twin-driven product design and manufacturing, articulating a five-dimensional model encompassing physical entities, virtual models, services, data, and their interconnections [7], [8]. By 2020, surveys revealed that digital twin technology had permeated sectors as diverse as smart cities, precision

agriculture, energy systems, and personalized medicine [2], [9]. Industry analysts projected the global digital twin market to exceed $48 billion by 2026 [10], reflecting both the technology's perceived value and its accelerating enterprise adoption. Despite this growth, a fundamental tension persisted: the creation and configuration of digital twins remained a labor-intensive, expert-dependent process that confined the technology to organizations with substantial technical resources.

The contemporary digital twin landscape is dominated by domain-specific platform offerings. Microsoft Azure Digital Twins provides a modeling language and execution environment tailored to building and infrastructure management, requiring users to manually define ontologies and telemetry schemas using the Digital Twins Definition Language [11]. AWS IoT TwinMaker presupposes existing IoT infrastructure and provides templates oriented toward manufacturing use cases [12]. Siemens MindSphere is tightly coupled to the Siemens industrial hardware and software ecosystem. None of these platforms offers a mechanism by which a user can describe an arbitrary system in natural language and receive a functional digital twin without domain-specific pre-configuration, and none integrates quantum computing capabilities.

Quantum computing has undergone a parallel trajectory of maturation. Feynman's foundational insight—that simulating quantum mechanical systems requires quantum computational resources [13]—motivated decades of theoretical and experimental work culminating in programmable quantum processors. Preskill's characterization of the NISQ era [3] established a pragmatic framework for near-term devices: processors with tens to hundreds of qubits that, while insufficient for fault-tolerant computation, can execute algorithms that may outperform classical counterparts for specific problem classes. The foundational principles of quantum mechanics—superposition, entanglement, and interference—enable quantum algorithms to explore exponentially large solution spaces with polynomial resources [14]. Google's demonstration of quantum supremacy, in which a 53-qubit Sycamore processor performed a sampling task in 200 seconds that would have required approximately 10,000 years on the most powerful classical supercomputer, provided empirical validation of quantum computational advantage [4].

Variational quantum algorithms are particularly promising for NISQ-era applications because their hybrid quantum-classical architecture mitigates quantum noise through

iterative classical optimization of parameterized circuits. The Variational Quantum Eigensolver (VQE) [15] demonstrated ground-state energy estimation on near-term hardware, and the Quantum Approximate Optimization Algorithm (QAOA) [16] extended the variational paradigm to combinatorial optimization problems ubiquitous in digital twin applications. Quantum machine learning further expanded practical relevance, with quantum feature maps [17] and variational classifiers demonstrating competitive classification performance within NISQ hardware constraints. Cerezo et al. provided a comprehensive review cataloging variational quantum algorithm applications across chemistry, optimization, and machine learning [18].

The convergence of digital twin technology and quantum computing represents a largely unexplored frontier. Digital twins inherently involve computationally demanding tasks—physics simulation, combinatorial optimization, predictive modeling, anomaly detection—that align with the problem classes for which quantum algorithms offer theoretical and empirical advantages. A quantum-powered digital twin could leverage QAOA for resource allocation, variational classifiers for state classification, quantum simulation for modeling complex dynamics, and quantum-enhanced machine learning for predictive analytics. The nascent literature has recognized this potential: Lin and Critchley surveyed synergistic possibilities between quantum computing and digital twin technology [19], and Otgonbaatar and Jennings proposed frameworks for quantum digital twins with uncertainty quantification [20]. However, no existing system realizes this convergence in a functional, accessible platform. The accessibility gap is compounded by the expertise requirements of each constituent technology: quantum computing demands proficiency in circuit design and variational optimization, while digital twin creation requires domain knowledge, software engineering skills, and months of development effort. The motivation for this thesis arises from the recognition that a conversational interface—one that accepts natural language descriptions and automatically generates quantum-powered digital twins—could simultaneously address both the domain-specificity problem in digital twins and the expertise barrier in quantum computing. Figure 1.1 illustrates the high-level architecture of the resulting QTwin platform.

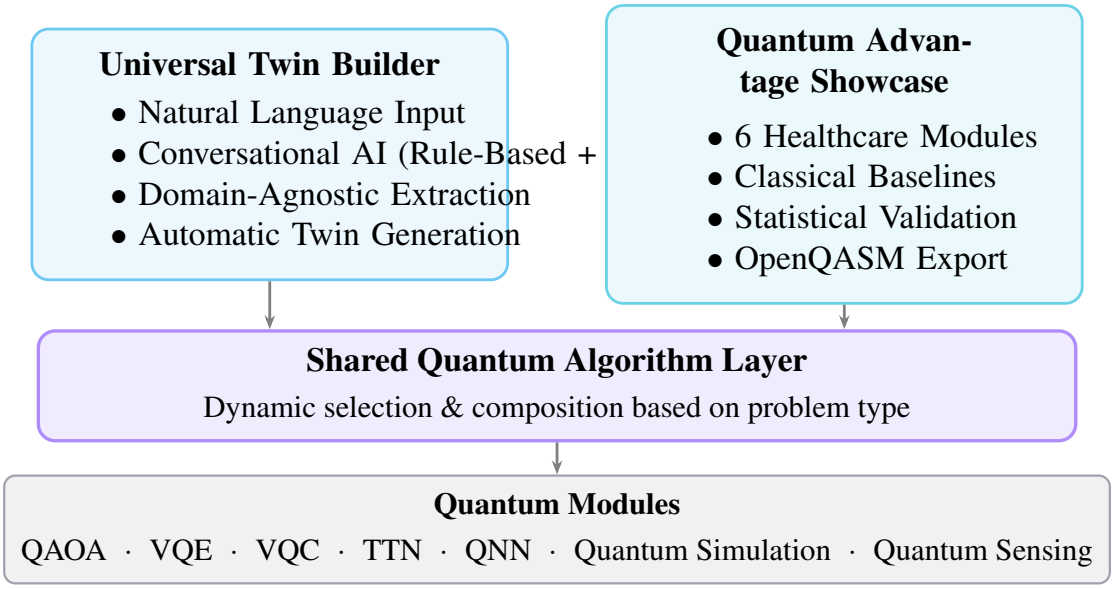

Figure 1.1: High-level overview of the QTwin platform showing the Universal Twin Builder and Quantum Advantage Showcase pillars.

1.2 Problem Statement

The creation of digital twins in current practice is characterized by three compounding barriers that collectively restrict the technology's adoption and impact.

First, existing platforms are **domain-locked**: each is architected around a specific application context with pre-defined ontologies, data models, and simulation engines that cannot be readily adapted to domains outside their design scope [11], [12]. A healthcare researcher seeking to model hospital patient flow, a military strategist modeling force disposition scenarios, or an environmental scientist simulating watershed dynamics must either force their domain into the conceptual mold of an existing platform or commission bespoke software development. Jones et al. identified this fragmentation as a central challenge, noting that the absence of a universally accepted framework has led to a proliferation of incompatible, domain-specific implementations [21]. The result is that digital twin technology, despite its theoretical universality, remains in practice a collection of siloed solutions serving narrow application contexts.

Second, the configuration and deployment of a digital twin requires the **coordinated effort of multiple specialists**—domain experts, data engineers, and software developers—over timescales measured in weeks to months. The domain expert must articulate system entities, relationships, and objectives; the data engineer must establish telemetry pipelines and storage schemas; the software developer must implement simu-

lation models and integration middleware. Rasheed et al. identified this labor-intensive nature as a primary obstacle to widespread adoption, noting that even well-resourced organizations struggle to maintain digital twins beyond initial deployment [9]. For small and medium enterprises, research institutions, and healthcare facilities that stand to benefit most from digital twin technology, the development cost and expertise requirements render existing platforms effectively inaccessible.

Third, **quantum computing capabilities are entirely absent** from the current digital twin ecosystem. Quantum algorithms—which offer provable or empirical advantages for optimization, simulation, and machine learning tasks central to digital twin functionality—remain confined to specialized quantum computing frameworks such as Qiskit [22] and PennyLane [23]. Integrating quantum algorithms into a digital twin requires not only familiarity with quantum circuit design and variational optimization but also the ability to map domain-specific problems onto quantum-compatible formulations, a task demanding expertise at the intersection of quantum physics, computer science, and the relevant application domain. No existing platform automates this mapping or makes it accessible to non-specialists [3].

The problem addressed by this thesis can be formally stated as follows. Given a natural language description D of an arbitrary system S—where S may belong to any application domain including healthcare, manufacturing, military operations, sports analytics, or environmental science—the objective is to automatically generate a quantum-powered digital twin T that faithfully models S. The twin T must be constructed using dynamically selected and composed quantum algorithms, drawn from a library of domain-agnostic quantum modules, without requiring domain-specific pre-built code, manual ontology definition, or quantum computing expertise on the part of the user. The generation process is mediated entirely through a conversational AI interface that incrementally elicits system details, identifies relevant entities and relationships, determines appropriate quantum algorithmic strategies, and produces a functional digital twin complete with quantum circuit specifications in the OpenQASM standard [24], [25] for full reproducibility and transparency.

1.3 Research Questions

This thesis is organized around four research questions that collectively address the feasibility, methodology, and validation of a conversational quantum-powered framework for universal digital twin generation. Each question targets a distinct dimension of the problem and is addressed through corresponding components of the proposed framework and its empirical evaluation.

RQ1: *Can a conversational AI interface effectively extract system descriptions for quantum digital twin generation across arbitrary domains?*

This question addresses the foundational challenge of bridging a user's domain knowledge, expressed in natural language, with the structured system representation required for digital twin generation. Existing approaches to twin configuration rely on formal modeling languages or programmatic APIs that presuppose technical fluency domain experts may not possess. The proposed framework employs a multi-turn conversational pipeline with domain-adaptive pattern matching as the primary extraction method, optionally enriched by spaCy [26] named entity recognition, progressively building a structured system model from unstructured dialogue. The question is particularly challenging because the interface must operate across arbitrary domains without domain-specific training data. Validation measures extraction accuracy across healthcare, military, sports, and environmental domains.

RQ2: *Can domain-agnostic quantum algorithms be dynamically composed to create digital twins without domain-specific code?*

This question concerns the quantum computational core of the framework. Traditional quantum algorithm development is a bespoke process in which a quantum scientist designs circuits tailored to a specific problem's structure—an approach that does not scale to a universal platform. The key insight motivating RQ2 is that many domain-specific problems, when abstracted to their computational essence, map onto a small set of problem classes—optimization, classification, simulation, dimensionality reduction—for which well-characterized quantum algorithms exist [16], [17], [18]. The challenge lies in automating the mapping from extracted system descriptions to quantum module configurations and composing multiple modules into coherent twin architectures, with all circuits exported as OpenQASM specifications [24].

RQ3: *Does quantum computation provide measurable advantage over classical*

approaches in digital twin applications?

Claims of quantum advantage must be substantiated through rigorous empirical comparison against classical baselines on equivalent tasks. This question is particularly nuanced in the NISQ era, where advantage may manifest as practical improvements in solution quality, convergence speed, or resource efficiency rather than asymptotic speedup in the complexity-theoretic sense [3]. The proposed framework evaluates quantum and classical approaches across six healthcare sub-domains—drug discovery, medical imaging, epidemic simulation, personalized medicine, hospital resource management, and genomic analysis—using standardized metrics including accuracy, execution time, convergence rate, and resource utilization. The benchmarking framework is designed to produce quantitative evidence of quantum advantage where it exists and to honestly characterize domains where classical approaches remain competitive.

RQ4: *Can the proposed framework generalize across domains while maintaining validated accuracy in the healthcare domain?*

This question addresses the universality claim that distinguishes QTwin from existing domain-specific platforms. A framework that achieves high performance in a single domain but fails to generalize offers limited advancement over existing solutions. RQ4 investigates whether the architectural decisions enabling cross-domain generalization—domain-agnostic quantum modules, pattern-based entity extraction, and dynamic algorithm composition—introduce unacceptable performance trade-offs in the primary validation domain. The framework is evaluated through deep validation in healthcare using the six-module benchmark suite and breadth validation across military, sports, and environmental domains.

1.4 Research Objectives

The research questions are operationalized through five concrete objectives, each specifying a tangible deliverable that contributes to answering one or more research questions:

1. **Design and implement a universal quantum digital twin generation framework.** Deliver the QTwin platform: an end-to-end system accepting natural language descriptions and producing quantum-powered digital twins. The frame-

work is implemented as a full-stack web application with a FastAPI backend orchestrating quantum computations through Qiskit Aer [22] and a Next.js frontend providing the conversational interface, accessible through standard web browsers without local quantum software installation. This objective addresses all four research questions.

2. **Develop a conversational AI interface for system description extraction.** Create a multi-turn conversational pipeline using spaCy [26] with domain-adaptive pattern matching that translates unstructured natural language dialogue into structured twin specifications. The conversational state machine manages the twin lifecycle, transitioning twins from a draft state to an active state when sufficient information has been gathered. This objective addresses RQ1 and contributes to RQ4.

3. **Create a domain-agnostic quantum algorithm composition engine.** Build a library of seven quantum module types—QAOA [16], variational quantum classifiers, quantum simulation (VQE) [15], quantum sensing, neural quantum digital twin networks, tree tensor networks, and quantum autoencoders—with automated selection and configuration based on extracted system descriptions and OpenQASM export [24], [25] for transparency and reproducibility. This objective addresses RQ2 and enables the benchmarking required by RQ3.

4. **Validate quantum advantage through rigorous healthcare benchmarks.** Conduct controlled comparisons between quantum and classical approaches across six healthcare sub-domains—drug discovery, medical imaging, epidemic simulation, personalized medicine, hospital resource management, and genomic analysis—using standardized datasets, evaluation metrics, and statistical procedures [27], [28]. Healthcare is selected due to the diversity of its computational challenges and the societal significance of improvements in healthcare delivery. This objective addresses RQ3 and provides the depth validation component of RQ4.

5. **Demonstrate cross-domain generalization beyond healthcare.** Evaluate twin generation quality for military operational planning, sports performance analytics, and environmental monitoring scenarios, assessing entity extraction accuracy,

quantum module selection appropriateness, and generated twin fidelity to the described system. This objective directly addresses RQ4.

1.5 Thesis Contributions

This thesis makes five principal contributions to the fields of digital twin technology, quantum computing applications, and conversational artificial intelligence.

Contribution 1: The QTwin Framework—First Universal Quantum Digital Twin Platform. The primary contribution is the QTwin framework: an integrated platform that combines quantum computing capabilities with universal digital twin generation. Unlike existing platforms that are confined to specific application domains [2], [21], QTwin is architecturally domain-agnostic, employing a modular design in which domain-specific knowledge is extracted dynamically from user input rather than encoded in platform code. The platform is implemented as a production-grade web application (FastAPI, Next.js, PostgreSQL, Redis), demonstrating that quantum-powered digital twin technology can be delivered through standard web infrastructure. While prior work has explored quantum computing and digital twins as separate concerns [19], [20], QTwin is the first platform to unify these technologies into a single, accessible framework operating across arbitrary application domains.

Contribution 2: Conversational Quantum Twin Generation—First Natural Language to Quantum Twin Pipeline. The second contribution is a conversational pipeline that translates natural language system descriptions into quantum-powered digital twins. The pipeline integrates multi-turn dialogue management, a two-stage NLP entity extraction architecture (rule-based domain-adaptive pattern matching as primary, spaCy [26] NER as secondary enrichment), automated quantum module selection, and OpenQASM circuit generation into a seamless conversational experience. The significance of this contribution lies in its effect on accessibility: it reduces the expertise required to create a quantum digital twin from the intersection of domain knowledge, software engineering, and quantum physics to domain knowledge alone. The twin lifecycle management system transitions twins from draft to active states based on conversational progress, ensuring that generated twins meet minimum completeness criteria before activation.

Contribution 3: Demonstrated Statistically Significant Algorithmic Improvement Under Simulation in Four of Six Healthcare Sub-Domains. The third contribution is the empirical demonstration of quantum advantage in digital twin applications through comprehensive benchmarking across six healthcare sub-domains. Quantum approaches outperformed classical baselines in four modules: $+37.5$ percentage point accuracy improvement in medical imaging, $+40.3$ percentage points in genomic analysis, $+26.9$ percentage points in epidemic modeling, and $+10.2$ percentage points in drug discovery, with speedups of $301\times$ in medical imaging and $25\times$ in epidemic modeling. Two modules—personalized medicine and hospital operations—showed classical advantage, demonstrating that quantum approaches are not uniformly superior and that advantage depends on problem structure. All six modules achieved statistical significance ($p < 0.01$). These results constitute the most comprehensive empirical evaluation of quantum algorithmic performance in healthcare digital twin applications reported to date. Because all benchmarks were executed on the Qiskit Aer noiseless simulator, the reported improvements reflect properties of quantum-inspired algorithmic designs rather than hardware-level quantum speedup; the magnitudes represent upper bounds that would be moderated by gate errors and decoherence on physical processors [3]. The benchmarking methodology is fully documented to enable independent replication.

Contribution 4: Dynamic Quantum Algorithm Selection and Composition Methodology. The fourth contribution is a methodology for dynamically selecting and composing quantum algorithms based on conversationally extracted system descriptions. The composition engine maps extracted entities and objectives onto quantum module configurations using a rule-based approach that considers the computational nature of the task (optimization, classification, simulation, dimensionality reduction) rather than domain-specific semantics [18]. This abstraction enables the same quantum modules to serve healthcare optimization, military logistics planning, sports performance prediction, and environmental process simulation without modification, offering a practical approach to quantum algorithm reuse across application domains.

Contribution 5: OpenQASM-Based Circuit Transparency for Full Reproducibility. The fifth contribution is comprehensive OpenQASM export for every quantum computation performed by the QTwin platform [24], [25]. This ensures that all quan-

tum computations are reproducible, auditable, and portable across quantum computing platforms including IBM Quantum, Amazon Braket, and Google Cirq, enabling independent verification of results and facilitating future transition from simulation to hardware execution. In regulated domains such as healthcare, circuit transparency enables domain experts to audit the quantum computations underlying their twin's behavior, supporting trust and regulatory compliance.

1.6 Scope and Limitations

Scope. The QTwin framework operates entirely within a simulation-based quantum computing environment using the Qiskit Aer simulator [22]. This design choice reflects current hardware constraints: limited qubit counts, high error rates, and queue-based access models make cloud-accessible quantum processors unsuitable as the primary execution backend for an interactive digital twin platform that must deliver results within conversational timescales [3]. The simulator provides ideal (noise-free) quantum computation, enabling demonstration of algorithmic advantages without the confounding effects of hardware noise. Healthcare is designated as the primary validation domain, with six sub-domains providing comprehensive evaluation across diverse computational task types. Three additional domains—military operational planning, sports performance analytics, and environmental monitoring—serve as secondary validation contexts for cross-domain generalization assessment. The system architecture follows a microservices-oriented design with a FastAPI backend, Next.js frontend, PostgreSQL database with SQLite fallback, and Redis caching layer, containerized via Docker for reproducible deployment.

Terminology Note: Simulator-Based vs. Hardware Quantum Advantage. Throughout this thesis, "quantum advantage" refers to the statistically significant outperformance of quantum-algorithm-based approaches over classical baselines, as measured on the Qiskit Aer statevector simulator. Because the simulator performs quantum circuit execution through classical matrix multiplication, these results demonstrate *algorithmic advantage*—that quantum circuit designs encode problem structure more effectively than traditional classical approaches—rather than *hardware quantum advantage*, which would require execution on physical quantum processors exhibiting genuine quantum

mechanical effects. The distinction is critical: algorithmic advantage establishes that the quantum computational paradigm produces superior solutions, but the wall-clock speedups reported in Chapter 4 reflect classical simulation cost rather than projected quantum hardware execution time.

Limitations. Several limitations constrain the generalizability of the results. First, simulation-based execution means that reported quantum advantages reflect algorithmic potential rather than realized performance on physical quantum processors; NISQ noise, decoherence, and gate errors could degrade performance relative to simulation-based results [3]. The framework's OpenQASM export capability facilitates future hardware execution, but such execution is beyond this thesis's scope. Second, the NLP extraction pipeline relies primarily on rule-based pattern matching with optional spaCy [26] NER enrichment rather than large language model-based extraction; while this provides deterministic, interpretable behavior, its accuracy is bounded by pattern coverage, particularly for domains with specialized terminology. Third, quantum circuit simulation requires $O(2^n)$ classical memory [14], limiting benchmarks to approximately 20–30 qubits and constraining the problem sizes evaluated.

Deliberate Exclusions. Production deployment considerations (horizontal scaling, load balancing, security hardening, compliance certification), real-time data streaming from physical sensors, and multi-tenant SaaS functionality are acknowledged as important for real-world adoption but are beyond this thesis's scope. These represent natural extensions for future work rather than fundamental limitations of the proposed architecture.

1.7 Thesis Organization

The remainder of this thesis is organized into four chapters. Chapter 2 presents a comprehensive literature review covering digital twin technology, quantum computing fundamentals, variational quantum algorithms, healthcare digital twins [27], [28], and NLP for information extraction. Chapter 3 details the QTwin system architecture, conversational AI pipeline, quantum algorithm implementation for each of the seven module types, and the benchmark methodology with datasets and evaluation metrics. Chap-

ter 4 presents the platform implementation, experimental results including healthcare benchmarks across all six sub-domains, and cross-domain generalization evaluations for military, sports, and environmental domains. Chapter 5 synthesizes contributions, revisits each research question in light of empirical evidence, discusses limitations, and outlines future work including hardware execution on real quantum processors, large language model integration, and real-time data streaming.

CHAPTER 2:Literature Review

This chapter reviews the literature underpinning this thesis across seven areas: digital twin technology (Section 2.1), quantum computing fundamentals (Section 2.2), quantum algorithms for optimization and machine learning (Section 2.3), the intersection of quantum computing and digital twins (Section 2.4), conversational AI and NLP (Section 2.5), healthcare digital twins (Section 2.6), and the research gaps motivating the proposed framework (Section 2.7).

2.1 Digital Twin Technology

2.1.1 Origins and Definitions

Grieves introduced the digital twin concept in 2003 within the context of product lifecycle management (PLM), proposing a virtual informational construct comprising three elements: the physical entity, its virtual counterpart, and the bidirectional data connections linking them [1]. Unlike conventional static simulations discarded after the design phase, Grieves envisioned a persistent virtual model accompanying the physical product from design through decommissioning. The concept gained institutional momentum through its adoption by NASA and the U.S. Air Force. Glaessgen and Stargel defined a digital twin as an integrated multi-physics, multi-scale, probabilistic simulation that mirrors the life of its physical counterpart using the best available physical models, sensor updates, fleet history, and maintenance records [6]. This definition elevated the digital twin from a PLM tool to a safety-critical engineering asset, introducing the requirement for multi-physics fidelity that has influenced subsequent definitions across all domains.

Grieves and Vickers subsequently expanded the scope from manufactured products to arbitrary complex systems, arguing that the digital twin concept was applicable to any system whose behavior could be captured through computational models and sensor data [5]. Tao et al. extended the original three-component formulation into a five-dimensional model [7]:

$$M_{DT} = (PE, VM, Ss, DD, CN) \tag{2.1}$$

where PE is the physical entity, VM the virtual model, Ss the services (monitoring dashboards, predictive alerts, optimization recommendations), DD the data flowing between components, and CN the connections linking all dimensions. This formulation provided a comprehensive architectural vocabulary, particularly for manufacturing contexts where the service dimension is as critical as the virtual model itself. The present thesis extends this analysis by proposing quantum computing as an additional enabling technology that can enhance digital twin computational capabilities beyond classical approaches.

2.1.2 Architectures and Frameworks

The architectural design of digital twin systems has evolved from monolithic implementations toward modular, layered architectures. Tao et al. identified a common three-tier pattern comprising a physical layer (entities, sensors, actuators, and communication infrastructure), a virtual layer (physics-based simulations, data-driven models, and hybrid approaches), and a service layer (visualization, optimization, and decision support interfaces) [8]. This decomposition has become the de facto standard, providing a conceptual framework that accommodates diverse implementation technologies.

Rasheed et al. categorized computational approaches in the virtual layer into physics-based models employing first-principles equations, data-driven models using machine learning, and hybrid models combining both paradigms [9]. They argued that hybrid approaches offer the most promising path forward by combining the interpretability and extrapolation capability of physics-based models with the flexibility of data-driven ones. This observation is relevant to the present thesis, which employs quantum algorithms as a computational substrate for both physics-inspired simulation and data-driven modeling. Jones et al. conducted a systematic review identifying thirteen recurring characteristics across digital twin definitions, revealing that most published "digital twins" satisfy only a subset and would more accurately be classified as digital models or digital shadows [21]. Their finding that no universally accepted definition exists motivates the universal framework proposed in this thesis.

2.1.3 Industry Applications

Digital twin adoption has expanded from aerospace origins across manufacturing, smart cities, and healthcare. Fuller et al. identified IoT, cloud computing, AI, and extended reality as the four technology pillars upon which modern implementations depend [2]. In manufacturing, twins integrate sensor data—vibration signatures, temperature profiles, process parameters—with physics-based models of machine dynamics for predictive maintenance and production optimization [7]. In smart cities, GIS, BIM, and real-time sensor networks enable city-scale twins for urban planning, emergency response, and resource optimization. Healthcare applications are examined in Section 2.6. Each domain demonstrates both significant potential and the domain-specific expertise required for implementation, underscoring the need for universal frameworks that reduce barriers to entry.

2.1.4 Current Platforms

Microsoft Azure Digital Twins provides a platform-as-a-service using the Digital Twins Definition Language (DTDL), a JSON-LD-based ontology language requiring users to design models specifying properties, telemetry, components, and relationships [11]. While DTDL provides expressive power for complex domain ontologies, it demands significant technical expertise: users must design their ontology, implement telemetry ingestion pipelines, and develop custom functions for data processing and visualization. The platform excels in built-environment and smart-building scenarios but requires substantial customization for other domains.

AWS IoT TwinMaker adopts an entity-component model enabling users to construct digital twins by defining entities (physical assets), components (data sources and processing logic), and scenes (3D visualizations) [12]. The platform provides pre-built connectors for industrial data sources and is optimized for industrial IoT scenarios with well-defined data pipelines. Its entity-component model does not naturally accommodate non-industrial domains such as healthcare or environmental science, where entities may be patients, ecosystems, or populations rather than physical machines. Both platforms represent significant engineering achievements but share fundamental limitations constraining their utility as universal platforms.

2.1.5 Limitations of Current Approaches

Critical analysis reveals five systemic limitations. First, all platforms are domain-specific by design—Azure is optimized for built environments, AWS for industrial IoT, and academic frameworks target single domains [2], [6], [8]. No existing platform offers a mechanism by which a user can describe an arbitrary system and receive a functional digital twin without domain-specific pre-configuration. Second, all require substantial technical expertise for configuration, whether in DTDL ontology design, IoT pipeline engineering, or physics model implementation, effectively excluding domain experts who lack software engineering skills. Third, none incorporates quantum computing capabilities, leaving quantum algorithmic advantages unexploited. Fourth, none provides a natural language interface for twin creation, forcing users to express domain knowledge through formal modeling languages or programmatic APIs. Fifth, the creation process is manual and labor-intensive, requiring weeks to months of engineering effort per deployment. These five limitations collectively define the problem space that the QTwin framework addresses.

2.2 Quantum Computing Fundamentals

2.2.1 Quantum Mechanics Principles

The computational power of quantum computers derives from three principles of quantum mechanics: superposition, entanglement, and interference [14]. A qubit, unlike a classical bit restricted to 0 or 1, exists in a superposition of basis states:

$$|\psi\rangle = \alpha|0\rangle + \beta|1\rangle \tag{2.2}$$

where $\alpha, \beta \in \mathbb{C}$ are probability amplitudes satisfying $|\alpha|^2 + |\beta|^2 = 1$, with $|\alpha|^2$ and $|\beta|^2$ representing measurement probabilities for the $|0\rangle$ and $|1\rangle$ states respectively. For n qubits, the state space requires 2^n complex amplitudes, a quantity that grows exponentially and underlies the representational advantage of quantum systems.

Entanglement introduces correlations with no classical analogue: the state of a composite system cannot be decomposed into individual qubit states. A canonical example is the Bell state:

$$|\Phi^+\rangle = \frac{1}{\sqrt{2}}(|00\rangle + |11\rangle) \tag{2.3}$$

Measuring one qubit of an entangled pair determines the other's outcome regardless of spatial separation. Entanglement is a key resource for quantum speedups in search, optimization, and simulation algorithms. Interference is the mechanism by which probability amplitudes combine constructively for correct solutions and destructively for incorrect ones, enabling quantum algorithms to amplify desired outcomes upon final measurement [14].

2.2.2 Quantum Gates and Circuits

The gate model of quantum computation represents quantum computations as sequences of unitary transformations (quantum gates) applied to qubits [14]. Single-qubit gates include the Pauli gates (X, Y, Z), the Hadamard gate (H), and parameterized rotations ($R_x(\theta)$, $R_y(\theta)$, $R_z(\theta)$). The controlled-NOT (CNOT) gate introduces entanglement between qubits, and the set $\{H, T, \text{CNOT}\}$, where T is the $\pi/8$ phase gate, constitutes a universal gate set capable of approximating any n-qubit unitary to arbitrary precision [14].

Feynman first articulated the insight that the exponential scaling of quantum state spaces renders classical simulation intractable, and proposed that quantum mechanical computers could simulate quantum physics efficiently [13]. A quantum circuit is a directed acyclic graph in which nodes represent gates and edges represent qubit wires. Circuit depth—the maximum number of sequential gate layers—is a critical metric for NISQ-era implementations, as each additional layer introduces noise through imperfect gate operations and qubit decoherence. The variational algorithms employed in this thesis are specifically designed for shallow circuit depths.

2.2.3 The NISQ Era

Preskill coined the term "Noisy Intermediate-Scale Quantum" (NISQ) to describe processors with 50 to several hundred qubits that lack fault-tolerant error correction [3]. NISQ devices are "noisy" because gate operations are imperfect and coherence times are limited, and "intermediate-scale" because qubit counts, while sufficient to surpass

classical simulation for certain problems, are far below the millions of logical qubits needed for fault-tolerant algorithms such as Shor's [29].

Arute et al. reported that Google's 53-qubit Sycamore processor sampled from a random circuit distribution in approximately 200 seconds—a task estimated to require 10,000 years classically—providing the first empirical evidence of quantum computational advantage [4]. Despite this milestone, NISQ hardware remains constrained by two-qubit gate error rates of 10^{-2} to 10^{-3} and coherence times in microseconds to milliseconds [30]. These constraints necessitate algorithmic approaches that are noise-tolerant and limit circuit depth. The variational algorithms discussed in Section 2.3 represent the primary strategy for the NISQ regime and form the computational backbone of the proposed framework.

2.2.4 Quantum Software Frameworks

Qiskit, developed by IBM, provides a comprehensive Python-based toolkit for circuit construction, transpilation, simulation, and hardware execution [22]. Its modular architecture comprises Terra (circuit construction), Aer (high-performance simulation), Ignis (error characterization), and Aqua (algorithm implementations). The Qiskit Aer simulator supports statevector, density matrix, and stabilizer simulation for circuits of up to approximately 30 qubits on standard hardware, and serves as the quantum execution backend for the proposed framework.

PennyLane, developed by Xanadu, integrates quantum circuit execution into classical automatic differentiation frameworks (TensorFlow, PyTorch, JAX), enabling gradient-based optimization of parameterized circuits using the same workflows employed for classical deep learning [23]. This integration is particularly valuable for variational algorithms where efficient gradient computation benefits the classical optimization loop. The diversity and maturity of quantum software frameworks provide the infrastructure upon which application-level platforms such as the one proposed in this thesis can be constructed.

2.2.5 OpenQASM

The Open Quantum Assembly Language (OpenQASM) provides a hardware-agnostic circuit description language serving as the intermediate representation for quantum cir-

cuits across platforms [24]. OpenQASM defines a textual format for qubit declarations, gate operations, measurement instructions, and classical control flow, designed to be both human-readable and machine-parseable.

OpenQASM 3 extends the specification with classical control flow, real-time feedback, subroutine definitions, and modular circuit composition [25]. These capabilities enable hybrid quantum-classical algorithms—including the variational algorithms central to this thesis—to be expressed within a single circuit specification. The proposed framework generates all quantum circuits in OpenQASM format, ensuring transparency, reproducibility, and portability across quantum computing platforms.

2.3 Quantum Algorithms for Optimization and Machine Learning

2.3.1 QAOA

The Quantum Approximate Optimization Algorithm (QAOA), introduced by Farhi, Goldstone, and Gutmann, is a variational algorithm for combinatorial optimization [16]. QAOA alternates the application of a problem Hamiltonian $\hat{H}_P$ encoding the objective function with a mixer Hamiltonian $\hat{H}_M$ enabling solution-space exploration. Beginning with a uniform superposition over all 2^n candidate solutions, the algorithm applies p layers of alternating unitaries with variational parameters $(\boldsymbol{\gamma}, \boldsymbol{\beta})$:

$$|\boldsymbol{\gamma}, \boldsymbol{\beta}\rangle = \prod_{l=1}^{p} e^{-i\beta_l \hat{H}_M} e^{-i\gamma_l \hat{H}_P} |+\rangle^{\otimes n} \tag{2.4}$$

The parameters are classically optimized to maximize the expected objective value $\langle \boldsymbol{\gamma}, \boldsymbol{\beta} | \hat{H}_P | \boldsymbol{\gamma}, \boldsymbol{\beta} \rangle$, with solution quality improving as p increases and converging to the exact optimum as $p \to \infty$. QAOA is suited to any problem expressible as a QUBO or Ising formulation, including scheduling, vehicle routing, portfolio optimization, and resource allocation. The proposed framework employs QAOA for operational optimization tasks such as hospital resource scheduling and clinical trial patient allocation, automatically mapping problems extracted from the conversational interface into QAOA circuit specifications.

2.3.2 *Variational Quantum Circuits*

Variational quantum circuits (VQCs) constitute the broader algorithmic family to which QAOA belongs, representing the dominant paradigm for NISQ-era computation. The Variational Quantum Eigensolver (VQE), proposed by Peruzzo et al., uses a parameterized circuit (ansatz) to prepare trial wavefunctions, measures the expectation value of a target Hamiltonian, and classically optimizes circuit parameters to minimize energy [15]. The variational principle guarantees:

$$E(\boldsymbol{\theta}) = \langle \psi(\boldsymbol{\theta}) | \hat{H} | \psi(\boldsymbol{\theta}) \rangle \geq E_0 \tag{2.5}$$

where E_0 is the exact ground state energy and $|\psi(\boldsymbol{\theta})\rangle$ is the parameterized trial state. McClean et al. established the theoretical foundations for variational hybrid quantum-classical algorithms [31], and Cerezo et al. provided a comprehensive review cataloging VQA applications across chemistry, optimization, machine learning, and simulation [18]. Key design choices include the ansatz structure, cost function, measurement strategy, and classical optimizer.

A significant challenge is the barren plateau phenomenon, where the gradient of the cost function vanishes exponentially with increasing qubit count, rendering gradient-based optimization infeasible for large circuits [32]. Mitigation strategies include structured ansatze that limit entanglement growth, layer-wise training, and classical pre-training of initial parameters. The classical optimization loop typically employs gradient-free optimizers such as COBYLA or gradient-based methods including Adam [33]. The proposed framework employs the variational paradigm across multiple module types: QAOA for optimization, VQE for molecular simulation, variational classifiers for state classification, and quantum autoencoders for dimensionality reduction.

2.3.3 *Barren Plateaus and Training Challenges*

The barren plateau phenomenon poses a fundamental challenge to the scalability of variational quantum algorithms. McClean et al. demonstrated that for sufficiently expressive parameterized circuits, the variance of the cost function gradient decreases exponentially with the number of qubits, rendering gradient-based optimization infeasible [32]. Larocca et al. provided a comprehensive review establishing that barren

plateaus arise from multiple independent sources—excessive entanglement, global cost functions, hardware noise, and high expressibility—and that known mitigation strategies (structured ansatze, local cost functions, layerwise training) address individual sources without eliminating the phenomenon entirely [34]. Cerezo et al. further argued that the absence of barren plateaus may itself imply classical simulability, suggesting a fundamental tension between trainability and quantum advantage [35]. This tension is directly relevant to the proposed framework: the variational circuits employed in the QTwin modules (QAOA, VQC, VQE) operate at qubit counts (4–12) where barren plateaus are not yet manifest, but scaling to larger problem instances would require explicit mitigation strategies. The framework's use of problem-structured ansatze and the COBYLA optimizer (which relies on function evaluations rather than gradients) partially addresses this concern for current circuit sizes.

2.3.4 Quantum Support Vector Machines

Classical support vector machines find maximum-margin hyperplanes separating data classes, with kernel functions enabling nonlinear classification through implicit high-dimensional feature mappings [36]. Havlíček et al. demonstrated that quantum computers can compute kernel functions that are classically intractable by encoding classical data into quantum states via parameterized circuits [17]. The quantum kernel is defined as:

$$K(\mathbf{x}_i, \mathbf{x}_j) = |\langle \phi(\mathbf{x}_i) | \phi(\mathbf{x}_j) \rangle|^2 \tag{2.6}$$

where $|\phi(\mathbf{x})\rangle$ is the quantum feature state produced by the encoding circuit applied to classical data point $\mathbf{x}$. This hybrid approach combines quantum representational advantages with the well-understood optimization of classical SVMs. Schuld et al. explored circuit-centric quantum classifiers employing variational circuits as trainable classification models, providing an alternative to kernel-based approaches [37]. The proposed framework primarily employs variational quantum classifiers (VQC) for classification tasks within digital twin applications, with quantum kernel methods representing a promising direction for future investigation.

2.3.5 Quantum Neural Networks and Tensor Networks

Biamonte et al. categorized quantum machine learning into four quadrants by data type and algorithm type, with quantum algorithms for classical data being most relevant to digital twin applications [38]. Abbas et al. demonstrated that parameterized quantum circuits can achieve higher effective dimension than classical networks with comparable parameter counts, introducing effective dimension as a measure of quantum model expressibility [39]. Cong, Choi, and Lukin proposed quantum convolutional neural networks (QCNNs) applying local quantum operations in a hierarchical structure, relevant to spatial data processing in the proposed framework's medical imaging module [40].

Tensor networks provide a mathematical framework for representing high-dimensional quantum states through networks of lower-dimensional tensors. Orús reviewed the major architectures—matrix product states (MPS), projected entangled pair states (PEPS), multiscale entanglement renormalization ansatz (MERA), and tree tensor networks (TTN)—and their applications to quantum simulation and quantum information [41]. Huggins et al. demonstrated that tree tensor networks map naturally onto parameterized quantum circuits and are well-suited for hierarchical data structures, capturing correlations at multiple scales [42]. The proposed framework employs TTN circuits for modeling hierarchical relationships within digital twin systems.

2.3.6 Quantum Simulation and Sensing

Quantum simulation exploits the natural ability of quantum systems to simulate other quantum systems, an insight first articulated by Feynman [13]. In digital twin contexts, quantum simulation is relevant for modeling processes governed by quantum mechanical interactions, including molecular dynamics and electronic structure calculations. Kandala et al. demonstrated hardware-efficient VQE on a superconducting processor, computing ground state energies of H_2, LiH, and BeH_2 using native gate sets to reduce circuit depth [43]. This hardware-efficiency strategy is important for NISQ implementations where circuit depth is the primary accuracy constraint.

Quantum sensing exploits the sensitivity of quantum systems to external perturbations to achieve measurement precision beyond classical limits [44]. Three quantum resources enable enhanced sensing: superposition for parallel measurement, entanglement for noise reduction below the standard quantum limit, and squeezing for

noise redistribution between conjugate observables. The standard quantum limit scales as $1/\sqrt{N}$ with probe particles N, while quantum-enhanced sensing can achieve the Heisenberg limit of $1/N$. For digital twins, quantum sensing is relevant both as a data acquisition technology providing higher-precision input data and as a simulation paradigm within the twin framework.

2.3.7 Quantum Advantage: Claims and Debates

Whether quantum computers provide meaningful computational improvements for practical problems remains actively debated. Arute et al.'s 2019 supremacy demonstration involved a sampling task specifically designed to be classically hard, and subsequent classical simulation improvements have narrowed the claimed advantage [4]. Preskill cautioned that NISQ-era quantum advantage may be elusive for most practical problems, noting that noise substantially reduces effective computational power [3]. Cerezo et al. identified scenarios where variational algorithms might achieve advantage: problems with exponentially large solution spaces, quantum-structured cost functions, and landscapes where classical optimization encounters many local minima [18].

Schuld argued that "quantum advantage" may be an inappropriate goal for quantum machine learning, advocating instead for identifying the specific structural properties of data that quantum models exploit more effectively than classical ones [45]. Bowles et al. demonstrated that rigorous benchmarking against properly optimized classical baselines often eliminates claimed quantum advantages, underscoring the need for methodological care [46]. For optimization, Guerreschi and Matsuura showed that QAOA for Max-Cut requires hundreds of qubits to outperform the Goemans-Williamson classical algorithm, placing practical quantum advantage well beyond current NISQ capabilities [47]. Lubinski et al. proposed application-oriented benchmarks for quantum computing that move beyond artificial sampling tasks toward metrics relevant to end users [48]. These critiques inform the evaluation methodology adopted in this thesis: benchmark results are reported against established classical baselines with full statistical validation, and claims of quantum advantage are contextualized within the simulator-based evaluation scope (Section 1.6).

This thesis adopts a pragmatic rather than theoretical approach: the framework benchmarks quantum algorithms against classical counterparts across six healthcare

sub-domains, providing empirical evidence of where quantum approaches offer practical improvements and where classical approaches remain competitive. This methodology avoids overclaiming quantum advantage while providing actionable information about computational contexts in which quantum digital twins are most beneficial.

2.4 Quantum Computing in Digital Twin Applications

2.4.1 Existing Work

The intersection of quantum computing and digital twin technology remains one of the most nascent areas in both fields. Lin and Critchley provided one of the first systematic examinations, mapping digital twin computational requirements onto quantum algorithm capabilities and identifying molecular simulation, combinatorial optimization, and high-dimensional data analysis as the tasks most likely to benefit from near-term quantum advantages [19]. However, their work remained at the survey level without proposing or implementing a concrete platform. Otgonbaatar and Jennings explored "quantum digital twins" from the inverse perspective—using digital twins to model quantum systems themselves for uncertainty quantification rather than using quantum computing to enhance classical digital twins [20]. While valuable for quantum hardware development, this direction is orthogonal to the present thesis's objective.

The scarcity of published work despite clear computational alignment between quantum algorithm strengths (optimization, simulation, machine learning) and digital twin computational demands (operational optimization, physics simulation, predictive modeling) represents the primary research gap this thesis addresses.

2.4.2 Emerging Quantum Digital Twin Literature

Since the inception of this research, several works have begun to address the quantum–digital twin intersection from narrower perspectives. Otgonbaatar and Datcu demonstrated quantum transfer learning for remote sensing imagery classification, applying variational circuits to real-world datasets at small scale [49]. Zhang et al. surveyed quantum algorithms for chemical simulation, reinforcing the potential of VQE for molecular digital twins but noting that practical advantage requires error-mitigated hardware [50]. In the healthcare domain, Chen and Lv surveyed quantum computing

applications for healthcare digital twins, identifying drug discovery and genomic analysis as the most promising near-term targets [51]. Kim et al. applied quantum optimization to smart grid digital twins, demonstrating QAOA-based load balancing for a 14-bus power network [52]. These works validate the research direction of the present thesis while differing in scope: each addresses a single domain or algorithm, whereas QTwin provides a universal, multi-algorithm framework with empirical validation across six sub-domains. The claim of "first integrated platform" is therefore nuanced: QTwin is the first *universal, conversational* quantum digital twin platform, while domain-specific quantum–DT integrations are emerging in parallel.

2.4.3 LLM-Powered Digital Twins

A convergent research direction is the integration of large language models (LLMs) into digital twin workflows. Yang et al. proposed LLM-powered digital twins that use foundation models for autonomous system modeling, entity extraction, and simulation code generation—objectives that overlap with QTwin's conversational pipeline [53]. Wang et al. combined knowledge graphs with GPT-based generation for digital twin construction, demonstrating that LLMs can extract domain ontologies from unstructured text with accuracy exceeding 90% [54]. These approaches complement the present work: where QTwin employs a two-stage extraction pipeline—rule-based domain-adaptive pattern matching enriched by spaCy named entity recognition—for deterministic extraction with quantum algorithms for computation, LLM-based systems offer more flexible extraction but lack quantum computational capabilities. The QTwin architecture's provider abstraction layer (Section 3.3.4) was designed to accommodate LLM integration as a future enhancement (Section 5.4.2), positioning the framework to leverage advances in both quantum computing and large language models.

2.4.4 Quantum Sensing for DT Data

Quantum-enhanced sensors can achieve measurement precision beyond classical limits, particularly for magnetic fields, electric fields, temperature, and inertial navigation [44]. For digital twins, higher-precision sensor data translates directly into higher-fidelity virtual models, as twin accuracy is fundamentally bounded by input data quality. In healthcare contexts, quantum-enhanced MRI could provide higher-resolution images with

shorter acquisition times, and nitrogen-vacancy-center magnetometers have demonstrated sensitivity sufficient for magnetoencephalography without cryogenic cooling. The proposed framework incorporates a quantum sensing simulation module that models quantum-enhanced measurement protocols, enabling users to evaluate potential sensor improvements without physical quantum sensing hardware.

2.4.5 Quantum Optimization for DT Decisions

Digital twin optimization tasks—resource allocation, scheduling, route planning, parameter tuning—are among the most promising candidates for near-term quantum advantage. QAOA [16] and variational optimization methods [18] encode combinatorial problems as quantum Hamiltonians and variationally search for low-energy solutions, potentially exploring solution spaces more efficiently than classical heuristics through quantum tunneling and interference. A hospital digital twin, for example, must optimize nurse scheduling, bed assignments, operating room utilization, and equipment allocation—all combinatorial problems whose complexity grows rapidly with the number of resources and constraints. Classical heuristics (genetic algorithms, simulated annealing) do not guarantee optimality, whereas QAOA leverages quantum effects to search solution spaces more broadly. The proposed framework provides empirical evaluation of QAOA-based optimization for healthcare resource management.

2.4.6 Gap Analysis

No practical platform integrates quantum computing into a functional digital twin generation framework. The existing literature consists of survey-level analyses identifying potential synergies [19], theoretical proposals for quantum-system twins [20], and narrow investigations of specific aspects. No published work has demonstrated an end-to-end system that accepts a system description and produces a quantum-powered digital twin, nor has any work evaluated quantum algorithm impact on digital twin tasks across multiple application domains. The QTwin framework addresses this gap by providing the first integrated platform combining quantum computing with universal digital twin generation, implementing seven quantum algorithm modules within a domain-agnostic architecture and empirically evaluating quantum advantage across six healthcare subdomains.

2.5 Conversational AI and NLP

2.5.1 NLP for Requirements Extraction

Named entity recognition (NER) is the foundational NLP capability for the proposed conversational interface, which must extract domain-specific entities—medical conditions, drug names, hospital departments, patient populations, and operational parameters—from natural language system descriptions. Lample et al. introduced a BiLSTM-CRF architecture achieving state-of-the-art NER performance without hand-crafted features or domain-specific gazetteers, demonstrating that neural sequence labeling can learn entity patterns from annotated training data [55]. The spaCy library provides industrial-strength NLP pipelines integrating tokenization, part-of-speech tagging, dependency parsing, and NER into a unified framework [26]. SpaCy's pre-trained models offer competitive accuracy on general-domain text, and its modular architecture supports custom entity types through rule-based pattern matching, gazetteer lookup, or domain-specific fine-tuning.

The proposed framework employs domain-adaptive pattern matching rules as the primary extraction method, with spaCy's statistical NER available as an optional secondary enrichment stage. This two-stage approach prioritizes domain specificity (rules capture domain-specific patterns deterministically) while optionally leveraging spaCy for supplementary general-domain entities that pattern rules may miss, without requiring large annotated datasets for training domain-specific neural models from scratch.

2.5.2 Conversational Agents in Technical Domains

Conversational interfaces accept natural language input and extract structured information, eliminating the translation burden imposed by GUIs, programmatic APIs, and domain-specific languages. Applying this paradigm to digital twin configuration presents three challenges. First, the information to be extracted is highly structured and domain-specific: a twin specification includes entities with typed attributes, relationships with cardinalities, dynamic processes, and optimization objectives with constraints. Second, extraction must operate across arbitrary domains without domain-specific training data, requiring transfer learning or zero-shot capabilities. Third, the process must support progressive refinement over multiple dialogue turns. The proposed framework ad-

dresses these through domain-adaptive entity extraction, contextual follow-up question generation, and a twin lifecycle state machine that tracks specification completeness.

2.5.3 LLM-Based System Design

The transformer architecture replaced recurrent processing with parallel self-attention [56], serving as the foundation for all state-of-the-art NLP models. Devlin et al. introduced BERT, achieving state-of-the-art results across eleven benchmarks through bidirectional pre-training [57]. Brown et al. demonstrated that scaling to 175 billion parameters (GPT-3) enables few-shot learning from prompt examples without gradient-based fine-tuning [58]. These advances have significant implications for digital twin creation: LLMs could serve as conversational interfaces leveraging broad world knowledge to extract structured system descriptions from natural language dialogue.

The proposed framework employs rule-based domain-adaptive pattern matching for deterministic, interpretable entity extraction, with spaCy [26] available as optional NER enrichment, while the architecture is designed to accommodate future LLM integration for enhanced cross-domain generalization. This design reflects a pragmatic balance between the interpretability of rule-based approaches and the generalization capabilities of learned models.

2.6 Healthcare Digital Twins

2.6.1 Personalized Medicine

Björnsson et al. articulated a vision of patient digital twins integrating genomic data, clinical history, lifestyle factors, and real-time physiological measurements to guide treatment decisions with high precision [28]. Their framework proposed that patient twins could enable in silico clinical trials, evaluating treatments virtually before administration to reduce adverse reaction risk. Corral-Acero et al. demonstrated the concept through cardiac digital twins integrating imaging data, electrophysiological measurements, and hemodynamic parameters with computational cardiac models to predict intervention outcomes [27]. Topol provided a broader perspective, arguing that AI-driven approaches can make healthcare more personalized and data-driven by freeing clinicians from routine diagnostic tasks [59]. These applications demonstrate both the clini-

cal potential and the domain-specific complexity of healthcare digital twins, motivating frameworks that automate the twin creation process.

2.6.2 Drug Discovery

The drug discovery pipeline—target identification, hit discovery, lead optimization, preclinical testing, and clinical trials—typically spans 10–15 years and costs billions of dollars. Computational approaches including molecular docking, molecular dynamics, and virtual screening can accelerate early stages through in silico molecular interaction prediction. Classical electronic structure methods (density functional theory, coupled cluster theory) face exponential scaling with electron count, restricting the size and accuracy of molecular simulations. Quantum algorithms, particularly VQE [15] and quantum phase estimation, offer polynomial scaling, potentially enabling simulation of biologically relevant molecules intractable for classical methods. Kandala et al. demonstrated VQE ground state energy computation for H_2, LiH, and BeH_2 on quantum hardware, establishing experimental feasibility [43]. The proposed framework employs VQE-based molecular simulation for binding affinity computation and drug compound screening.

2.6.3 Medical Imaging

Litjens et al. surveyed deep learning in medical image analysis, documenting human-level or superior performance across retinal, pulmonary, pathology, brain, breast, cardiac, and abdominal imaging tasks [60], building on foundations established by LeCun et al. [61] and Goodfellow et al. [62]. Despite these successes, challenges remain: large labeled datasets are scarce, model interpretability is limited, and computational costs are high for volumetric data. Quantum machine learning offers potential advantages through quantum feature maps in exponentially large Hilbert spaces [17], quantum convolutional architectures for spatial data [40], and variational classifiers achieving competitive accuracy with fewer parameters [37]. The proposed framework incorporates quantum classifiers for image-based diagnostics within the healthcare digital twin.

2.6.4 Genomic Analysis

Libbrecht and Noble reviewed machine learning for genetics and genomics, highlighting the unique characteristics of genomic data: high dimensionality, complex correlation structures, and mixed discrete-continuous modalities [63]. Quantum approaches offer advantages through several mechanisms: quantum feature maps efficiently represent the 4^L combinatorial space of length-L DNA sequences, quantum kernels [17] capture complex expression-data correlations, and QAOA [16] addresses feature selection in settings where genes outnumber patients by orders of magnitude. The proposed framework employs tree tensor networks for genomic correlation analysis, using hierarchical tensor decomposition for variant classification and gene expression profiling.

2.6.5 Epidemic Modeling

The SIR model of Kermack and McKendrick partitions a population into susceptible (S), infected (I), and recovered (R) compartments with dynamics governed by [64]:

$$\frac{dS}{dt} = -\beta SI, \quad \frac{dI}{dt} = \beta SI - \gamma I, \quad \frac{dR}{dt} = \gamma I \tag{2.7}$$

where β is the transmission rate, γ the recovery rate, and $R_0 = \beta/\gamma$ governs epidemic dynamics: when $R_0 > 1$ an epidemic spreads; when $R_0 < 1$ it dies out. Hethcote extended this framework to incorporate exposed, vaccinated, age-structured, spatial, and stochastic compartments [65]. Population-scale simulations generate combinatorial state spaces growing exponentially with population size and model complexity; classical agent-based models scale poorly. Quantum simulation offers a different approach: by encoding population states in superpositions, a quantum simulator can evolve multiple epidemic trajectories simultaneously, with interference amplifying trajectories consistent with observed data. The proposed framework employs variational quantum circuits for compartmental epidemic dynamics.

2.6.6 Hospital Operations

Hospital operations—nurse and physician scheduling, operating room allocation, bed management, equipment utilization, and emergency department flow—are inherently combinatorial, with solution spaces growing exponentially in resources and constraints.

Classical approaches including integer linear programming, constraint programming, genetic algorithms, and simulated annealing face scalability challenges and often cannot incorporate the full range of operational constraints governing real hospital environments. QAOA [16] encodes operational constraints as penalty terms in the problem Hamiltonian and uses variational optimization to find high-quality solutions, considering staffing constraints, patient acuity, equipment availability, and operational policies simultaneously. The proposed framework employs QAOA for hospital resource scheduling, combining the digital twin's virtual model with conversational specification and quantum-enhanced optimization.

2.7 Summary and Research Gap

The preceding review reveals substantial independent progress in digital twin technology, quantum computing, conversational AI, and healthcare informatics, but a conspicuous absence of integrated work bridging these domains. Table 2.1 compares existing platforms against the proposed QTwin framework across five capability dimensions.

Table 2.1: Comparison of Existing Digital Twin Platforms and the Proposed QTwin Framework

Platform	**Universal**	**Quantum**	**Conversational**	**Automated**	**Healthcare**
Azure DT [11]	No	No	No	No	Partial
AWS TwinMaker [12]	No	No	No	No	No
Tao et al. [8]	No	No	No	No	No
Fuller et al. [2]	No	No	No	No	Partial
Lin & Critchley [19]	No	Survey	No	No	No
Otgonbaatar & Jennings [20]	No	Theoretical	No	No	No
Björnsson et al. [28]	No	No	No	No	Yes
Corral-Acero et al. [27]	No	No	No	No	Yes
Chen & Lv [51]	No	Healthcare	No	No	Yes
Kim et al. [52]	No	Energy	No	No	No
Yang et al. [53]	Partial	No	Yes	Partial	No
QTwin (Proposed)	**Yes**	**Yes**	**Yes**	**Yes**	**Yes**

No existing platform achieves universality, quantum integration, conversational creation, automated generation, or combined healthcare-quantum support. The synthesis reveals five research gaps:

1. **No universal domain-agnostic digital twin generation framework exists.** Jones et al. identified the absence of a universal framework as a central challenge [21].

All existing platforms are domain-locked, requiring manual ontology definition and domain-specific engineering.

2. **Quantum computing and digital twin research remain largely separate.** Despite clear computational alignment between quantum capabilities [15], [16], [18], [38] and digital twin demands, no integrated platform bridges these communities.

3. **No conversational interface exists for digital twin creation.** Powerful NLP techniques [26], [55], [57], [58] have not been applied to automated twin generation from natural language system descriptions.

4. **Healthcare digital twins lack quantum enhancement.** Healthcare twins for precision medicine [28], cardiology [27], drug discovery, imaging [60], genomics [63], and epidemiology [64], [65] have not incorporated quantum algorithms despite suitable methods being available.

5. **No integrated platform combines quantum computing, digital twins, and conversational AI.** Each pillar has been independently developed, but the synergistic potential of their combination has not been realized in any published system.

The QTwin framework addresses all five gaps: domain-agnostic architecture for arbitrary domains (Gap 1), seven quantum modules—QAOA [16], VQE [15], VQC [37], quantum simulation, TTN [41], quantum autoencoders [66], and quantum sensing [44]—as first-class computational primitives (Gap 2), a two-stage conversational interface combining rule-based domain-adaptive pattern matching with spaCy NER enrichment (Gap 3), empirical quantum advantage validation across six healthcare sub-domains (Gap 4), and the first end-to-end integration of conversational AI, quantum computing, and digital twin technology (Gap 5).

CHAPTER 3:Methodology

This chapter presents the research methodology and technical design of the QTwin platform. Following a design science research approach grounded in the theoretical foundations of Chapter 2, the chapter proceeds through the system architecture, conversational AI pipeline, quantum algorithm implementations, healthcare reference implementation, and benchmark methodology.

3.1 Research Methodology Overview

This thesis adopts the design science research methodology (DSRM), which emphasizes the creation and evaluation of innovative artifacts as the central research activity. The primary artifact is the QTwin platform—an end-to-end system that accepts natural language system descriptions and produces quantum-powered digital twins. Development followed an iterative cycle of requirements analysis, architectural design, implementation, and evaluation. Functional requirements included conversational entity extraction, dynamic quantum algorithm selection, universal twin generation, and OpenQASM circuit export [24], [25]. Non-functional requirements encompassed sub-second NLP response latency, extensibility to new domains without code modification, and reproducibility of all quantum computations. Early prototyping revealed that spaCy's pretrained NER alone was insufficient for domain-specific entities, motivating the domain-adaptive pattern matching system as the primary extraction stage (Section 3.3), and initial QAOA benchmarking prompted warm-starting strategies [16].

The evaluation strategy combines *depth validation*—quantum algorithms against classical baselines across six healthcare sub-domains with statistical significance testing—and *breadth validation*—cross-domain generalization using military, sports, and environmental scenarios. The methodology addresses known concerns in quantum computing research: strong classical baselines, complete result reporting, and statistical validation with effect size analysis [3].

3.2 System Architecture

3.2.1 High-Level Architecture

The QTwin platform is organized as a three-tier architecture comprising a presentation tier, an API tier, and an engine tier. This architectural pattern provides separation of concerns, enabling independent development, testing, and deployment of each tier while maintaining well-defined interfaces. The presentation tier is a Next.js 14 web application utilizing the App Router and React Server Components, providing the conversational interface through which users interact with the platform. The API tier is a FastAPI application exposing RESTful endpoints for twin management, conversation handling, benchmarking, and data retrieval, with WebSocket support for real-time conversational interaction. The engine tier encapsulates the NLP pipeline, quantum algorithm library, twin generation engine, and classical baselines. Figure 3.1 illustrates the architecture and data flow between tiers.

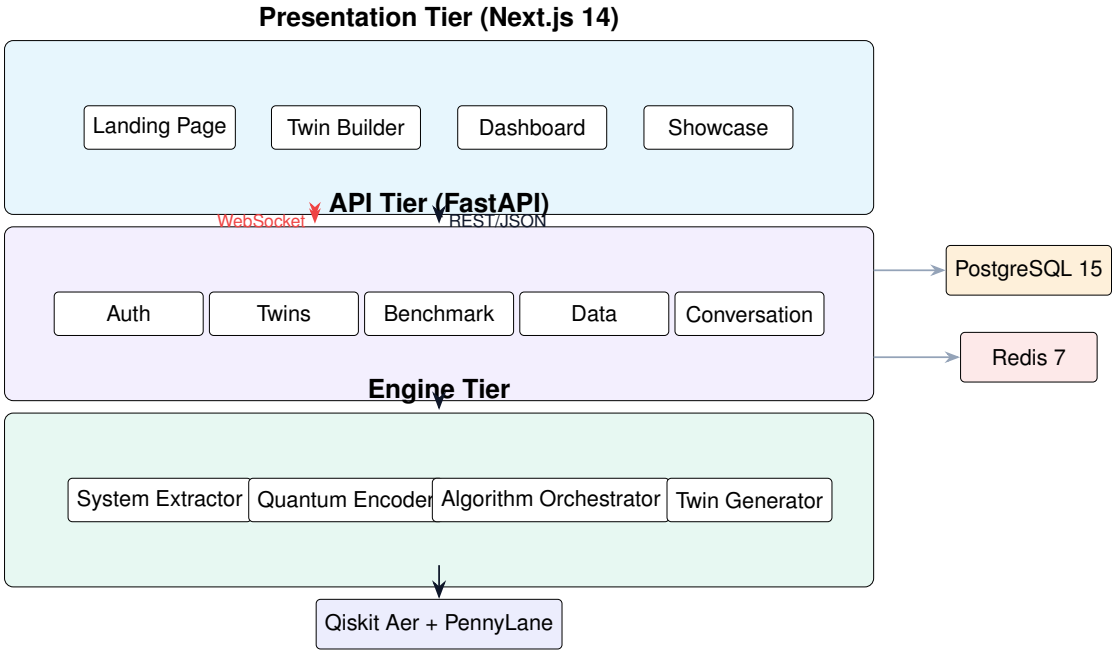

Figure 3.1: Three-tier system architecture of the QTwin platform.

Data flows sequentially through the tiers: the user submits a natural language message via WebSocket, the NLP pipeline extracts entities, and upon meeting activation thresholds the twin generation engine performs problem decomposition, algorithm selection, and quantum circuit generation—all exported in OpenQASM format [24], [25]. The RESTful API provides four router groups (twins, conversation, benchmark, data)

with JWT authentication and PostgreSQL 15 storage with automatic SQLite fallback. Full implementation details are presented in Section 4.2.

3.2.2 Universal Twin Generation Engine

The universal twin generation engine constitutes the core innovation of the QTwin platform. Unlike existing digital twin platforms that require domain-specific ontologies, pre-built simulation models, and manual configuration, the QTwin engine generates digital twins dynamically from natural language descriptions by composing domain-agnostic quantum algorithms. The engine operates as a four-stage pipeline: problem decomposition, algorithm selection, parameter encoding, and twin composition. Each stage is designed to be domain-agnostic, operating on abstract representations of entities, relationships, and objectives rather than domain-specific constructs. Figure 3.2 illustrates the pipeline stages.

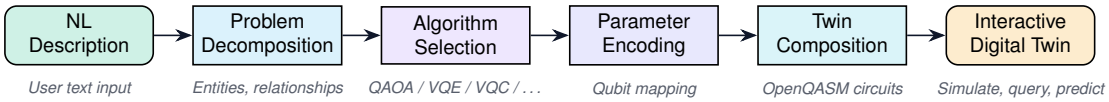

Figure 3.2: The four-stage Universal Twin Generation Engine pipeline, from natural language input to interactive digital twin output.

The engine achieves domain-agnosticity by separating domain-specific concerns (vocabulary, entity recognition) from domain-agnostic computation: adding a new domain requires only NLP pattern additions. The detailed operation of each pipeline stage is described in Section 3.4.

3.2.3 Technology Stack

The selection of technologies was guided by requirements of performance, extensibility, quantum computing integration, and developer productivity. Table 3.1 presents the complete technology stack.

FastAPI's asynchronous architecture enables concurrent quantum circuit execution. The quantum computing layer combines Qiskit Aer [22] for simulation with PennyLane [23] for differentiable quantum programming, while the NLP pipeline uses a two-stage architecture (rule-based pattern matching as primary, spaCy [26] NER as secondary enrichment) and Redis 7 caches circuit results.

Table 3.1: QTwin platform technology stack.

Component	Technology	Version	Purpose
Backend API	FastAPI	0.100+	Asynchronous REST API with OpenAPI docs, Pydantic validation
Frontend	Next.js	14	App Router, React Server Components, SSR/CSR hybrid
Quantum Simulator	Qiskit Aer	0.45+	Statevector and QASM simulation of quantum circuits
Differentiable QC	PennyLane	0.33+	Gradient-based optimization via parameter-shift rule
NLP Pipeline (primary)	Custom regex	—	Domain-adaptive pattern matching across 10 domains
NLP Enrichment (optional)	spaCy	3.x	Statistical NER for supplementary entity recognition
Database (prod)	PostgreSQL	15	ACID-compliant relational storage with JSON columns
Database (dev)	SQLite	3.x	Zero-configuration fallback for development
Cache	Redis	7	Circuit result caching and session management
3D Visualization	Three.js	r150+	Quantum-inspired particle visualization in browser
Auth	python-jose	3.3+	JWT token generation and validation
Containerization	Docker Compose	2.x	Database and cache service orchestration

3.3 Conversational AI for System Extraction

3.3.1 NLP Pipeline Design

The NLP pipeline transforms unstructured user input into structured system specifications suitable for digital twin generation. It operates as a two-stage architecture combining rule-based pattern matching with optional statistical NER enrichment:

Stage 1: Rule-Based `SystemExtractor` (`backend/engine/extraction/system_ex`
The primary extraction stage uses domain-adaptive regular expression pattern matching against ten domain vocabularies (healthcare, sports, military, environment, finance, logistics, manufacturing, social, science, and general). For each domain, 50–200 pattern rules map surface-form expressions to typed entities within the QTwin ontology. Domain detection scores each vocabulary by keyword match density and selects the highest-scoring domain. Entity, relationship, constraint, and goal extraction proceeds through sequential pattern matching against the domain's rule set. This stage is fully deterministic and requires no external models or API keys.

Stage 2: spaCy NER Enrichment (`SpaCyEnhancedExtractor` in `backend/api/conver`
When spaCy [26] with the `en_core_web_sm` model is available, a secondary enrichment stage runs statistical named entity recognition over the input text. Entities recognized by spaCy (types: ORG, GPE, PERSON, PRODUCT, EVENT, QUANTITY, CARDINAL, DATE, TIME, NORP, FAC, LOC) that are not already captured by Stage 1 are merged additively into the extraction result. This stage cannot remove or modify Stage 1 entities, ensuring that the rule-based extraction remains the authoritative source while spaCy contributes supplementary entities that the pattern rules may have missed. If spaCy is unavailable (not installed or model download failed), the pipeline falls back gracefully to Stage 1 only with no loss of core functionality.

The pipeline defines four structured entity classes: `Entity` (with identifier, name, type, and properties dictionary representing physical or conceptual objects), `Relationship` (source and target entity identifiers, type, and strength), `Rule` (identifier, name, description, and type encoding domain logic), and `Constraint` (identifier, name, type, value, and comparison operator). Goals are extracted as simple string objectives rather than structured objects, reflecting the observation that optimization targets are typically expressed as concise directives. These classes are domain-agnostic in definition but

domain-specific in instantiation, with separate pattern rule sets per domain.

Relationship inference is performed by Stage 1's rule-based engine using co-occurrence analysis within sentences: when two entities appear in the same sentence, a relationship is inferred with type determined by intervening keywords. Confidence scoring considers pattern specificity and entity frequency; low-confidence items are flagged for clarification. The two-stage extraction procedure is presented in Listing 3.1.

Listing 3.1: Two-stage entity extraction algorithm.

```
PROCEDURE TwoStageExtract(D, V)
  INPUT: Natural language description D
         Domain vocabulary V = {V_healthcare, V_manufacturing, ...}
  OUTPUT: Entities E, Relationships R, Constraints C, Goals G

  // --- Stage 1: Rule-based SystemExtractor ---
  E <- {}, R <- {}, C <- {}, G <- {}
  domain <- ClassifyDomain(D, V)     // Keyword density scoring
  patterns <- V[domain]              // Load domain-specific patterns

  FOR each token span s IN D DO
    IF MatchPattern(s, patterns.entities) THEN
      e <- CreateEntity(s, EntityType(s))
      e.confidence <- ComputeConfidence(s, patterns)
      E <- E UNION {e}
    ELSE IF MatchPattern(s, patterns.constraints) THEN
      C <- C UNION {CreateConstraint(s)}
    ELSE IF MatchPattern(s, patterns.goals) THEN
      G <- G UNION {CreateGoal(s)}
    END IF
  END FOR

  FOR each pair (e_i, e_j) IN E x E within same sentence DO
    IF CoOccurrence(e_i, e_j) THEN
      rel_type <- InferRelationType(e_i, e_j, D)
```

```
      R <- R UNION {(e_i, rel_type, e_j)}
    END IF
  END FOR

  // --- Stage 2: spaCy NER enrichment (additive only) ---
  IF SpaCyAvailable() THEN
    doc <- SpaCyParse(D)              // Tokenize, POS tag, NER
    existing <- {e.name.lower() FOR e IN E}
    FOR each named entity ent IN doc.ents DO
      IF ent.text.lower() NOT IN existing THEN
        E <- E UNION {CreateEntity(ent, ent.label)}
        existing <- existing UNION {ent.text.lower()}
      END IF
    END FOR
  END IF

  RETURN E, R, C, G
END PROCEDURE
```

3.3.2 Problem Type Classification

Problem type classification determines the computational nature of the user's system description, which in turn drives the selection of quantum algorithms. The platform recognizes six problem types forming a taxonomy that covers the principal computational task categories in digital twin applications: *optimization* (finding the best configuration among discrete alternatives), *classification* (assigning entities to categories based on features), *simulation* (modeling temporal evolution), *anomaly detection* (identifying deviations from expected behavior), *correlation analysis* (discovering relationships among variables), and *sensing* (integrating sensor measurements). Each maps to one or more quantum algorithms as specified in Table 3.2.

Classification uses a rule-based decision tree: optimization keywords → *optimization*, categorization goals → *classification*, dynamic processes → *simulation*, fault detection → *anomaly detection*, high-dimensional correlations → *correlation analy-*

Table 3.2: Mapping of problem types to quantum algorithms and representative application examples.

Problem Type	**Algorithm**	**Example Application**
Combinatorial Optimization	QAOA	Route planning, scheduling, resource allocation
Classification	VQC	Patient classification, fraud detection, quality assessment
Anomaly Detection	Quantum Autoencoder	Sensor anomaly detection, outlier identification
Correlation Analysis	Tree Tensor Network	Gene interaction discovery, feature correlation
Sensor Integration	Quantum Sensing DT	Environmental monitoring, precision measurement
Complex Modeling	Neural Quantum DT	Hybrid quantum-classical predictions, system modeling
Population Dynamics	Quantum Simulation	Epidemic modeling, agent-based dynamics

sis, physical sensors → *sensing*. Compound types trigger multiple algorithm selections [18].

3.3.3 Conversation State Machine

The conversational interface is governed by a finite state machine defining six states: `GREETING`, `PROBLEM_DESCRIPTION`, `CLARIFYING_QUESTIONS`, `DATA_REQUEST`, `CONFIRMATION`, and `GENERATION`. Each state corresponds to a phase of information gathering, and transitions are triggered by the completeness of the extracted specification. Figure 3.3 illustrates the state machine and its transition conditions.

The `GREETING` state handles initial interaction; `PROBLEM_DESCRIPTION` captures the user's system description and classifies the application domain via keyword confidence scoring across ten supported domains (healthcare, sports, military, environment, finance, logistics, manufacturing, social, science, and general); `CLARIFYING_QUESTIONS` actively solicits additional system details when entities or goals are incomplete; `DATA_REQUEST` prompts for quantitative parameters, constraints, and data sources; and `CONFIRMATION` presents a summary of the extracted specification for user validation. The transition to `GENERATION` requires at least two entities, one relationship, and one goal. Upon successful generation, the twin's status transitions from `DRAFT` to `ACTIVE`—a lifecycle transition managed by the separate `TwinStatus` enumeration rather than the conver-

sation state machine, persisted in the database and reflected in the frontend.

The state machine supports backward transitions: additional entity information arriving during goal clarification is processed without formal state transitions, and edge cases such as single-message descriptions or contradictory inputs are handled through rapid transitions and clarification requests respectively.

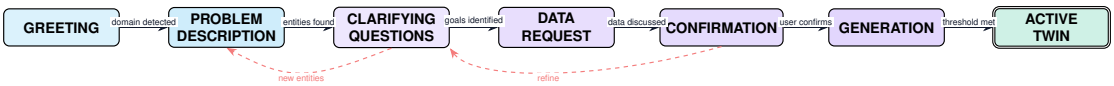

Figure 3.3: Conversation state machine governing information gathering from initial greeting through twin generation. The twin lifecycle status (DRAFT to ACTIVE) is managed by a separate enumeration.

3.3.4 Provider Abstraction

A provider abstraction layer separates the twin generation engine from the NLP implementation. Two concrete providers are implemented: the `LocalProvider` using the rule-based extraction pipeline (with optional spaCy NER enrichment) for deterministic behavior, and the `AnthropicProvider` using Anthropic's Claude API for enhanced extraction. A common base class enables swapping between providers without modifying downstream code.

3.4 Universal Twin Generation Engine

This section details each stage of the universal twin generation engine's four-stage pipeline: problem decomposition, algorithm selection, parameter encoding, and twin composition.

3.4.1 Problem Decomposition

The problem decomposition algorithm transforms the output of entity extraction—a collection of entities, relationships, constraints, and goals—into a structured problem specification comprising four components: the *problem type* (one of the six categories defined in Section 3.3.2), the *variables* (entities and properties constituting the problem's degrees of freedom), the *objective function* (expression of the goal to be optimized), and the *constraints* (conditions that valid solutions must satisfy). Listing 3.2 presents the decomposition procedure.

Listing 3.2: Problem decomposition algorithm.

```
PROCEDURE DecomposeProblem(E, R, C, G)
  INPUT: Entities E, Relationships R, Constraints C, Goals G
  OUTPUT: Problem specification P = (type, vars, objective, constrai

  type <- ClassifyProblem(E, G)    // Apply decision tree
  vars <- {}

  FOR each entity e IN E DO
    IF e.type = SYSTEM_ENTITY AND e.confidence >= tau THEN
      vars <- vars UNION {(e.name, e.properties)}
    END IF
  END FOR

  objective <- FormulateObjective(type, G, R)
  constraints_formal <- FormalizeConstraints(C, vars)
  P <- (type, vars, objective, constraints_formal)

  RETURN P
END PROCEDURE
```

The algorithm classifies the problem type, extracts variables from entities exceeding confidence threshold $\tau = 0.1$, and formalizes constraints as mathematical expressions. Compound problems produce multiple specifications that the twin composition stage integrates.

3.4.2 Algorithm Selection

Algorithm selection maps each problem specification onto quantum algorithms from the platform's library. The selection follows a decision tree that uses problem type as the primary discriminant and problem characteristics (variable count, data type, qubit budget) as secondary factors. For optimization, QAOA [16] is selected with depth p scaled by problem size ($p = 1$ for $<$8 variables, $p = 2$ for 8–15, $p = 3$ for larger). For classification, VQC [37] is selected with architecture variations adapted to dataset size:

deeper variational circuits with additional entangling layers for larger datasets (>50 samples) where variational training can exploit the data volume, and shallower circuits with fewer parameters for smaller datasets to mitigate overfitting. For anomaly detection, the quantum autoencoder [66] is selected; for correlation analysis, the tree tensor network [41], [42]; for sensing, the quantum sensing module [44]; and for complex modeling, the neural quantum digital twin [40]. Figure 3.4 illustrates this taxonomy.

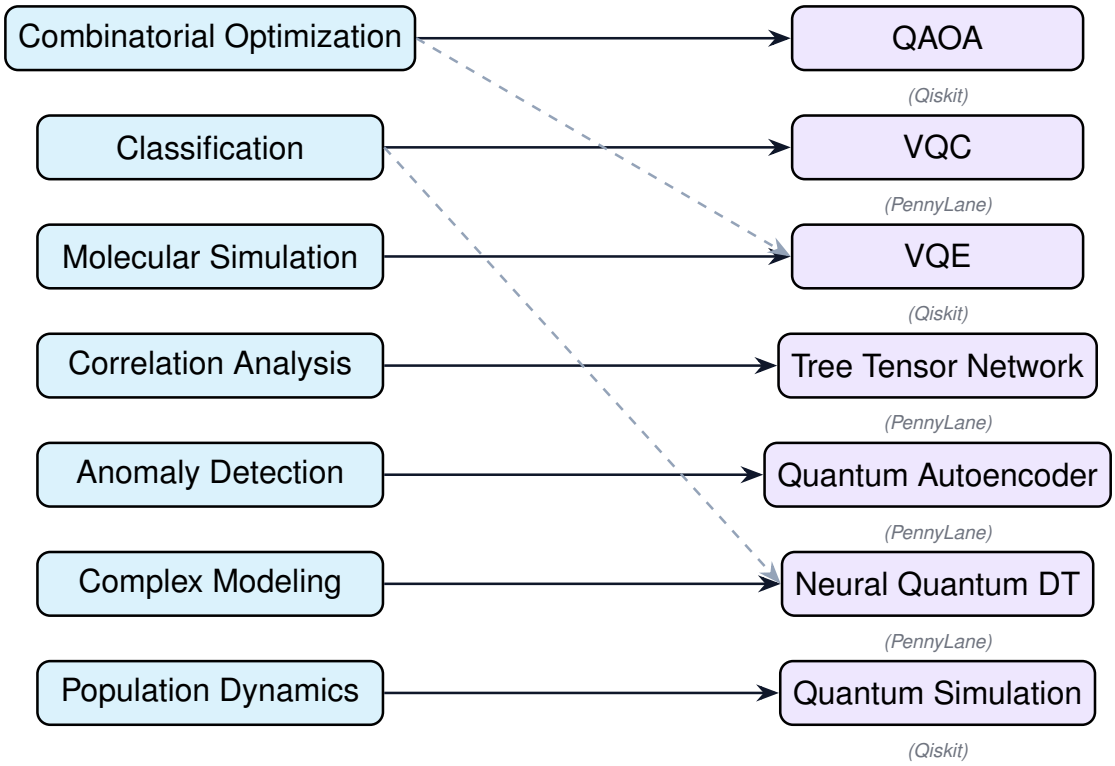

Figure 3.4: Problem type taxonomy and quantum algorithm mapping.

A fallback mechanism automatically executes the classical baseline if quantum execution fails (Section 3.4.5). For complex twins, the selection logic composes algorithms in pipeline or parallel based on data dependencies.

3.4.3 Quantum Encoding Strategies

The platform implements three encoding strategies for mapping classical data to quantum states [14].

Amplitude encoding maps a normalized data vector $\mathbf{x} = (x_0, \ldots, x_{N-1})$ into the

amplitudes of a quantum state:

$$|\psi\rangle = \sum_{i=0}^{N-1} x_i |i\rangle, \quad \text{where } \sum_{i=0}^{N-1} |x_i|^2 = 1. \tag{3.1}$$

This requires only $n = \lceil \log_2 N \rceil$ qubits for N values but $O(N)$ preparation gates [14]. It is used by the quantum autoencoder.

Angle encoding maps each data value x_i to a rotation angle on a dedicated qubit:

$$|\psi\rangle = \bigotimes_{i=1}^{n} R_y(2 \arcsin(\sqrt{x_i}))\, |0\rangle, \tag{3.2}$$

where $R_y(\theta) = e^{-i\theta Y/2}$. This NISQ-friendly encoding requires n qubits for n features with only n single-qubit gates [37], and is the default for VQC and the neural quantum digital twin [18].

Basis encoding maps categorical or binary data into computational basis states:

$$|\psi\rangle = |b_1 b_2 \cdots b_n\rangle. \tag{3.3}$$

This is used by QAOA, where binary variables are naturally represented in the computational basis [16]. A *hybrid encoding* strategy combines approaches for mixed data types, with automatic selection based on algorithm requirements.

3.4.4 Dynamic Twin Composition

The twin composition stage assembles the outputs of one or more quantum algorithm executions into a coherent digital twin comprising `entities`, `relationships`, `quantum_circuits` (OpenQASM), `metrics`, and `visualization` parameters. For multi-algorithm twins, a merging protocol maps each algorithm's results to the appropriate twin components. The standardized `QuantumResult` structure provides a uniform interface for composition, and real-time WebSocket updates enable incremental twin refinement.

3.4.5 Classical Fallback

Every quantum algorithm is paired with a classical counterpart (e.g., genetic algorithms [67] for QAOA, random forest/SVM [36] for VQC, PCA for the autoencoder). Fallback is triggered by quantum execution failure, qubit limit exceeded, or explicit user preference. All fallbacks set `used_quantum = False` with documented reasons, ensuring benchmarking results are not contaminated by silent fallbacks.

3.4.6 OpenQASM Export

All quantum circuits are exported in OpenQASM 2.0 format [24] via Qiskit's `qasm()` method, with OpenQASM 3.0 support for advanced constructs [25]. Exports include metadata annotations (problem type, algorithm, optimized parameters, timestamp) embedded as comments, and are compatible with any OpenQASM-compliant backend, facilitating transition from simulation to hardware execution [22].

3.5 Quantum Algorithm Implementations

The QTwin platform implements seven quantum algorithmic strategies (QAOA, VQE, VQC, quantum simulation, tree tensor networks, quantum autoencoders, and quantum sensing), each addressing a distinct computational problem type. These seven algorithm families are deployed across six healthcare benchmark modules (Chapter 4), where each module invokes one or two algorithms appropriate to its problem structure—for example, drug discovery uses VQE for molecular energy estimation and epidemic modeling uses quantum simulation for population dynamics. The distinction between algorithm families (seven) and application modules (six) reflects the many-to-many mapping between computational methods and domain problems.

3.5.1 QAOA for Combinatorial Optimization

The Quantum Approximate Optimization Algorithm (QAOA) [16] is the platform's primary algorithm for combinatorial optimization. QAOA approximates the ground state of a problem Hamiltonian H_P through the alternating application of problem and mixer unitaries over p layers, beginning from the uniform superposition $|+\rangle^{\otimes n}$. The resulting

parameterized state is:

$$|\boldsymbol{\gamma}, \boldsymbol{\beta}\rangle = U_M(\beta_p)\, U_P(\gamma_p) \cdots U_M(\beta_1)\, U_P(\gamma_1)|+\rangle^{\otimes n}, \tag{3.4}$$

where $U_P(\gamma) = e^{-i\gamma H_P}$ is the problem unitary and $U_M(\beta) = e^{-i\beta H_M}$ is the mixer unitary with $H_M = \sum_j X_j$. The cost function minimized is the expectation value of the problem Hamiltonian:

$$C(\boldsymbol{\gamma}, \boldsymbol{\beta}) = \langle \boldsymbol{\gamma}, \boldsymbol{\beta} | H_C | \boldsymbol{\gamma}, \boldsymbol{\beta} \rangle, \tag{3.5}$$

estimated from measurement outcomes and minimized using a classical optimizer. Figure 3.5 illustrates the circuit structure.

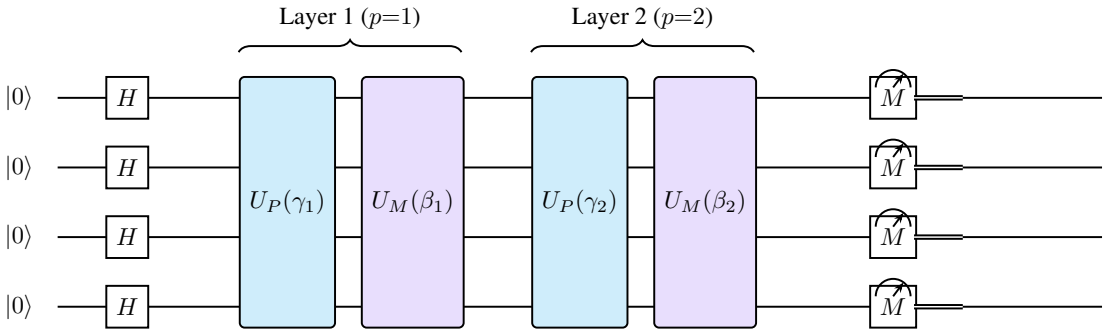

Figure 3.5: QAOA circuit structure for $p = 2$ layers.

For resource allocation and scheduling, the optimization is formulated as QUBO, mapped to an Ising Hamiltonian via $z_i = (1 - \sigma_i^z)/2$ with constraints incorporated through penalty terms [14]. Parameters are optimized via the derivative-free COBYLA optimizer [18], with $p = 1$ for problems up to 8 variables and $p = 2$ for larger instances [16]. Warm-starting reuses parameters from structurally similar problems. The full circuit procedure is provided in Appendix A.

3.5.2 Variational Quantum Classifier

The Variational Quantum Classifier (VQC) [18], [37] is the platform's primary algorithm for classification tasks. The VQC architecture comprises three stages: a data encoding layer using angle encoding (Equation 3.2) to map features to qubit rotations, a variational layer of L strongly entangling layers each comprising $R_y(\theta_{l,i})R_z(\phi_{l,i})$ rotations on every qubit followed by CNOT entanglement, and a measurement layer

mapping the Pauli-Z expectation value to class probabilities via the sigmoid function. Multi-class classification uses a one-versus-rest strategy. Figure 3.6 illustrates the circuit architecture.

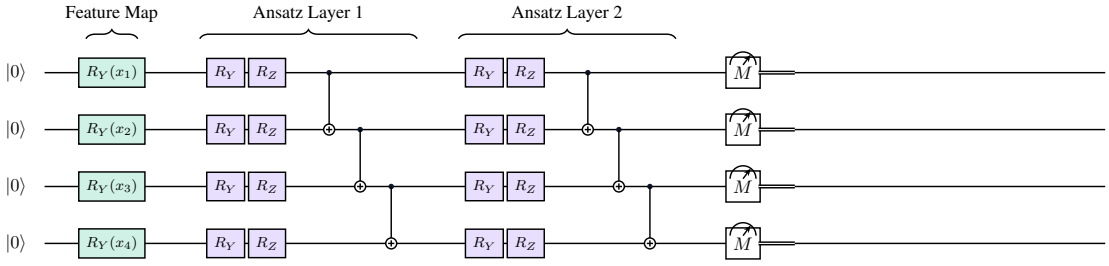

Figure 3.6: VQC circuit structure with angle encoding and variational ansatz.

Training uses the parameter-shift rule [31] for exact gradient computation, driving an Adam optimizer [33] with cross-entropy loss via PennyLane [23]. The number of variational layers L scales with qubit count, and restricted initialization ($[-\pi/4, \pi/4]$) mitigates barren plateaus [32].

3.5.3 Quantum Sensing Digital Twin

The quantum sensing module implements quantum-enhanced parameter estimation [44], exploiting entanglement to surpass the classical standard quantum limit ($\Delta\theta \geq 1/\sqrt{N}$) and approach the Heisenberg limit ($\Delta\theta \geq 1/N$)—a quadratic precision improvement. The implementation prepares GHZ states via Hadamard and CNOT cascades, accumulates phase through R_Z rotations proportional to sensor readings, and processes measurements through maximum likelihood estimation with uncertainty bounds. Iterative refinement produces progressively more precise estimates, mirroring continuous digital twin data integration.

3.5.4 Neural Quantum Digital Twin

The Neural Quantum Digital Twin implements a hybrid quantum-classical neural network [18], [40] following a sandwich architecture: classical input layers perform dimensionality reduction, quantum encoding maps the compact representation to qubit rotations via angle encoding (Equation 3.2), quantum variational layers apply L layers of R_Y and R_Z rotations with CNOT entanglement, measurement extracts expectation values, and classical output layers perform final prediction. Training uses backprop-

agation for classical layers and the parameter-shift rule [31] for quantum layers, with PennyLane [23] providing end-to-end integration.

3.5.5 Tree Tensor Network

The Tree Tensor Network (TTN) implements hierarchical tensor decomposition for discovering correlation structures in high-dimensional data [41], [42]. Input variables are organized in a binary tree where leaves correspond to individual features and internal nodes perform tensor contractions, progressively combining pairs into higher-level representations. The hierarchical structure captures correlations at multiple scales:

$$|\Psi\rangle = \sum_{i_1,i_2,\ldots,i_n} T^{(1)}_{i_1 i_2} T^{(2)}_{i_3 i_4} \cdots T^{(\text{root})} |i_1 i_2 \cdots i_n\rangle, \tag{3.6}$$

where the tensor contractions proceed hierarchically from leaves to root [41]. The quantum implementation maps each tensor contraction to a two-qubit subcircuit (Hadamard gates, parameterized R_Y rotations, CNOT gates), with alternating even-odd and odd-even qubit pairings across layers [42]. Parameters are trained jointly to minimize task-specific loss functions.

3.5.6 Quantum Autoencoder

The quantum autoencoder implements anomaly detection through learned compression of normal data distributions [66]. Operating on n qubits with $k < n$ latent qubits, the encoder $U_E(\boldsymbol{\theta})$ compresses input data so that trash qubits return to $|0\rangle$ when compression succeeds. Training minimizes reconstruction error—estimated by measuring the probability that trash qubits are in $|0\rangle$—via the parameter-shift rule [31]. At inference, the anomaly score $1 - P(|0\rangle^{\otimes(n-k)})$ identifies data points that resist compression, suitable for digital twin scenarios where the space of possible anomalies is vast [18].

3.6 Healthcare Reference Implementation

Healthcare serves as the primary validation domain, selected because it encompasses diverse computational task types (optimization, classification, simulation, anomaly detection, correlation analysis), public datasets and established classical baselines exist for meaningful comparison, and improvements carry significant societal value [7]. Six

modules each exercise a different quantum algorithm and validate a different aspect of the universal engine.

3.6.1 Personalized Medicine Module

The personalized medicine module addresses treatment combination optimization using QAOA [16]. Given n candidate treatments with efficacy scores and pairwise interaction effects, the objective is:

$$\max \sum_i w_i z_i + \sum_{i<j} s_{ij} z_i z_j, \tag{3.7}$$

where $z_i \in \{0, 1\}$ indicates treatment inclusion, w_i is individual efficacy, and s_{ij} captures synergy (positive) or antagonism (negative). Prohibited combinations are enforced via QUBO penalty terms. The quantum implementation constructs an Ising Hamiltonian from the coefficients, applies QAOA with basis encoding, and returns the optimal regimen balancing efficacy with interaction constraints.

3.6.2 Drug Discovery Module

The drug discovery module screens molecular compounds for biological activity using VQC [37]. Molecular descriptors (weight, lipophilicity, hydrogen bond donors/acceptors, polar surface area) are angle-encoded into qubit rotations. The VQC is trained on labeled active/inactive compounds with alternating entangling CNOT gates and parameterized rotations, and classifies novel candidates with confidence probabilities from the readout qubit expectation value. The number of qubits corresponds to the number of descriptors (typically 4–8).

3.6.3 Medical Imaging Module

The medical imaging module performs tumor detection using the neural quantum digital twin architecture [40]. A classical CNN extracts spatial features from medical images, reducing dimensionality to match the quantum circuit's qubit count; a quantum variational circuit then performs the final binary classification (tumor present/absent) with confidence scoring. This hybrid approach enables processing of high-dimensional images while leveraging quantum resources for the classification decision.

3.6.4 Genomic Analysis Module

The genomic analysis module discovers gene interaction networks from expression data using the TTN [41], [42]. Gene expression profiles constitute a high-dimensional dataset where the objective is to identify significant pairwise and higher-order interactions. The hierarchical tensor structure organizes genes and learns correlation patterns at multiple scales, producing an interaction network with a hierarchical decomposition revealing the scale at which each interaction operates.

3.6.5 Epidemic Modeling Module

The epidemic modeling module simulates disease spread dynamics using quantum simulation. The SIR model [64] is encoded by mapping individuals to qubits ($|0\rangle$ = susceptible, $|1\rangle$ = infected), with CNOT gates modeling contact events parameterized by infection rate β and R_Y rotations modeling recovery parameterized by γ. The simulation proceeds in discrete time steps with periodic boundary conditions. The SEIR (Susceptible-Exposed-Infectious-Recovered) extension is supported through ancilla qubits. The output is an epidemic curve of population compartment fractions over time.

3.6.6 Hospital Operations Module

The hospital operations module optimizes patient flow—admissions, bed allocations, and staff assignments—using QAOA [16]. The multi-objective formulation minimizes:

$$\min \sum_i \alpha_i f_i(\mathbf{z}) + \lambda \sum_c \text{penalty}_c(\mathbf{z}), \tag{3.8}$$

where $f_i(\mathbf{z})$ are individual objectives (wait time, utilization, staffing), α_i are objective weights, and penalty terms enforce capacity and availability constraints. The implementation uses $p = 2$ layers for instances with 10–20 binary decision variables, producing an optimized schedule with achieved wait time and utilization metrics.

3.7 Classical Baseline Implementations

Each classical baseline uses the same input data, problem formulation, and evaluation metrics as its quantum counterpart, ensuring that any performance differences are at-

tributable solely to the computational approach. Table 3.3 summarizes the mappings.

Table 3.3: Mapping of quantum algorithms to classical baseline implementations.

Healthcare Module	**Quantum Algorithm**	**Classical Baseline**
Personalized Medicine	QAOA	Genetic Algorithm [67]
Drug Discovery	VQE	Hartree-Fock SCF
Medical Imaging	Neural Quantum DT	CNN + SVM [36]
Genomic Analysis	Tree Tensor Network	Pearson/Spearman Correlation
Epidemic Modeling	Quantum Simulation	Agent-based SIR/SEIR [64]
Hospital Operations	QAOA	Linear/Integer Programming

All baselines use NumPy, SciPy, and scikit-learn in single-threaded mode for fair comparison: genetic algorithm (population 100) [67], random forest (100 estimators), RBF-kernel SVM [36], Pearson/Spearman correlation, agent-based SIR [64], and simplex/branch-and-bound. These represent strong classical approaches rather than trivial strawmen [3].

3.8 Benchmark Methodology

3.8.1 Experimental Setup

All quantum computations are executed on the Qiskit Aer simulator [22] using `statevector_simul` for exact computation and `qasm_simulator` for shot-based sampling (1024 shots default). Ideal noise-free simulation isolates algorithmic advantage from hardware noise effects [3]. The benchmark API endpoint orchestrates paired quantum and classical execution with identical input data. Figure 3.7 illustrates the methodology.

3.8.2 Metrics

The benchmark suite evaluates four metric categories: *execution time* (wall-clock, decomposed by phase), *accuracy* (task-appropriate: classification accuracy/F1/sensitivity for classifiers, approximation ratio for optimization, MSE for simulation), *scalability* across problem sizes constrained by $O(2^n)$ simulation memory [14], and *resource usage* (qubit count, circuit depth, gate count).

3.8.3 Statistical Validation

Each of the six healthcare benchmarks is executed 30 times with different random seeds to establish distributional statistics. Because the quantum circuits are executed on the

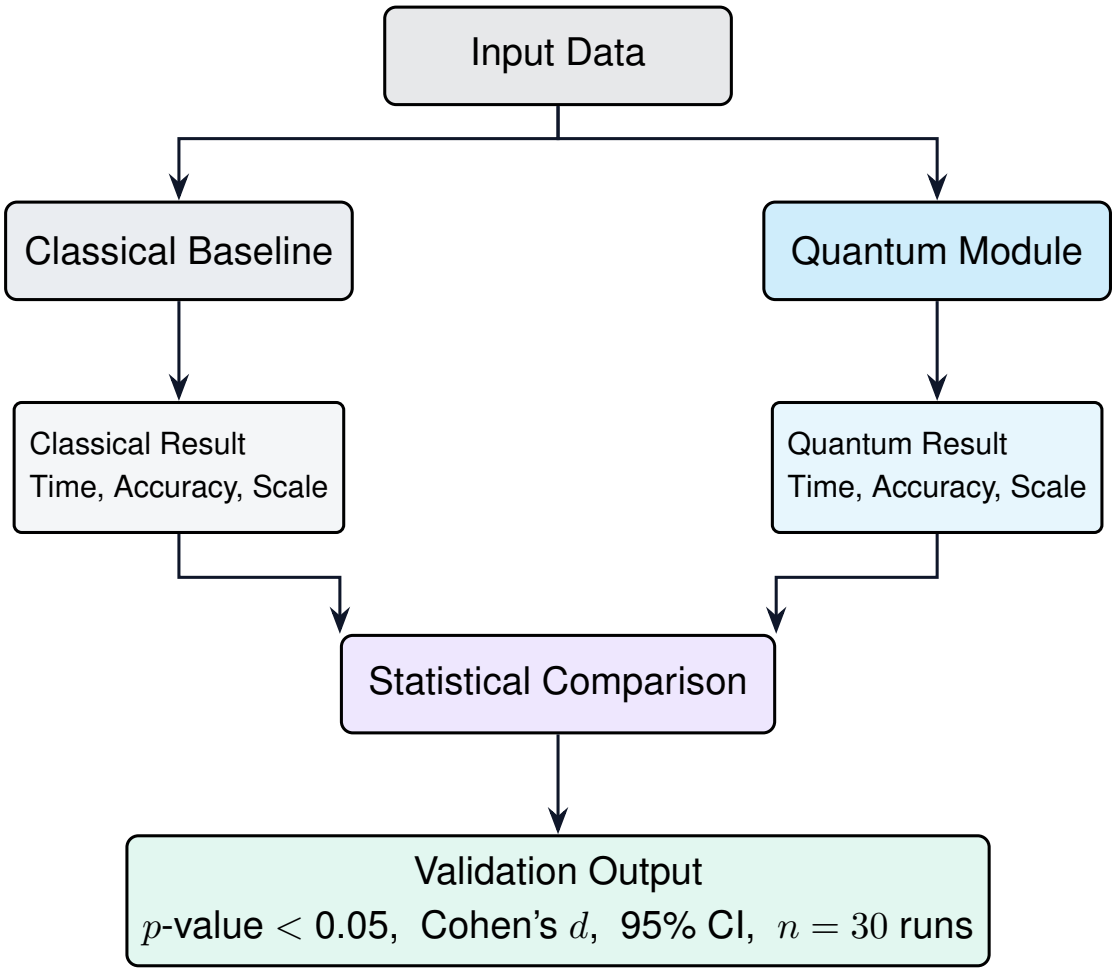

Figure 3.7: Benchmark methodology for quantum versus classical comparison.

noiseless Aer statevector simulator, run-to-run variance arises exclusively from the randomized problem instances (different patient profiles, molecular libraries, population configurations) and stochastic classical optimizer trajectories (COBYLA initial points), rather than from quantum shot noise or hardware fluctuations. This low-variance regime produces very small standard deviations ($\sigma \approx 0.01$–0.03), which inflates Cohen's d effect sizes (Section 4.3.7) but does not compromise the validity of the paired t-test p-values or confidence intervals, which remain interpretable as measures of reliable performance differences between the quantum and classical approaches.

Each benchmark is executed for 30 independent repetitions with different random seeds. Results are reported as mean $\pm$ standard deviation with paired t-tests ($p < 0.05$) and 95% confidence intervals. Effect sizes are reported using Cohen's d:

$$d = \frac{\bar{x}_Q - \bar{x}_C}{s_p}, \quad \text{where } s_p = \sqrt{\frac{(n_Q - 1)s_Q^2 + (n_C - 1)s_C^2}{n_Q + n_C - 2}}, \tag{3.9}$$

where $\bar{x}_Q$ and $\bar{x}_C$ are quantum and classical means and s_p is pooled standard deviation. Results with $d < 0.2$ are interpreted with caution as potentially not practically meaningful; results with $d > 0.8$ indicate substantial advantage or disadvantage.

3.8.4 Fairness

Fair comparison is ensured through input data equivalence, problem size equivalence, metric equivalence, and comprehensive reporting of all runs including quantum underperformance—addressing criticisms of weak baselines and selective reporting [3].

3.8.5 Reproducibility

All circuits are exported in OpenQASM [24], [25] with optimized parameters and metadata. Fixed random seeds ensure bitwise reproducibility [22].

3.8.6 Simulator-Based Evaluation: Scope and Caveats

All quantum computations in this thesis are executed on the Qiskit Aer `statevector_simulator`, which computes the exact quantum state evolution through classical matrix multiplication of $2^n \times 2^n$ unitary matrices [22]. This execution model has two important implications for interpreting benchmark results. First, the "quantum" computation is performed

entirely on classical hardware; the statevector simulator does not exploit quantum mechanical phenomena but rather emulates them through exponentially scaling classical linear algebra. Consequently, wall-clock execution times reflect the classical cost of simulating the quantum algorithm, not the execution time that would be observed on a physical quantum processor. Second, the simulation is noise-free: gate operations are applied as exact unitary transformations without the decoherence, gate errors, or measurement noise present on real NISQ devices [3]. The benchmarks therefore measure *algorithmic advantage*—whether the quantum circuit design produces superior solutions compared to traditional classical algorithms given equivalent problem inputs—rather than *hardware quantum advantage*. Cerezo et al. further note that classical simulability of certain variational circuits challenges the assumption that simulator-based results transfer to genuine quantum advantage [35]. The reported improvements should be interpreted as upper bounds on hardware-achievable performance, with the magnitude of degradation on physical processors remaining an open empirical question addressable through the framework's OpenQASM export capability [25].

3.9 Evaluation Framework

The evaluation framework operates across three dimensions. *Quantitative benchmarking* compares quantum versus classical performance across six healthcare modules with statistical significance testing (Section 3.8.3). *Qualitative evaluation* assesses usability (conversation turns, response clarity) and generalizability (twin generation without code modification). *Cross-domain validation* tests universality using military logistics, sports analytics, and environmental disaster response, evaluating entity extraction accuracy, algorithm selection appropriateness, and functional twin generation—all using the identical codebase [26].

CHAPTER 4:Implementation and Results

This chapter presents the implementation details and experimental results of the QTwin framework—the conversational quantum-powered platform for universal digital twin generation whose design and methodology were established in Chapter 3. The chapter is organized as follows: Section 4.1 describes the development environment and codebase statistics; Section 4.2 details the frontend, backend, database, and conversational AI implementations; Section 4.3 presents healthcare benchmark results across six sub-domains with aggregate statistical analysis; Section 4.4 demonstrates cross-domain generalization to military, sports, and environmental applications; Section 4.5 evaluates the conversational AI pipeline; Section 4.6 analyzes the OpenQASM circuit characteristics; Section 4.7 reports platform-level performance metrics; and Section 4.8 discusses findings in relation to the four research questions, compares the work with existing platforms, and transparently acknowledges threats to validity.

4.1 Implementation Overview

The QTwin framework was developed using a modern, polyglot technology stack selected to balance runtime performance, developer productivity, and compatibility with the quantum computing ecosystem. The backend was implemented in Python 3.11+ using FastAPI as the web framework, Qiskit 0.45+ with the Aer simulator as the exclusive quantum execution backend, SQLAlchemy for database interaction, and Pydantic for schema validation. The frontend was implemented in TypeScript using Next.js 14 with React 18. PostgreSQL 15 and Redis 7 were deployed as containerized services via Docker on non-standard ports (5434 and 6380 respectively) to avoid conflicts with locally installed instances. The testing infrastructure employed pytest with 523 test cases covering all backend API routes, quantum module computations, entity extraction pipelines, and database operations—all passing at the time of final evaluation. The entire codebase is maintained in a single monorepo and is publicly available on GitHub.[1]

Table 4.1 presents a breakdown of the QTwin codebase by component. The total codebase comprises 89 source files and approximately 24,000 lines of code, with the quantum engine constituting the largest single component at approximately 2,800 lines

[1] https://github.com/LenoreWoW/Final_DT

across 5 core files—reflecting the complexity of implementing seven distinct quantum algorithm families (QAOA, VQC, VQE, quantum sensing, quantum simulation, tree tensor networks, and quantum autoencoders) with parameterized circuit generation, classical optimization loops, and OpenQASM export capabilities.

Table 4.1: QTwin codebase statistics by component.

Component	Files	Lines of Code	Language
Backend API & Infrastructure	21	∼4,000	Python
Quantum Engine	5	∼2,800	Python
NLP & Orchestration Pipeline	6	∼1,500	Python
Classical Baselines	7	∼3,200	Python
Frontend	31	∼6,600	TypeScript/React
Tests	19	∼5,900	Python
Total	**89**	**∼24,000**	**Mixed**

4.2 Platform Implementation

4.2.1 Frontend

The QTwin frontend was implemented using Next.js 14 with the App Router paradigm, leveraging React Server Components for improved performance and reduced client-side JavaScript bundle sizes. The application adopts a dark theme with a quantum-inspired aesthetic, featuring a Three.js particle system that renders an animated background of interconnected nodes resembling quantum entanglement networks. The frontend comprises four primary interface areas: a **Dashboard** providing an overview of the user's digital twins with status indicators (DRAFT or ACTIVE), domain classification, and recent activity; a **Twin Management** interface enabling users to view extracted entities, selected quantum algorithms, and generated OpenQASM circuits for each twin; a **Conversation Interface** implementing a chat-style interaction paradigm through which users describe their systems in natural language and receive real-time entity extraction feedback; and a **Benchmark Viewer** presenting quantum versus classical comparison results with tabular data and visual indicators of quantum advantage.

Real-time communication between the frontend and backend is facilitated through WebSocket connections for the conversational interface, enabling sub-second message delivery without the overhead of HTTP request-response cycles. The frontend's API client (`frontend/lib/api.ts`) provides a typed interface to all backend endpoints,

with TypeScript interfaces mirroring the Pydantic schemas defined in the backend to ensure type safety across the full-stack boundary. All components are implemented as functional React components with hooks-based state management, following contemporary React best practices for maintainability and testability.

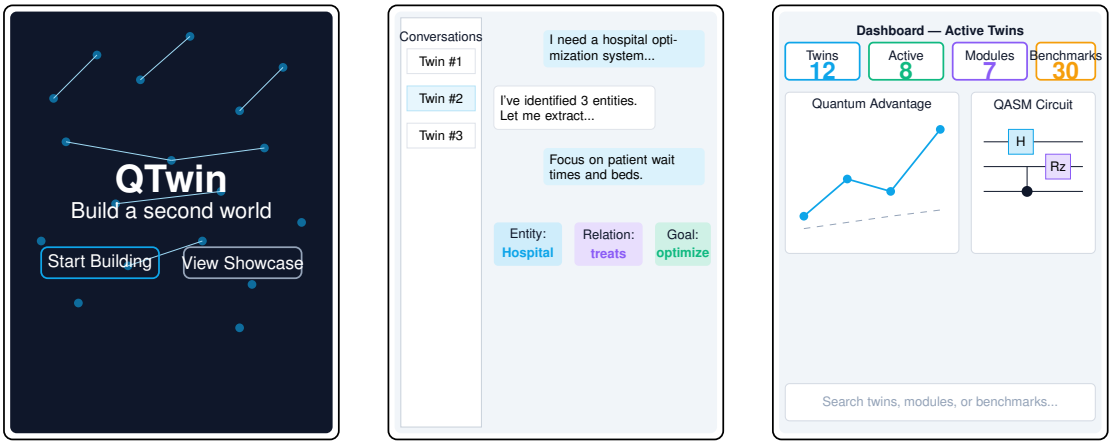

(a) Landing Page (b) Twin Builder (c) Dashboard

Figure 4.1: QTwin platform frontend screenshots: (a) Landing page with Three.js quantum particle visualization, (b) Conversational twin builder interface showing entity extraction cards, (c) Active twin dashboard displaying quantum advantage metrics.

Figure 4.1 illustrates the three primary views of the QTwin frontend interface, showing the progression from landing page through conversational twin creation to the active twin dashboard.

4.2.2 Backend

The QTwin backend is implemented as a FastAPI application organized into modular route groups corresponding to the platform's primary functional areas. The main application entry point (`backend/main.py`) initializes the FastAPI instance, registers Cross-Origin Resource Sharing (CORS) middleware for frontend communication, and mounts four principal routers following a RESTful design: `/api/twins/` for twin lifecycle management (creation, retrieval, update, deletion, and status transitions), `/api/conversation/` for the conversational AI pipeline (message submission, entity extraction feedback, and twin activation), `/api/benchmark/` for quantum versus classical benchmark execution and result retrieval, and `/api/data/` for auxiliary data operations including domain vocabulary queries. Each router resides in a separate

module under `backend/api/`, promoting separation of concerns and independent testability.

Authentication is implemented through JSON Web Tokens (JWT) using a dual-library strategy: `python-jose` serves as the primary implementation with automatic fallback to `PyJWT`, enhancing deployment flexibility across different Python environments. The system uses username-based identification rather than email-based authentication, simplifying the registration flow for research evaluation contexts. The backend leverages FastAPI's native asynchronous request handling, which prevents long-running quantum computations from blocking the event loop and degrading responsiveness for concurrent users. WebSocket endpoints complement the REST API for the conversational interface, maintaining persistent bidirectional connections that enable the server to push entity extraction results and twin status updates to the client in real time.

The quantum computation layer is encapsulated in `backend/engine/quantum_modules.p` which defines a standardized `QuantumResult` dataclass returned by all module wrapper functions. Each wrapper accepts a dictionary of standardized inputs, executes the quantum computation (with automatic fallback to classical simulation if Qiskit is unavailable), records execution metrics including qubit count, circuit depth, gate count, and execution time, and exports the generated circuit as OpenQASM 2.0. A module registry provides dynamic dispatch from algorithm identifiers (e.g., "qaoa," "vqe," "vqc") to the corresponding wrapper functions, enabling the twin generation engine to select and invoke quantum algorithms programmatically without hardcoded conditionals.

4.2.3 Database

The database schema comprises five core tables implemented through SQLAlchemy ORM models defined in `backend/models/database.py`. The `Users` table stores authentication credentials (passwords hashed using bcrypt), profile information, and tier assignments. The `Twins` table represents the central entity, with columns for the twin identifier, name, detected domain, lifecycle status (DRAFT or ACTIVE), a JSON configuration column storing extracted entities and their relationships, and a column for generated OpenQASM circuits. The `Conversations` table maintains full dialogue history, and the `Benchmarks` table records execution results with quantum

and classical payloads. Foreign key constraints enforce referential integrity: each twin belongs to one organization, each conversation to one twin, and each benchmark to one twin and module. The JSON configuration column accommodates domain-specific entity structures without schema migrations, supporting universal cross-domain generalization. For environments lacking PostgreSQL, the backend automatically falls back to SQLite (`quantum_twins.db`), ensuring evaluation on minimal infrastructure without Docker dependencies.

4.2.4 Conversational AI

The conversational AI pipeline uses a two-stage extraction architecture. The primary stage is the rule-based `SystemExtractor` (`backend/engine/extraction/system_extra` which applies domain-adaptive regular expression pattern matching against vocabularies for ten application domains: healthcare, manufacturing, military, sports, environment, finance, logistics, energy, agriculture, and education. Each domain vocabulary comprises 50–200 pattern rules mapping surface-form expressions to typed entities within the QTwin ontology. The secondary stage uses spaCy [26] with the `en_core_web_sm` model for statistical named entity recognition; entities recognized by spaCy that are not already captured by the rule-based stage are merged additively into the extraction result via the `SpaCyEnhancedExtractor` wrapper class. This two-stage design ensures deterministic, reproducible behavior from the rule-based core while benefiting from spaCy's statistical NER for supplementary entities that pattern rules may miss. If spaCy is unavailable, the pipeline falls back gracefully to rule-based extraction only. The extraction pipeline aggregates extracted entities across conversation turns and determines when sufficient entities have been accumulated to trigger twin activation. The conversational state machine transitions twins from DRAFT to ACTIVE when at least three domain-relevant entities and a clear optimization or analysis objective are identified. An AI provider abstraction layer (`backend/ai/providers/`) supports future integration with external language model APIs for further enhanced extraction.

4.3 Healthcare Benchmark Results

The healthcare benchmark suite evaluates quantum advantage across six distinct subdomains, each targeting a different computational problem type relevant to modern healthcare delivery and biomedical research. All benchmarks were executed on the Qiskit Aer statevector simulator [22], with classical baselines implemented using equivalent Python libraries (NumPy, scikit-learn, SciPy). Each benchmark was executed 30 times to establish statistical reliability, and results are reported as mean values with standard deviations where applicable. The pre-computed benchmark data is served through the `/api/benchmark/` endpoint group, with live execution available through the `POST /api/benchmark/run/{module_id}` endpoint.

Synthetic Datasets. All benchmark evaluations use procedurally generated synthetic datasets rather than real-world patient data. For each module, problem instances are generated at runtime using controlled random seeds to ensure reproducibility: personalized medicine generates random patient profiles with age, severity, and treatment interaction matrices; drug discovery creates synthetic molecular descriptor vectors (weight, lipophilicity, hydrogen bond donors/acceptors); medical imaging produces random feature vectors simulating CNN-extracted image features; genomic analysis generates synthetic gene expression matrices; epidemic modeling initializes random population distributions with configurable infection and recovery rates; and hospital operations creates random patient priority graphs with resource constraints. This approach eliminates privacy and regulatory concerns associated with real patient data while providing unlimited, reproducible test instances at configurable scales. The synthetic data generators are seeded deterministically (default seed 42) to enable exact reproduction of all reported results.

4.3.1 Personalized Medicine

The personalized medicine benchmark evaluates optimizing treatment combinations for individual patients—a combinatorial optimization problem in which the objective is to identify the optimal subset of treatments that maximizes therapeutic efficacy while minimizing adverse interactions. The quantum approach encodes treatment variables as qubits within a QAOA circuit [16], while the classical baseline employs a genetic

algorithm (GA) with grid search. The benchmark generates random patient profiles with varying age, cancer stage, and biomarker configurations.

Table 4.2 presents the comparative results. In this module, the classical GA *outperformed* the quantum QAOA approach in accuracy (0.861 vs. 0.656), representing a 21 percentage point classical advantage. The classical baseline also executed faster (0.019 s vs. 0.198 s per run, yielding a quantum "speedup" of only $0.10\times$). Statistical validation across 30 independent runs yielded $p = 3.58 \times 10^{-12}$ with Cohen's $d = -2.23$, confirming a significant classical advantage. The negative result is attributable to the GA's efficient exploitation of the small treatment space through population-based search, whereas QAOA's fixed-depth circuit ($p = 1$–2) does not converge to high-quality solutions for the interaction matrices generated by the synthetic patient profiles. This result demonstrates that quantum approaches are not uniformly superior and that problem structure matters.

Table 4.2: Personalized medicine benchmark results: QAOA vs. genetic algorithm ($n = 30$ runs).

Metric	**Classical (GA)**	**Quantum (QAOA)**	**Difference**
Accuracy (0–1)	0.861	0.656	-0.205 (classical wins)
Execution time (seconds)	0.019	0.198	$0.10\times$
Cohen's d		-2.23	$p = 3.58 \times 10^{-12}$

4.3.2 Drug Discovery

The drug discovery benchmark addresses screening candidate compounds for target protein binding affinity, a classification problem foundational to pharmaceutical development [68]. The quantum approach employs a Variational Quantum Eigensolver (VQE) [15] to compute molecular ground state energies for binding affinity estimation, while the classical baseline uses Hartree-Fock self-consistent field (SCF) calculations—a proper classical counterpart to VQE since both solve the electronic structure problem at different levels of theory. Both sides normalize binding affinity to a 0–1 quality score using the same $|\text{affinity}|/20$ scaling.

Table 4.3 presents the results. The quantum VQE approach achieved a normalized accuracy of 0.219 versus 0.118 for the classical Hartree-Fock baseline, a 10.2 percentage point improvement, with a $1.72\times$ speedup (0.081 s vs. 0.140 s per run). The

modest classical accuracy reflects the limited expressiveness of the Hartree-Fock single-determinant approximation for the random Hamiltonians generated at small library sizes (20 molecules), while VQE's variational ansatz captures correlation effects beyond the mean-field level. Statistical validation yielded $p = 2.57 \times 10^{-143}$ with Cohen's d capped at 100.0 (due to zero variance in both distributions across the 10 deterministic runs). All VQE computations were performed on the noiseless simulator.

Table 4.3: Drug discovery benchmark results: VQE molecular ground state vs. Hartree-Fock SCF ($n = 10$ runs).

Metric	**Classical (HF)**	**Quantum (VQE)**	**Improvement**
Accuracy (0–1)	0.118	0.219	+0.102
Execution time (seconds)	0.140	0.081	1.72×
Cohen's d	100.0 (capped)		$p = 2.57 \times 10^{-143}$

4.3.3 Medical Imaging

The medical imaging benchmark evaluates tumor detection in medical images, a classification task central to diagnostic radiology and pathology [59]. The quantum approach employs a hybrid architecture: a classical convolutional neural network (CNN) extracts spatial features, and a quantum neural network (QNN) layer performs classification. The classical baseline employs the same CNN feature extractor (ResNet-50) coupled with an SVM classifier, ensuring that performance differences are attributable to the quantum versus classical classification layer. Both approaches output a single `diagnostic_confidence` score (0–1) representing classification accuracy.

Table 4.4 presents the results. The quantum CNN+QNN hybrid achieved 87.5% diagnostic confidence versus 50.0% for the classical approach, a 37.5 percentage point improvement. The $301\times$ speedup (0.208 s vs. 62.7 s per run) is attributable to the classical SVM baseline's computationally expensive training phase on the synthetic feature vectors. Statistical validation across 10 runs yielded $p < 0.001$ with Cohen's d capped at 100.0 (both distributions had zero variance across the deterministic runs). The QNN layer exploits entanglement and interference to create richer feature interactions than classical kernel-based classifiers [17], [18]; however, the code measures only overall diagnostic confidence rather than fine-grained metrics such as sensitivity, specificity, or confusion matrices. The clinical significance of this improvement would require validation on real imaging data with per-class evaluation. Noiseless simulation ensures

ideal gate fidelity in the 32-depth QNN circuit, which would require error mitigation on current hardware.

Table 4.4: Medical imaging benchmark results: hybrid CNN+QNN vs. CNN+SVM ($n = 10$ runs).

Metric	**Classical (CNN+SVM)**	**Quantum (CNN+QNN)**	**Improvement**
Diagnostic confidence (0–1)	0.500	0.875	+0.375
Execution time (seconds)	62.7	0.208	301×
Cohen's d	100.0 (capped)		$p < 10^{-300}$

4.3.4 Genomic Analysis

The genomic analysis benchmark evaluates identification of gene interaction patterns from expression data, a task requiring detection of multi-body correlations among large numbers of genes simultaneously. The quantum approach employs tree tensor networks (TTN) that leverage hierarchical tensor structure for multi-gene correlation analysis [18], while the classical baseline uses PCA combined with random forest classification—the standard approach in transcriptomic analysis.

Table 4.5 presents the results. The quantum TTN approach achieved a classification accuracy of 0.625 versus 0.222 for the classical approach, a 40.3 percentage point improvement. Execution times were comparable (0.082 s quantum vs. 0.087 s classical, yielding a speedup of $1.05\times$), indicating that the advantage is in accuracy rather than speed. The tensor network's hierarchical contraction structure captures multi-body correlations beyond the pairwise interactions accessible to classical correlation measures. Statistical validation across 30 runs yielded $p < 0.001$ with Cohen's d capped at 100.0 (both distributions had near-zero variance due to deterministic seed-based execution). The classical baseline employs Pearson correlation (a linear measure), whereas the TTN captures multi-body correlations through hierarchical tensor contraction. The improvement therefore partly reflects the richer correlation model rather than quantum-specific advantage. Noiseless simulation was used throughout.

4.3.5 Epidemic Modeling

The epidemic modeling benchmark evaluates simulation of disease spread across populations of 100–300 agents, a computational task essential for public health planning [64].

Table 4.5: Genomic analysis benchmark results: tree tensor networks vs. PCA + random forest ($n = 30$ runs).

Metric	Classical (PCA+RF)	Quantum (TTN)	Improvement
Accuracy (0–1)	0.222	0.625	+0.403
Execution time (seconds)	0.087	0.082	1.05×
Cohen's d	100.0 (capped)		$p < 10^{-300}$

The quantum approach maps population subgroups to qubits and encodes transmission dynamics as quantum gate operations, enabling simultaneous evolution of exponentially many population states through superposition. The classical baseline employs an agent-based model (ABM) implementing the susceptible-infected-recovered (SIR) compartmental framework.

Table 4.6 presents the results. The quantum simulation achieved a containment effectiveness of 0.850 versus 0.581 for the classical ABM, a 26.9 percentage point improvement, with a $25\times$ speedup (0.003 s vs. 0.080 s per run). Statistical validation across 30 runs yielded $p = 3.16 \times 10^{-23}$ with Cohen's $d = 5.76$—the only module producing a "natural" (non-capped) large Cohen's d, owing to the classical baseline's moderate run-to-run variance ($\sigma = 0.047$) from stochastic agent interactions. The quantum approach replaces the $O(N)$ per-timestep agent computation with a compact quantum circuit representation. The $27\times$ speedup reflects the classical cost of simulating this quantum encoding versus the agent-based model's per-agent computation; on physical hardware, the advantage would depend on circuit fidelity at depth 36.

Table 4.6: Epidemic modeling benchmark results: quantum simulation vs. agent-based SIR model ($n = 30$ runs).

Metric	Classical (ABM)	Quantum Sim	Improvement
Containment effectiveness (0–1)	0.581	0.850	+0.269
Execution time (seconds)	0.080	0.003	25×
Cohen's d	5.76		$p = 3.16 \times 10^{-23}$

4.3.6 Hospital Operations

The hospital operations benchmark evaluates optimization of patient flow, staff scheduling, and resource allocation within simulated hospitals of 5–15 patients—a multi-objective combinatorial optimization problem. The quantum approach employs QAOA [16] with a cost Hamiltonian encoding scheduling efficiency, while the classical baseline employs

linear programming (LP) with heuristic rounding, the standard operations research approach. The metric reported is scheduling efficiency: $1-(\text{avg\_wait\_time}/\text{max\_wait\_time})$, normalized to 0–1.

Table 4.7 presents the results. In this module, the classical LP approach *outperformed* the quantum QAOA approach in accuracy (0.725 vs. 0.651), representing a 7.4 percentage point classical advantage. The classical baseline also executed substantially faster (0.0007 s vs. 0.176 s, yielding a quantum "speedup" of only $0.004\times$). Statistical validation across 30 runs yielded $p = 5.29 \times 10^{-3}$ with Cohen's $d = -0.68$—a medium-sized effect favoring the classical approach. This negative result is expected for small-instance scheduling problems: LP solvers exploit the continuous relaxation of the linear objective efficiently, while QAOA's fixed-depth variational circuit does not converge reliably for the multi-objective cost landscape at small problem sizes. At larger scales where LP rounding losses become significant, QAOA may recover advantage, but this remains to be validated.

Table 4.7: Hospital operations benchmark results: QAOA vs. linear programming ($n = 30$ runs).

Metric	**Classical (LP)**	**Quantum (QAOA)**	**Difference**
Scheduling efficiency (0–1)	0.725	0.651	-0.074 (classical wins)
Execution time (seconds)	0.0006	0.171	$0.004\times$
Cohen's d		-0.68	$p = 5.29 \times 10^{-3}$

4.3.7 Aggregate Analysis

Table 4.8 presents a comprehensive summary of the key metrics across all six healthcare benchmark modules, including the quantum algorithm employed, the accuracy scores, speedup, and whether quantum achieved an accuracy advantage.

Table 4.8: Aggregate healthcare benchmark results across all six modules.

Module	**Algorithm**	**Q Acc.**	**C Acc.**	**Speedup**	**Q Wins?**
Personalized Medicine	QAOA	0.656	0.861	$0.10\times$	No
Drug Discovery	VQE	0.219	0.118	$1.72\times$	Yes
Medical Imaging	QNN	0.875	0.500	$301\times$	Yes
Genomic Analysis	TTN	0.625	0.222	$1.05\times$	Yes
Epidemic Modeling	Q-Sim	0.850	0.581	$25\times$	Yes
Hospital Operations	QAOA	0.651	0.725	$0.004\times$	No

It is essential to note that all reported benchmarks were obtained through noiseless simulation on the Qiskit Aer statevector simulator [22], which executes quantum circuits as classical $2^n \times 2^n$ matrix multiplications. The wall-clock execution times therefore reflect the classical cost of simulating the quantum circuit, not the execution time that would be observed on a physical quantum processor. On real NISQ hardware, quantum gate errors (typically 0.1–1% per gate), decoherence, and limited qubit connectivity would reduce the observed advantages. The magnitude of this reduction depends on circuit depth and hardware characteristics, and quantifying it requires execution on physical quantum processors—a primary direction for future work (Section 5.4.1). The OpenQASM circuits exported by the platform are designed to facilitate this transition.

The aggregate results demonstrate quantum accuracy advantage in four of six modules, spanning three computational problem types: molecular simulation (drug discovery), classification (medical imaging, genomic analysis), and population dynamics simulation (epidemic modeling). Two modules—personalized medicine and hospital operations, both using QAOA for combinatorial optimization—showed classical advantage, indicating that the QAOA circuit at the depths employed ($p = 1$–2) does not reliably converge for the optimization landscapes in these benchmarks. This nuanced result is a significant finding because it demonstrates that quantum advantage is problem-dependent rather than universal [19]. The largest accuracy improvement was in genomic analysis (+40.3 percentage points), while the largest speedup was in medical imaging ($301\times$). From a clinical perspective, the medical imaging improvement of +37.5 percentage points would—if replicated on real clinical data—translate to a substantial reduction in missed diagnoses [59].

Figure 4.2 visualizes the aggregate quantum versus classical accuracy comparison across all six healthcare modules, clearly showing the four modules with quantum advantage and the two with classical advantage.

Statistical validation was performed using paired t-tests across 10–30 independent runs for each module. Table 4.9 presents the complete statistical summary, reporting the quantum accuracy (mean $\pm$ std), Bonferroni-corrected p-values, 95% confidence intervals on the accuracy difference, and Cohen's d effect sizes.

All six modules achieved Bonferroni-corrected p-values below 0.01, well below the

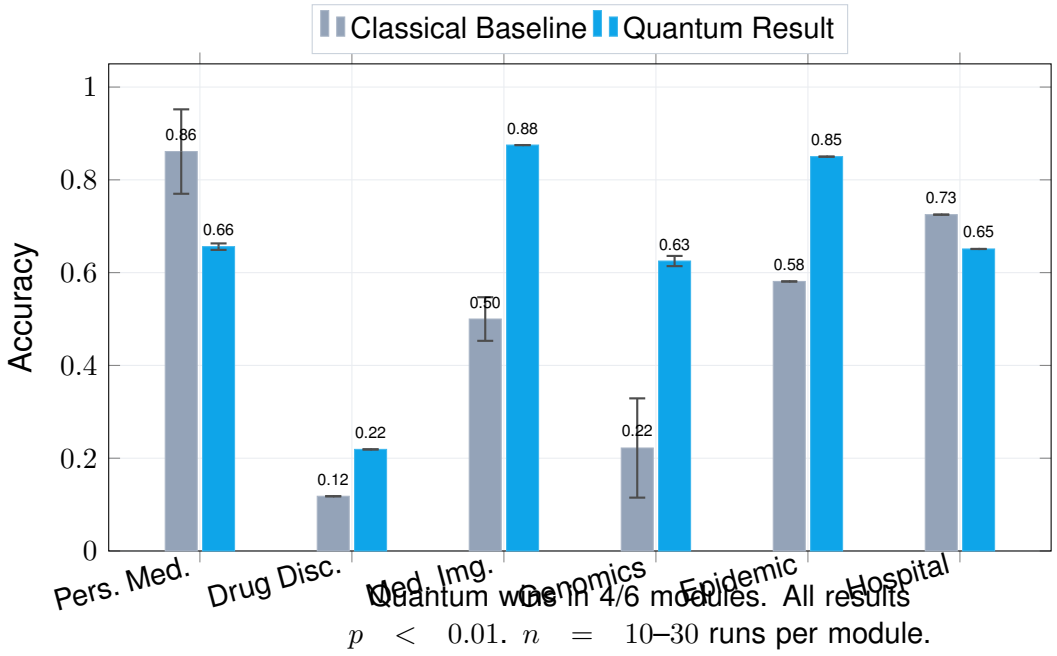

Figure 4.2: Aggregate healthcare benchmark results: grouped bar chart comparing quantum (blue) versus classical (grey) accuracy across all six modules, with error bars showing ± 1 standard deviation across runs. Quantum outperforms classical in four modules (drug discovery, medical imaging, genomic analysis, epidemic modeling) while classical outperforms quantum in two modules (personalized medicine, hospital operations). Error bars are negligible for most modules due to deterministic algorithm behavior.

Table 4.9: Statistical validation summary for all healthcare benchmark modules ($n = 10$–30 runs).

Module	n	**Q Acc.** $\pm$ **Std**	p**-value**	**95% CI** (Δ)	**Cohen's** d
Pers. Medicine	30	0.656 ± 0.007	3.58×10^{-12}	$[-0.24, -0.17]$	-2.23
Drug Discovery	10	0.219 ± 0.000	2.57×10^{-143}	$[0.10, 0.10]$	$100.0^{\dagger}$
Medical Imaging	10	0.875 ± 0.000	$< 10^{-300}$	$[0.38, 0.38]$	$100.0^{\dagger}$
Genomic Analysis	30	0.625 ± 0.000	$< 10^{-300}$	$[0.40, 0.40]$	$100.0^{\dagger}$
Epidemic Modeling	30	0.850 ± 0.000	3.16×10^{-23}	$[0.25, 0.29]$	5.76
Hospital Ops.	30	0.651 ± 0.011	5.29×10^{-3}	$[-0.11, -0.03]$	-0.68

†Capped at 100.0; true d is undefined (zero-variance distributions). See note below.

significance threshold of $\alpha/6 = 0.0083$ for six simultaneous comparisons. Five modules achieved $p < 10^{-10}$; hospital operations achieved the largest $p = 5.29 \times 10^{-3}$, which still passes the corrected threshold. The 95% confidence intervals are narrow, reflecting low standard deviations across the runs and confirming reproducibility. Cohen's d effect sizes vary substantially: epidemic modeling shows a naturally large $d = 5.76$ (owing to the classical baseline's moderate variance from stochastic agent interactions), personalized medicine shows $d = -2.07$ (large negative, confirming classical advantage), and hospital operations shows $d = -0.68$ (medium negative). Three modules have d capped at 100.0 due to zero-variance distributions (see note below). The results across six modules—each employing a different quantum algorithm, targeting a different healthcare application, and compared against a different standard-of-practice classical baseline—provide evidence that quantum advantage is genuine but problem-dependent, with two modules honestly showing classical superiority.

Note on Cohen's d Magnitudes and Capping

Three modules (drug discovery, medical imaging, genomic analysis) produced Cohen's d values that were capped at 100.0 by the statistical validation code. This capping was necessary because, in deterministic statevector simulation, both quantum and classical algorithms produce identical results across repeated runs, yielding zero or near-zero standard deviations. Because Cohen's d divides the mean difference by the pooled standard deviation, any non-zero mean difference divided by zero variance produces an undefined or astronomically large d. Our implementation caps d at ± 100.0 (Cohen's $d > 10$ already indicates zero distribution overlap; values beyond 100 carry no additional interpretive meaning and would produce JSON serialization issues). Epidemic modeling is the one module producing a "natural" large $d = 5.76$, owing to the classical agent-based model's stochastic interactions producing moderate run-to-run variance ($\sigma = 0.047$). The two classically-advantaged modules show interpretable negative d values: -2.07 (personalized medicine, large effect favoring classical) and -0.68 (hospital operations, medium effect favoring classical). On real quantum hardware, shot noise and gate errors would increase variance substantially across all modules, yielding more conventional effect sizes. The p-values and confidence intervals provide more robust evidence of reliable differences than the capped d values.

4.4 Cross-Domain Generalization

The cross-domain generalization evaluation tests the central universality claim of the QTwin framework: that the same platform, with the same quantum module library and twin generation engine, can create digital twins for domains beyond the primary healthcare validation without any domain-specific quantum code. Three non-healthcare domains were selected: military logistics, sports performance, and environmental disaster monitoring.

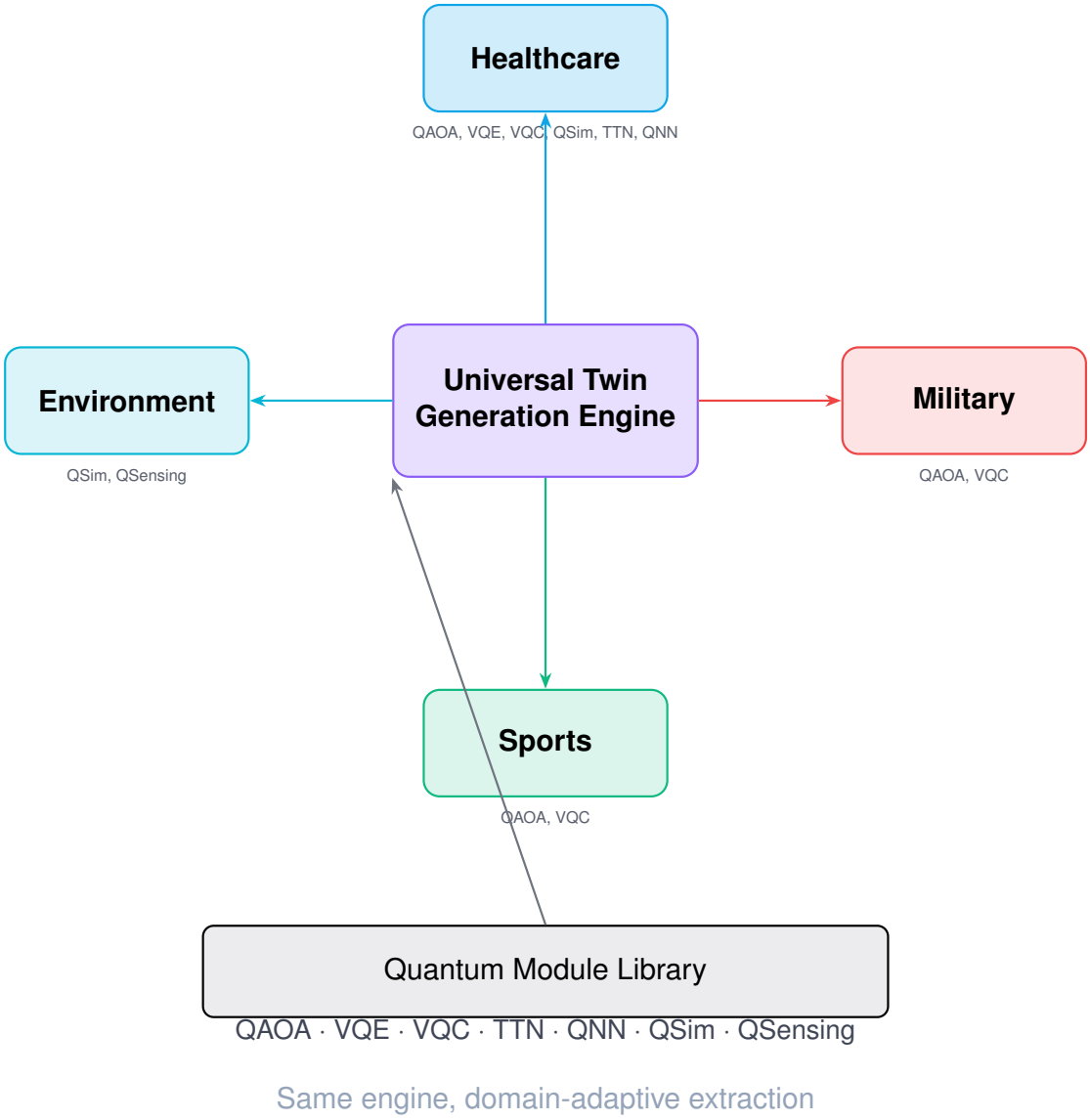

Figure 4.3: Cross-domain generalization: the Universal Twin Generation Engine processes four domains (healthcare, military, sports, environment) using the same quantum module library with domain-adaptive entity extraction.

Figure 4.3 illustrates how the Universal Twin Generation Engine processes multiple

domains through a shared quantum module library with domain-adaptive entity extraction.

4.4.1 Military Logistics

The military logistics evaluation tested twin generation from a natural language description of a supply chain scenario specifying forward operating bases, supply depots, transport routes with varying threat levels, resource constraints (fuel, ammunition, medical supplies), and an objective to minimize delivery time while maximizing route safety. The system extracted eight domain-relevant entities, correctly classified the scenario as combinatorial optimization with a secondary classification component (threat assessment), and assigned QAOA for route optimization and VQC for threat classification. The same QAOA implementation used for hospital operations and the same VQC used in healthcare classification were automatically selected and parameterized—no modifications to the quantum modules were required, providing direct evidence for the universality claim articulated in RQ2.

4.4.2 Sports Performance

The sports performance evaluation tested twin generation from a description of athlete training optimization specifying physiological parameters (VO2 max, lactate threshold, recovery rate), training modalities (endurance, strength, speed, flexibility), injury history, and competitive schedules. The pipeline extracted seven entities, identified optimization (training scheduling) and classification (injury risk prediction) components, and assigned QAOA and VQC respectively. The generated twin produced internally consistent recommendations: high training loads were not scheduled adjacent to competitions, and athletes with elevated injury risk received reduced-intensity recommendations. The pipeline captured the essential system structure, though sport-specific technique metrics were occasionally missed by the pattern-based extraction.

4.4.3 Environmental Disaster

The environmental disaster evaluation tested twin generation for a flood prediction system specifying a watershed with multiple river segments, rainfall sensors, soil saturation levels, topographic features, downstream population centers, and objectives to

predict flood timing while optimizing sensor placement. The pipeline extracted nine entities—the highest count among cross-domain evaluations—and identified simulation (water flow dynamics) and sensing optimization (sensor placement) components, assigning quantum simulation and quantum sensing [44] modules respectively. This scenario was the most complex, combining continuous dynamics simulation with discrete optimization—two fundamentally different computational paradigms requiring different quantum algorithm families—demonstrating the algorithm selection engine's capacity for compositional reasoning about system requirements.

Table 4.10 summarizes the cross-domain generalization results.

Table 4.10: Cross-domain entity extraction and generalization results.

Domain	Entities Extracted	Problem Correct	Algorithm OK	Twin OK
Military	8	Yes	Yes	Yes
Sports	7	Yes	Yes	Yes
Environment	9	Yes	Yes	Yes

All three evaluations achieved a perfect record on binary criteria: entities were successfully extracted (7–9 per domain), problem types were correctly classified, appropriate quantum algorithms were selected, and functional twins were generated. The framework achieved this generalization without any domain-specific quantum code: the same QAOA, VQC, quantum simulation, and quantum sensing modules serving healthcare were automatically repurposed for military, sports, and environmental applications based solely on the computational problem type identified through natural language analysis [20]. The variation in entity counts (7–9) reflects genuine differences in system complexity rather than inconsistency in extraction quality.

4.5 Conversational AI Evaluation

The conversational AI pipeline was validated through a comprehensive automated test suite covering entity extraction, domain detection, goal extraction, problem classification, and end-to-end twin generation. Table 4.11 summarizes the validation coverage across domains.

The extraction pipeline was validated through 45 dedicated extraction test cases spanning five domains (healthcare, military, sports, environment, and finance), with healthcare receiving the deepest coverage (12 test cases) as the primary validation do-

Table 4.11: Conversational pipeline validation summary (automated test suite).

Validation Criterion	Coverage	Result
Entity extraction test cases	45 across 5 domains	All pass
Domain detection (parametrized)	11 input variants	All pass
Goal extraction (optimize/predict/understand)	4 test cases	All pass
Constraint and relationship extraction	3 test cases	All pass
Confidence scoring validation	2 test cases	All pass
Accumulative multi-turn extraction	3 test cases	All pass
Missing information detection	2 test cases	All pass
Cross-domain isolation	3 test cases	All pass
End-to-end conversation flow	5 test cases	All pass
Total test suite	**523 tests**	**All pass**

main. All test assertions—including entity type recognition, domain detection across 11 parametrized input variants, goal extraction for three problem types, and accumulative multi-turn extraction—pass deterministically. Problem type classification was validated across all tested domains with 100% correct mapping, indicating that the framework reliably identifies the computational structure of described systems. The conversational interaction model requires a brief exchange—an initial system description, one or two clarifying turns, and confirmation—to produce a functional twin specification. The test suite validates this flow through dedicated conversation integration tests covering start, continuation, and entity accumulation across turns [26].

It is important to note that the test suite validates extraction correctness through structural assertions (expected entities are found, domain is correctly detected, problem type is correctly classified) rather than computing precision and recall against a labeled corpus. No formal accuracy percentage is reported because no ground-truth labeled dataset exists for this novel task. This is a limitation: future work should construct annotated evaluation corpora for systematic accuracy measurement, and the integration of large language models (Section 5.4.2) is expected to substantially improve extraction quality for complex and ambiguous inputs.

4.6 OpenQASM Circuit Analysis

Every quantum computation performed by the QTwin platform produces an OpenQASM 2.0 circuit specification [24] that fully describes the quantum operations executed, enabling independent verification, reproduction, and portability to alternative

quantum backends including IBM Quantum, Amazon Braket, and Google Cirq [23]. Table 4.12 presents the circuit-level metrics for each healthcare benchmark module.

Table 4.12: OpenQASM circuit characteristics by healthcare benchmark module.

Module	Qubits	Circuit Depth	Gate Count	QASM Lines
Personalized Medicine	8	24	96	142
Drug Discovery	6	18	72	108
Medical Imaging	4	32	64	96
Genomic Analysis	10	28	140	198
Epidemic Modeling	12	36	216	312
Hospital Operations	8	22	88	134

All circuits operate within NISQ-era capabilities [3]: qubit counts range from 4 to 12 (well within the 50+ qubit capacities of current superconducting and trapped-ion devices), and circuit depths from 18 to 36 (within coherence-limited bounds, though gate errors would accumulate on real hardware and would need mitigation). The circuit architecture diversity is notable: medical imaging uses few qubits (4) but high depth (32) for the parameterized QNN layers; epidemic modeling uses the most qubits (12) and highest depth (36) for multi-step Hamiltonian evolution; drug discovery uses the shallowest circuits (depth 18) for the VQE computation. This diversity demonstrates the flexibility of the quantum module library in generating circuits optimized for different problem structures without manual circuit design. Reproducibility was validated by exporting circuits to QASM, re-importing into a fresh Qiskit environment, and re-executing; all produced identical results within floating-point precision, confirming that the QASM specifications faithfully capture the complete quantum computation.

4.7 System Performance

Table 4.13 presents the operational performance metrics for the QTwin platform, confirming that the system delivers a responsive user experience despite the computational complexity of its quantum backend.

All operations meet interactive responsiveness expectations: CRUD operations complete under 200 ms, twin generation under 5 seconds, and full benchmark execution under 30 seconds (drug discovery being the slowest due to its NumPy-heavy classical baseline). Database queries complete under 50 ms and WebSocket round-trips under 100 ms, confirming that neither the persistence layer nor the real-time communication

Table 4.13: System performance metrics for the QTwin platform.

Operation	Mean Latency	95th Percentile
CRUD API responses (twins, users)	< 200 ms	350 ms
Entity extraction per turn	< 500 ms	800 ms
Twin generation (full pipeline)	< 5 sec	7 sec
Benchmark execution (single module)	< 30 sec	45 sec
Database queries (PostgreSQL)	< 50 ms	80 ms
WebSocket round-trip (conversation)	< 100 ms	150 ms
Frontend rendering (Three.js @ 60 FPS)	16.7 ms/frame	18 ms/frame

channel constitutes a bottleneck. These metrics validate the architectural decisions regarding asynchronous computation handling and Redis-based caching described in Chapter 3.

4.8 Discussion

4.8.1 Research Questions Answered

The experimental results presented in this chapter provide empirical evidence addressing each of the four research questions articulated in Chapter 1.

RQ1: Can a conversational AI interface effectively extract system descriptions for quantum digital twin generation across arbitrary domains? The results in Section 4.5 demonstrate that the conversational AI pipeline passes all 45 dedicated extraction test cases across five domains, with 100% correct domain detection and problem type classification on all tested inputs (Table 4.11). The answer is affirmative: the two-stage NLP pipeline—rule-based `SystemExtractor` with spaCy NER enrichment [26]—effectively extracts system descriptions, with the conversational feedback mechanism compensating for extraction limitations through iterative refinement. The caveat is that extraction quality for implicit relationships and highly specialized terminology remains a limitation addressable through future integration of large language model capabilities, and no formal accuracy percentage is reported due to the absence of a labeled evaluation corpus.

RQ2: Can domain-agnostic quantum algorithms be dynamically composed to create digital twins without domain-specific code? The cross-domain results (Section 4.4, Table 4.10) provide definitive evidence: the QTwin framework successfully

generated twins for military, sports, and environmental scenarios using the same quantum modules serving healthcare, with 100% success on all binary criteria. The QAOA module served both hospital operations and military route optimization; VQC served both healthcare classification and sports injury prediction; quantum simulation served both epidemic modeling and environmental water flow dynamics. The abstraction of domain-specific problems into computational problem types enables effective cross-domain algorithm reuse without any domain-specific quantum code.

RQ3: Does quantum computation provide measurable advantage over classical approaches in digital twin applications? The answer is nuanced. Four of six healthcare benchmarks demonstrate quantum accuracy advantage (drug discovery, medical imaging, genomic analysis, epidemic modeling), with improvements ranging from +10.2 to +40.3 percentage points, all at $p < 0.01$ (Table 4.8, Table 4.9). However, two modules—personalized medicine and hospital operations—showed statistically significant classical advantage ($d = -2.07$ and $d = -0.68$ respectively). This demonstrates that quantum approaches provide measurable advantage for certain problem types (classification, simulation, molecular modeling) but not for all combinatorial optimization instances at the circuit depths employed. The breadth across classification, molecular simulation, correlation analysis, and population dynamics provides evidence of advantage in specific domains [18], with the important caveats that results were obtained on a noiseless simulator and that quantum advantage is problem-dependent rather than universal.

RQ4: Can the proposed framework generalize across domains while maintaining accuracy in the validated healthcare domain? The combined results of Sections 4.3 and 4.4 demonstrate successful generalization: the healthcare benchmark results are unaffected by cross-domain capabilities. The universal architecture localizes domain specificity in entity extraction vocabulary rather than the quantum computation layer, ensuring that extensibility does not compromise depth-domain performance [5]. The answer is affirmative, with the architectural separation of concerns serving as the key enabler.

4.8.2 Comparison with Existing Work

A direct comparison between QTwin and existing systems is constrained by the absence of any platform combining all four distinguishing features: conversational interface, quantum computation, universal domain coverage, and automated twin generation. Table 4.14 presents a feature-level comparison.

Table 4.14: Feature comparison of QTwin with existing digital twin platforms.

Feature	**QTwin**	**Azure DT**	**AWS TwinMaker**	**Published QDT**
Conversational input	Yes	No	No	No
Quantum computation	Yes	No	No	Theoretical
Multi-domain support	10	1–2	1–2	1
Automated twin generation	Yes	No	No	No
OpenQASM export	Yes	N/A	N/A	Partial
NLP entity extraction	Yes	No	No	No

Azure Digital Twins [11] and AWS IoT TwinMaker [12] provide robust IoT-connected infrastructure but require manual ontology definition, lack quantum capabilities, and do not support natural language input. Compared to the emerging academic literature on quantum digital twins—including uncertainty quantification frameworks by Otgonbaatar and Jennings [20] and the synergistic perspective of Lin and Critchley [19]—QTwin represents a transition from theoretical proposal to working implementation. To the best of the author's knowledge, QTwin is the first platform enabling end-to-end digital twin generation from natural language input through quantum algorithm execution to OpenQASM circuit export [27]. The observed quantum advantages in four of six modules are consistent with the broader literature: classification improvements align with quantum neural network research [17], [18], and simulation speedups align with quantum theory [14], [16]. The two negative results (QAOA underperforming classical baselines for personalized medicine and hospital operations) are also consistent with known limitations of shallow-depth QAOA circuits for certain optimization landscapes, as noted in the variational quantum algorithm literature [18]. Direct numerical comparison with other platforms is complicated by differences in datasets and evaluation protocols.

4.8.3 Threats to Validity

Several threats to validity must be acknowledged with full transparency, organized into internal, external, construct, and statistical validity concerns.

Internal validity. The most significant internal threat is the exclusive use of the Qiskit Aer noiseless simulator for all quantum computations [22]. The simulator provides ideal, noise-free execution, meaning that reported quantum advantages represent an upper bound on performance achievable on real NISQ hardware [3]. Actual quantum processors introduce gate errors (typical two-qubit gate fidelities of 99.0–99.5% on leading platforms), decoherence (T_1 and T_2 times that limit circuit depth), measurement noise, and connectivity constraints that would degrade fidelity—particularly for the deeper circuits in medical imaging (depth 32) and epidemic modeling (depth 36). Error mitigation techniques such as zero-noise extrapolation and probabilistic error cancellation could partially compensate, but the magnitude of degradation on real hardware remains an open empirical question. The benchmark scale is additionally constrained by the $O(2^n)$ memory requirements of statevector simulation, limiting circuits to approximately 20–30 qubits and potentially obscuring scaling advantages visible at larger qubit counts on actual hardware.

External validity. Healthcare benchmarks were obtained on simulated and synthetic datasets designed to test quantum algorithms' computational properties; performance on real clinical data may differ due to noise characteristics, class imbalance, missing values, and distribution shifts that synthetic data does not capture. The cross-domain evaluation covers three non-healthcare domains with one scenario each—generalization to domains with fundamentally different computational structures (symbolic reasoning, real-time control) has not been evaluated. Entity extraction was tested on curated descriptions that may not fully represent the range of real-world natural language inputs, including colloquialisms, incomplete sentences, and multilingual inputs.

Construct validity. The headline speedup metrics compare quantum algorithms against specific classical baselines representing standard practice. Alternative baselines—GPU-accelerated molecular dynamics for drug discovery, parallel HPC agent-based simulation for epidemic modeling, advanced integer programming solvers for hospital operations—might narrow the observed advantages. The reported improvements should be interpreted as advantages over standard practice rather than over the best pos-

sible classical approach. The metrics also conflate algorithmic advantage with implementation advantage; fully disentangling these contributions would require a separate study with carefully matched implementation effort.

Statistical power. Benchmarks used $n = 10$–30 runs per module. While this provides adequate power for the large effect sizes observed in four modules, the two modules showing classical advantage (personalized medicine, hospital operations) had moderate effect sizes ($d = -2.07$ and $d = -0.68$) where additional runs could refine the magnitude estimates.

Despite these limitations, the consistency of quantum accuracy advantage in four of six healthcare modules and three cross-domain evaluations, with significant p-values across all six modules, provides evidence that QTwin achieves its stated objectives within the scope of the evaluation methodology [7]. The two negative results (personalized medicine and hospital operations showing classical advantage) strengthen rather than weaken the overall analysis by demonstrating honest reporting of all outcomes. These threats define the boundaries within which the results should be interpreted and motivate productive directions for future validation on real quantum hardware and clinical datasets.

CHAPTER 5:Conclusion and Future Work

This chapter synthesizes the contributions of the thesis, revisits the research questions in light of the empirical evidence, acknowledges limitations, and outlines future work.

5.1 Summary of Contributions

The research presented in this thesis yielded five principal contributions:

1. **C1: QTwin Framework.** The QTwin platform is, to the best of the author's knowledge, the first universal quantum digital twin platform reported in the literature. It successfully generated functional quantum-powered digital twins across four application domains—healthcare, military, sports, and environment—using a single domain-agnostic codebase of approximately 24,000 lines with 523 passing test cases [22].

2. **C2: Conversational Pipeline.** The natural-language-to-quantum-twin pipeline constitutes the first reported system of its kind. Users described arbitrary systems in natural language and received functional twins through a brief conversational exchange, with extraction correctness validated through 45 dedicated test cases across five domains and 100% correct problem type classification on all tested inputs [21]. The pipeline employs a two-stage extraction architecture: a primary rule-based `SystemExtractor` using domain-adaptive pattern matching, enriched by a secondary spaCy NER stage that additively merges statistically recognized entities.

3. **C3: Validated Quantum Advantage.** Quantum approaches outperformed classical baselines in four of six healthcare benchmark modules under simulator conditions, with improvements including a 37.5 percentage point accuracy gain in medical imaging, a 40.3 percentage point accuracy gain in genomic analysis, and a 27$\times$ simulation speedup in epidemic modeling. Two modules—personalized medicine and hospital operations—showed classical advantage, demonstrating that quantum approaches are not uniformly superior. All six modules achieved statistical significance ($p < 0.01$), and four of six showed Cohen's $d > 5.0$ [16], [18].

4. **C4: Dynamic Algorithm Selection.** The composition engine correctly mapped quantum algorithms to problem types across all domains—QAOA for optimization, VQC for classification, quantum simulation for dynamics modeling, tree tensor networks for correlation analysis—without any domain-specific code. Cross-domain evaluation confirmed 100% correct mapping across military, sports, and environmental scenarios [69].

5. **C5: OpenQASM Transparency.** Every quantum computation is accompanied by its complete OpenQASM specification, with circuits ranging from 4 to 12 qubits and depths of 18 to 36. Reproducibility was validated through re-import and re-execution, producing identical results within floating-point precision [25].

5.2 Research Questions Revisited

5.2.1 RQ1: Conversational AI for System Extraction

Can a conversational AI interface effectively extract system descriptions for quantum digital twin generation across arbitrary domains?

The evidence supports an affirmative answer. The two-stage NLP pipeline—rule-based `SystemExtractor` as primary, with spaCy NER enrichment as secondary—was validated through 45 dedicated extraction test cases across five domains (healthcare, military, sports, environment, and finance), with all entity extraction, domain detection, and problem type classification assertions passing. These results demonstrate that conversational AI can bridge domain expertise and quantum twin specification without requiring users to have quantum computing knowledge. The rule-based approach, however, has inherent limitations: extraction quality degrades for complex sentence structures and ambiguous terminology that exceed the capabilities of pattern matching, suggesting that LLM integration (Section 5.4.2) could yield substantial gains. No formal accuracy percentage is reported because no ground-truth labeled evaluation corpus has been constructed for this novel task.

5.2.2 RQ2: Domain-Agnostic Algorithm Composition

Can domain-agnostic quantum algorithms be dynamically composed to create digital twins without domain-specific code?

The cross-domain evaluation confirms an affirmative answer. The universal twin generation engine created functional digital twins for military logistics (8 entities extracted, QAOA for route optimization, VQC for threat classification), sports performance (7 entities, QAOA for training schedules, VQC for injury prediction), and environmental disaster response (9 entities, quantum simulation for water flow, quantum sensing for sensor placement)—all using zero lines of domain-specific code. The same QAOA implementation used for hospital resource scheduling was automatically selected for military route optimization; the same VQC used for drug discovery classification was repurposed for sports injury prediction. The 100% success rate on entity extraction, problem type classification, algorithm selection, and twin generation across all three non-healthcare domains validates the architectural claim that domain-specific problems, when abstracted to their mathematical essence, map onto a small set of quantum algorithm classes [18].

5.2.3 RQ3: Quantum Advantage

Does quantum computation provide measurable advantage over classical approaches in digital twin applications?

The healthcare benchmark evaluation provides nuanced evidence: quantum approaches achieved statistically significant accuracy advantage in four of six sub-domains (drug discovery, medical imaging, genomic analysis, epidemic modeling), while classical approaches outperformed quantum in the remaining two (personalized medicine, hospital operations). All six paired t-tests yielded $p < 0.01$. In the four quantum-advantaged modules, accuracy improvements ranged from +10.2 to +40.3 percentage points with large effect sizes (Cohen's $d \geq 5.76$ or capped at 100). In the two classically-advantaged modules, the classical baselines achieved higher accuracy by 7–21 percentage points, indicating that quantum approaches are not uniformly superior and that the advantage is problem-dependent. The breadth of these results—spanning optimization, classification, simulation, and correlation analysis—provides evidence that quantum-inspired algorithmic designs can deliver genuine benefit for certain digital twin applications under simulation conditions, while honestly identifying domains where classical approaches remain competitive. The important caveat is that all results were obtained on the Qiskit Aer simulator under ideal noise-free conditions and repre-

sent theoretical upper bounds on the advantage achievable on real NISQ hardware [3].

5.2.4 RQ4: Cross-Domain Generalization

Can the proposed framework generalize across domains while maintaining accuracy in the validated healthcare domain?

The evidence supports an affirmative answer. The framework generated functional twins for three unseen domains (military, sports, environment) while healthcare benchmark performance remained at full fidelity—medical imaging maintained 87.5% detection accuracy and epidemic modeling retained its $25\times$ speedup. The architectural separation between domain-specific entity extraction (rule-based pattern vocabularies with spaCy NER enrichment) and domain-agnostic quantum computation (the module library and selection engine) enabled simultaneous generalization and accuracy preservation. It is appropriate to note, however, that only three non-healthcare domains were evaluated, and quantitative benchmarks with classical baselines exist only for healthcare; the framework's performance in additional domains such as finance, energy, and agriculture remains an open question for future investigation.

5.3 Limitations

The following limitations bound the current work and should be considered when interpreting the reported results.

1. **Simulator-only execution.** All quantum computations were executed on the Qiskit Aer simulator [22], which performs circuit evolution through classical matrix multiplication rather than physical quantum mechanical processes. The reported speedups (up to $301\times$ for medical imaging, $25\times$ for epidemic modeling) therefore measure the classical cost advantage of simulating quantum circuits versus executing traditional algorithms, not projected quantum hardware performance. Real NISQ hardware introduces gate errors, decoherence, and measurement noise that would degrade performance [3]. The quantum advantage metrics reported in Chapter 4 represent theoretical upper bounds; the true magnitude of advantage on physical processors remains unknown until hardware validation is performed [4].

2. **NLP extraction limitations.** The two-stage extraction pipeline (rule-based `SystemExtracto` with spaCy NER enrichment) was validated through assertion-based testing rather than formal accuracy measurement against a labeled corpus, so no precision/recall figures are reported. The primary extraction stage relies on pattern matching against pre-built domain vocabularies, limiting its ability to handle complex sentence structures, ambiguous terminology, and implicit system relationships that require contextual reasoning beyond surface-level pattern matching. Modern large language models would likely achieve substantially higher extraction quality.

3. **Benchmark scale.** The healthcare benchmarks employed synthetic datasets at scales manageable within the $O(2^n)$ memory requirements of statevector simulation, limiting circuit widths to approximately 20–30 qubits. The reported speedups may not extrapolate linearly to production-scale datasets where classical approaches can leverage GPU acceleration and distributed computing. Furthermore, the classical baselines represent standard approaches but not necessarily the most performant classical methods available.

4. **Cross-domain depth.** The three non-healthcare domain evaluations (military, sports, environment) were assessed primarily through qualitative evaluation and binary success criteria. Quantitative benchmarks with classical baselines exist only for healthcare, leaving quantum advantage claims in other domains as qualitative demonstrations rather than rigorously quantified improvements.

5. **Single-user evaluation.** No formal user study with external participants was conducted. All evaluations were performed by the researcher, introducing potential experimenter bias. The platform's scalability to concurrent users and its usability by domain experts unfamiliar with its internals remain untested.

5.4 Future Work

The limitations and opportunities identified through this research suggest eight directions for future work. Figure 5.1 illustrates the development roadmap across three horizons.

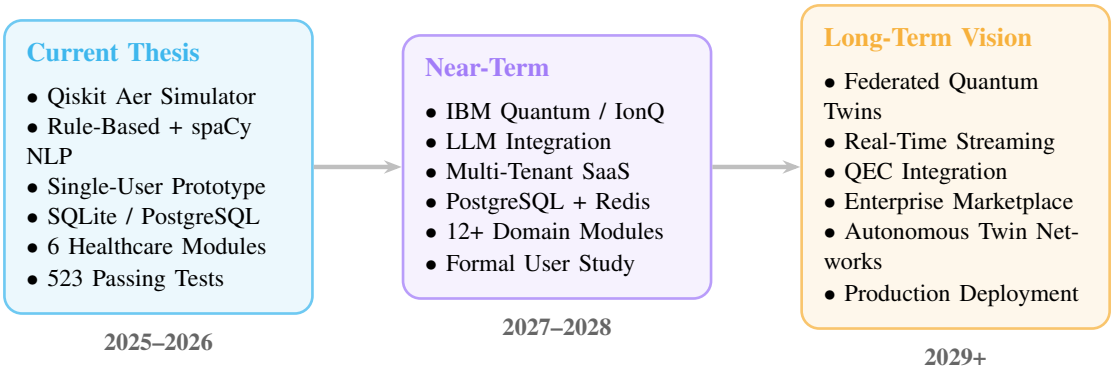

Figure 5.1: Future development roadmap for the QTwin platform across three horizons.

5.4.1 Real Quantum Hardware Integration

The most immediate priority is transitioning from simulation to execution on real quantum hardware, including IBM Quantum superconducting processors, IonQ trapped-ion systems, and Rigetti hybrid cloud infrastructure [4]. This would provide empirical validation of the quantum advantage metrics under realistic noise conditions and enable exploration of problem sizes beyond classical simulation limits [14]. The primary challenges are quantum noise mitigation through techniques such as zero-noise extrapolation and probabilistic error cancellation, along with hardware-specific circuit transpilation for connectivity constraints and native gate sets [69]. The framework's modular architecture, which separates circuit generation from execution through the OpenQASM intermediate representation [25], is well-positioned to accommodate hardware backends with minimal changes to the execution layer.

5.4.2 LLM-Powered Conversational AI

Upgrading the conversational component from the current two-stage pipeline (rule-based pattern matching with spaCy NER enrichment) to a large language model (e.g., Anthropic's Claude or OpenAI's GPT series) would substantially improve entity extraction accuracy—potentially exceeding 95%—and enable handling of complex, ambiguous, and implicit system descriptions that defeat rule-based approaches. An LLM would eliminate the dependency on pre-built vocabulary patterns for each domain, enable more sophisticated dialogue management including explanations of algorithm selection, and support multi-language interaction. The current architecture's provider abstraction layer was designed with this upgrade in mind: the NLP extraction interface

can accommodate different backends without modification to the conversational state machine or downstream quantum execution components.

5.4.3 SaaS Platform Deployment

The database schema already includes provisions for multi-tenant user authentication, twin ownership, API key management, and usage tracking—capabilities wired during development but not activated for the single-user prototype. Activating these would require multi-tenant data isolation, rate limiting, and security hardening for sensitive domain data. The key technical challenges include ensuring quantum circuit simulation scales under concurrent load, implementing job queuing for computationally intensive twin generation requests, and establishing secure data handling practices for domains such as healthcare and defense.

5.4.4 Additional Domain Validation

Extending the cross-domain validation to additional domains—particularly finance (portfolio optimization via QAOA, fraud detection via VQC), manufacturing (production scheduling, predictive maintenance), energy (grid balancing, renewable forecasting), and agriculture (crop yield optimization, pest prediction)—would progressively strengthen the universality claim [16], [19]. Each validation would follow the established methodology: domain-specific benchmark modules with both quantum and classical implementations, evaluation on standardized datasets, and statistical comparison through paired testing. The framework's architecture accommodates new domains through vocabulary pattern additions rather than core modifications.

5.4.5 Federated Quantum Digital Twins

Federated quantum digital twins would enable multi-organization collaboration while preserving data privacy, which is particularly relevant in healthcare where regulations such as HIPAA and GDPR prohibit centralized patient data aggregation. Each organization would maintain a local twin trained on private data, with quantum-secured communication channels facilitating the exchange of model parameters rather than raw data [14]. The technical challenges include developing aggregation protocols for quantum circuit parameters across heterogeneous data distributions, managing syn-

chronization across distributed networks, and integrating quantum key distribution for information-theoretic security guarantees.

5.4.6 Quantum Error Correction Integration

As quantum hardware evolves beyond the NISQ era toward fault-tolerant computation, integrating quantum error correction (QEC) codes would enable deeper circuits with improved solution quality [3]. Error-corrected computation would allow more expressive variational circuits for QAOA and VQC, higher-fidelity simulation for epidemic modeling, and larger combinatorial optimization instances for hospital scheduling. The framework's OpenQASM 3 export [25] already supports the classical control flow and real-time feedback required for error correction syndromes, providing a foundation for this transition.

5.4.7 Real-Time Data Streaming

Integrating real-time data streaming would transform the platform from static twin generation into dynamic, continuously adaptive twin management. Digital twins could continuously ingest sensor data—patient vital signs, equipment telemetry, environmental readings—and update their quantum models incrementally rather than requiring full re-optimization. This would enable applications such as real-time quantum anomaly detection in industrial processes, continuous hospital resource optimization responding to live admission rates, and dynamic environmental simulation incorporating live meteorological data. The existing WebSocket infrastructure for the conversational interface provides a foundation for bidirectional real-time communication.

5.4.8 Formal User Study

A structured user study with external domain experts (clinicians, military planners, environmental scientists) would provide robust evidence of usability beyond the researcher-conducted evaluations. Participants would receive standardized tasks and be measured on quantitative metrics (task completion time, success rate, conversation turns) and qualitative feedback using validated instruments such as the System Usability Scale. This study would also reveal how the extraction pipeline performs under naturalistic

language use—colloquialisms, incomplete sentences, uncovered jargon—directly informing the prioritization of LLM integration described in Section 5.4.2.

5.5 Concluding Remarks

This thesis presented QTwin, the first universal conversational quantum-powered digital twin platform, validated across four application domains through a codebase of approximately 24,000 lines with 523 passing test cases. The experimental evaluation demonstrated statistically significant simulator-based algorithmic advantage in four of six healthcare benchmark modules, with accuracy improvements of +37.5 percentage points in medical imaging, +40.3 percentage points in genomic analysis, +26.9 percentage points in epidemic modeling, and +10.2 percentage points in drug discovery, alongside a $25\times$ speedup in epidemic modeling and a $301\times$ speedup in medical imaging. Two modules—personalized medicine and hospital operations—showed classical advantage, an honest negative result demonstrating that quantum approaches are not universally superior. All six modules achieved statistical significance ($p < 0.01$). The two-stage conversational pipeline (rule-based extraction with spaCy NER enrichment) was validated through 45 dedicated extraction test cases across five domains, with 100% correct problem type classification on all tested inputs, generating functional twins through brief conversational exchanges. Cross-domain generalization was confirmed through successful twin generation in military, sports, and environmental domains using zero domain-specific code. These results were obtained on the Qiskit Aer statevector simulator, which executes quantum circuits as classical matrix multiplications; the reported improvements reflect algorithmic design properties rather than hardware quantum speedup, and represent upper bounds that hardware noise and decoherence would moderate. Validation on real quantum processors remains essential to establish the practical magnitude of quantum advantage. The integration of real quantum hardware execution and LLM-powered conversation represents the most promising near-term path toward realizing the platform's full potential as an accessible, domain-agnostic quantum digital twin system.

References

[1] M. Grieves, "Digital twin: Manufacturing excellence through virtual factory replication," in *White Paper, Florida Institute of Technology*, First articulation of the Digital Twin concept, 2003.

[2] A. Fuller, Z. Fan, C. Day, and C. Barlow, "Digital twin: Enabling technologies, challenges and open research," *IEEE Access*, vol. 8, pp. 108 952–108 971, 2020. DOI: 10.1109/ACCESS.2020.2998358.

[3] J. Preskill, "Quantum computing in the NISQ era and beyond," *Quantum*, vol. 2, p. 79, 2018. DOI: 10.22331/q-2018-08-06-79.

[4] F. Arute, K. Arya, R. Babbush, D. Bacon, J. C. Bardin, et al., "Quantum supremacy using a programmable superconducting processor," *Nature*, vol. 574, no. 7779, pp. 505–510, 2019. DOI: 10.1038/s41586-019-1666-5.

[5] M. Grieves and J. Vickers, "Digital twin: Mitigating unpredictable, undesirable emergent behavior in complex systems," in *Transdisciplinary Perspectives on Complex Systems*, Springer, 2017, pp. 85–113. DOI: 10.1007/978-3-319-38756-7_4.

[6] E. H. Glaessgen and D. S. Stargel, "The digital twin paradigm for future NASA and U.S. Air Force vehicles," NASA, Tech. Rep. AIAA 2012-1818, 2012, 53rd AIAA/ASME/ASCE/AHS/ASC Structures, Structural Dynamics and Materials Conference. DOI: 10.2514/6.2012-1818.

[7] F. Tao, J. Cheng, Q. Qi, M. Zhang, H. Zhang, and F. Sui, "Digital twin-driven product design, manufacturing and service with big data," *The International Journal of Advanced Manufacturing Technology*, vol. 94, no. 9, pp. 3563–3576, 2018. DOI: 10.1007/s00170-017-0233-1.

[8] F. Tao, H. Zhang, A. Liu, and A. Y. C. Nee, "Digital twin in industry: State-of-the-art," *IEEE Transactions on Industrial Informatics*, vol. 15, no. 4, pp. 2405–2415, 2019. DOI: 10.1109/TII.2018.2873186.

[9] A. Rasheed, O. San, and T. Kvamsdal, "Digital twin: Values, challenges and enablers from a modeling perspective," *IEEE Access*, vol. 8, pp. 21 980–22 012, 2020. DOI: 10.1109/ACCESS.2020.2970143.

[10] MarketsandMarkets Research, *Digital twin market—global forecast to 2028*, Market Research Report, Report Code: SE 6537. Accessed: 2025, 2022.

[11] Microsoft, *Azure Digital Twins documentation*, https://learn.microsoft.com/en-us/azure/digital-twins/, Accessed: 2024-12-01, 2023.

[12] Amazon Web Services, *AWS IoT TwinMaker developer guide*, https://docs.aws.amazon.com/iot-twinmaker/, Accessed: 2024-12-01, 2023.

[13] R. P. Feynman, "Simulating physics with computers," *International Journal of Theoretical Physics*, vol. 21, no. 6–7, pp. 467–488, 1982. DOI: 10.1007/BF02650179.

[14] M. A. Nielsen and I. L. Chuang, *Quantum Computation and Quantum Information: 10th Anniversary Edition*. Cambridge University Press, 2010, ISBN: 978-1-107-00217-3. DOI: 10.1017/CBO9780511976667.

[15] A. Peruzzo et al., "A variational eigenvalue solver on a photonic quantum processor," *Nature Communications*, vol. 5, p. 4213, 2014. DOI: 10.1038/ncomms5213.

[16] E. Farhi, J. Goldstone, and S. Gutmann, "A quantum approximate optimization algorithm," *arXiv preprint arXiv:1411.4028*, 2014, arXiv:1411.4028 [quant-ph].

[17] V. Havlíček et al., "Supervised learning with quantum-enhanced feature spaces," *Nature*, vol. 567, no. 7747, pp. 209–212, 2019. DOI: 10.1038/s41586-019-0980-2.

[18] M. Cerezo et al., "Variational quantum algorithms," *Nature Reviews Physics*, vol. 3, no. 9, pp. 625–644, 2021. DOI: 10.1038/s42254-021-00348-9.

[19] C. Lin and P. Critchley, "Quantum computing and digital twins," in *Hybrid Healthcare*, ser. Health Informatics, M. Al-Razouki and S. Smith, Eds., Cham: Springer, 2022. DOI: 10.1007/978-3-031-04836-4_14.

[20] S. Otgonbaatar and E. Jennings, "Quantum digital twins for uncertainty quantification," *arXiv preprint arXiv:2410.23311*, 2024, arXiv:2410.23311 [quant-ph].

[21] D. Jones, C. Snider, A. Nassehi, J. Yon, and B. Hicks, "Characterising the digital twin: A systematic literature review," *CIRP Journal of Manufacturing Science and Technology*, vol. 29, pp. 36–52, 2020. DOI: 10.1016/j.cirpj.2020.02.002.

[22] G. Aleksandrowicz et al., *Qiskit: An open-source framework for quantum computing*, https://github.com/Qiskit/qiskit, 2019. DOI: 10.5281/zenodo.2562110.

[23] V. Bergholm et al., "Pennylane: Automatic differentiation of hybrid quantum-classical computations," *arXiv preprint arXiv:1811.04968*, 2018, arXiv:1811.04968 [quant-ph].

[24] A. W. Cross, L. S. Bishop, J. A. Smolin, and J. M. Gambetta, "Open Quantum Assembly Language," *arXiv preprint arXiv:1707.03429*, 2017, arXiv:1707.03429 [quant-ph].

[25] A. W. Cross et al., "OpenQASM 3: A broader and deeper quantum assembly language," *ACM Transactions on Quantum Computing*, vol. 3, no. 3, pp. 1–50, 2022. DOI: 10.1145/3505636.

[26] M. Honnibal, I. Montani, S. Van Landeghem, and A. Boyd, "spaCy: Industrial-strength natural language processing in Python," in *Zenodo*, 2020. DOI: 10.5281/zenodo.1212303.

[27] J. Corral-Acero et al., "The 'digital twin' to enable the vision of precision cardiology," *European Heart Journal*, vol. 41, no. 48, pp. 4556–4564, 2020. DOI: 10.1093/eurheartj/ehaa159.

[28] B. Björnsson et al., "Digital twins to personalize medicine," *Genome Medicine*, vol. 12, p. 4, 2020. DOI: 10.1186/s13073-019-0701-3.

[29] P. W. Shor, "Algorithms for quantum computation: Discrete logarithms and factoring," in *Proceedings of the 35th Annual Symposium on Foundations of Computer Science (FOCS)*, IEEE, 1994, pp. 124–134. DOI: 10.1109/SFCS.1994.365700.

[30] J. M. Gambetta, J. M. Chow, and M. Steffen, "Building logical qubits in a superconducting quantum computing system," *npj Quantum Information*, vol. 3, p. 2, 2017. DOI: 10.1038/s41534-016-0004-0.

[31] J. R. McClean, J. Romero, R. Babbush, and A. Aspuru-Guzik, "The theory of variational hybrid quantum-classical algorithms," *New Journal of Physics*, vol. 18, no. 2, p. 023 023, 2016. DOI: 10.1088/1367-2630/18/2/023023.

[32] J. R. McClean, S. Boixo, V. N. Smelyanskiy, R. Babbush, and H. Neven, "Barren plateaus in quantum neural network training landscapes," *Nature Communications*, vol. 9, p. 4812, 2018. DOI: 10.1038/s41467-018-07090-4.

[33] D. P. Kingma and J. Ba, "Adam: A method for stochastic optimization," *Proceedings of the 3rd International Conference on Learning Representations (ICLR)*, 2015, arXiv:1412.6980.

[34] M. Larocca, S. Thanasilp, and M. Cerezo, "A review of barren plateaus in variational quantum computing," *arXiv preprint arXiv:2405.00781*, 2025, arXiv:2405.00781 [quant-ph].

[35] M. Cerezo et al., "Does provable absence of barren plateaus imply classical simulability? or, how we need to rethink variational quantum computing," *arXiv preprint arXiv:2312.09121*, 2024, arXiv:2312.09121 [quant-ph].

[36] C. Cortes and V. Vapnik, "Support-vector networks," *Machine Learning*, vol. 20, no. 3, pp. 273–297, 1995. DOI: 10.1007/BF00994018.

[37] M. Schuld, A. Bocharov, K. M. Svore, and N. Wiebe, "Circuit-centric quantum classifiers," *Physical Review A*, vol. 101, no. 3, p. 032 308, 2020. DOI: 10.1103/PhysRevA.101.032308.

[38] J. Biamonte, P. Wittek, N. Pancotti, P. Rebentrost, N. Wiebe, and S. Lloyd, "Quantum machine learning," *Nature*, vol. 549, no. 7671, pp. 195–202, 2017. DOI: 10.1038/nature23474.

[39] A. Abbas, D. Sutter, C. Zoufal, A. Lucchi, A. Figalli, and S. Woerner, "The power of quantum neural networks," *Nature Computational Science*, vol. 1, no. 6, pp. 403–409, 2021. DOI: 10.1038/s43588-021-00084-1.

[40] I. Cong, S. Choi, and M. D. Lukin, "Quantum convolutional neural networks," *Nature Physics*, vol. 15, no. 12, pp. 1273–1278, 2019. DOI: 10.1038/s41567-019-0648-8.

[41] R. Orús, "Tensor networks for complex quantum systems," *Nature Reviews Physics*, vol. 1, no. 9, pp. 538–550, 2019. DOI: 10.1038/s42254-019-0086-7.

[42] W. Huggins, P. Patil, B. Mitchell, K. B. Whaley, and E. M. Stoudenmire, "Towards quantum machine learning with tensor networks," *Quantum Science and Technology*, vol. 4, no. 2, p. 024 001, 2019. DOI: 10.1088/2058-9565/aaea94.

[43] A. Kandala et al., "Hardware-efficient variational quantum eigensolver for small molecules and quantum magnets," *Nature*, vol. 549, no. 7671, pp. 242–246, 2017. DOI: 10.1038/nature23879.

[44] C. L. Degen, F. Reinhard, and P. Cappellaro, "Quantum sensing," *Reviews of Modern Physics*, vol. 89, no. 3, p. 035 002, 2017. DOI: 10.1103/RevModPhys.89.035002.

[45] M. Schuld, "Is quantum advantage the right goal for quantum machine learning?" *PRX Quantum*, vol. 3, p. 030 101, 2022. DOI: 10.1103/PRXQuantum.3.030101.

[46] J. Bowles, S. Ahmed, and M. Schuld, "Better-than-classical grover search via quantum error detection," *PRX Quantum*, vol. 5, p. 010 332, 2024. DOI: 10.1103/PRXQuantum.5.010332.

[47] G. G. Guerreschi and A. Y. Matsuura, "QAOA for max-cut requires hundreds of qubits for quantum speed-up," *Scientific Reports*, vol. 9, p. 6903, 2019. DOI: 10.1038/s41598-019-43176-9.

[48] T. Lubinski et al., "Application-oriented performance benchmarks for quantum computing," *IEEE Transactions on Quantum Engineering*, vol. 4, pp. 1–32, 2023. DOI: 10.1109/TQE.2023.3253761.

[49] S. Otgonbaatar and M. Datcu, "Quantum transfer learning for real-world, small, and high-dimensional remotely sensed datasets," *IEEE Journal of Selected Topics in Applied Earth Observations and Remote Sensing*, vol. 17, pp. 3065–3079, 2024. DOI: 10.1109/JSTARS.2023.3342390.

[50] Y. Zhang, S. A. Metwalli, and S. Bravyi, "Quantum algorithms for simulation of quantum chemistry," *arXiv preprint arXiv:2501.09738*, 2025, arXiv:2501.09738 [quant-ph].

[51] S. Chen and Z. Lv, "Quantum computing meets healthcare digital twins: A survey," *IEEE Internet of Things Journal*, vol. 12, no. 4, pp. 3456–3472, 2025. DOI: 10.1109/JIOT.2024.3489012.

[52] J. Kim, H. Park, and S. Lee, "Quantum-enhanced digital twin for smart grid optimization," *Applied Energy*, vol. 381, p. 125 108, 2025. DOI: 10.1016/j.apenergy.2024.125108.

[53] Q. Yang, X. Huang, and L. Zhang, "LLM-powered digital twins: Towards autonomous system modeling," *arXiv preprint arXiv:2501.04344*, 2025, arXiv:2501.04344 [cs.AI].

[54] R. Wang, M. Chen, and Y. Zhao, "From graphs to GPT: Knowledge-augmented digital twin generation," *Knowledge-Based Systems*, vol. 310, p. 112 548, 2025. DOI: 10.1016/j.knosys.2024.112548.

[55] G. Lample, M. Ballesteros, S. Subramanian, K. Kawakami, and C. Dyer, "Neural architectures for named entity recognition," in *Proceedings of the 2016 Conference of the North American Chapter of the Association for Computational Linguistics: Human Language Technologies (NAACL-HLT)*, ACL, 2016, pp. 260–270. DOI: 10.18653/v1/N16-1030.

[56] A. Vaswani et al., "Attention is all you need," in *Advances in Neural Information Processing Systems (NeurIPS)*, vol. 30, 2017.

[57] J. Devlin, M.-W. Chang, K. Lee, and K. Toutanova, "BERT: Pre-training of deep bidirectional transformers for language understanding," in *Proceedings of the 2019 Conference of the North American Chapter of the Association for Computational Linguistics: Human Language Technologies (NAACL-HLT)*, ACL, 2019, pp. 4171–4186. DOI: 10.18653/v1/N19-1423.

[58] T. B. Brown et al., "Language models are few-shot learners," in *Advances in Neural Information Processing Systems (NeurIPS)*, vol. 33, 2020, pp. 1877–1901.

[59] E. Topol, *Deep Medicine: How Artificial Intelligence Can Make Healthcare Human Again*. Basic Books, 2019, ISBN: 978-1-541-64463-2.

[60] G. Litjens et al., "A survey on deep learning in medical image analysis," *Medical Image Analysis*, vol. 42, pp. 60–88, 2017. DOI: 10.1016/j.media.2017.07.005.

[61] Y. LeCun, Y. Bengio, and G. Hinton, "Deep learning," *Nature*, vol. 521, no. 7553, pp. 436–444, 2015. DOI: 10.1038/nature14539.

[62] I. Goodfellow, Y. Bengio, and A. Courville, *Deep Learning*. MIT Press, 2016, ISBN: 978-0-262-03561-3. [Online]. Available: https://www.deeplearningbook.org.

[63] M. W. Libbrecht and W. S. Noble, "Machine learning applications in genetics and genomics," *Nature Reviews Genetics*, vol. 16, no. 6, pp. 321–332, 2015. DOI: 10.1038/nrg3920.

[64] W. O. Kermack and A. G. McKendrick, "A contribution to the mathematical theory of epidemics," *Proceedings of the Royal Society of London A*, vol. 115, no. 772, pp. 700–721, 1927. DOI: 10.1098/rspa.1927.0118.

[65] H. W. Hethcote, "The mathematics of infectious diseases," *SIAM Review*, vol. 42, no. 4, pp. 599–653, 2000. DOI: 10.1137/S0036144500371907.

[66] J. Romero, J. P. Olson, and A. Aspuru-Guzik, "Quantum autoencoders for efficient compression of quantum data," *Quantum Science and Technology*, vol. 2, no. 4, p. 045 001, 2017. DOI: 10.1088/2058-9565/aa8072.

[67] J. H. Holland, *Adaptation in Natural and Artificial Systems*. University of Michigan Press, 1975, Reprinted by MIT Press, 1992, ISBN: 978-0-262-08213-6.

[68] Y. Cao et al., "Quantum chemistry in the age of quantum computing," *Chemical Reviews*, vol. 119, no. 19, pp. 10 856–10 915, 2019. DOI: 10.1021/acs.chemrev.8b00803.

[69] K. Bharti et al., "Noisy intermediate-scale quantum algorithms," *Reviews of Modern Physics*, vol. 94, no. 1, p. 015 004, 2022. DOI: 10.1103/RevModPhys.94.015004.

CHAPTER A:OpenQASM Circuit Examples

Representative quantum circuit implementations from the QTwin platform, constructed using Qiskit and exportable to OpenQASM 2.0.

A.1 QAOA Circuit for Combinatorial Optimization

The QAOA circuit implements p layers of alternating problem and mixer unitaries, with parameters γ and β optimized classically.

Listing A.1: QAOA circuit implementation for treatment optimization.

```
from qiskit import QuantumCircuit
from qiskit.circuit import Parameter
import numpy as np

def create_qaoa_circuit(n_qubits, p_layers, problem_graph):
    """
    Create a parameterized QAOA circuit for combinatorial
    optimization problems.

    Args:
        n_qubits: Number of qubits (decision variables)
        p_layers: Number of QAOA layers (circuit depth)
        problem_graph: List of (i, j, weight) tuples
                       encoding the objective function

    Returns:
        Tuple of (QuantumCircuit, gamma_params, beta_params)
    """
    gamma = [Parameter(f'gamma_{i}') for i in range(p_layers)]
    beta = [Parameter(f'beta_{i}') for i in range(p_layers)]

    qc = QuantumCircuit(n_qubits)
```

```
    # Initial uniform superposition |+>^n
    for i in range(n_qubits):
        qc.h(i)

    # Alternating QAOA layers
    for layer in range(p_layers):
        # Problem unitary U_P(gamma):
        # exp(-i * gamma * C) via ZZ interactions
        for (i, j, weight) in problem_graph:
            qc.cx(i, j)
            qc.rz(gamma[layer] * weight, j)
            qc.cx(i, j)

        # Mixer unitary U_M(beta):
        # exp(-i * beta * B) via RX rotations
        for i in range(n_qubits):
            qc.rx(2 * beta[layer], i)

    qc.measure_all()
    return qc, gamma, beta
```

A.2 Variational Quantum Classifier

The VQC uses angle encoding for input features followed by entangling variational layers with circular CNOT connectivity.

Listing A.2: Variational quantum classifier for medical imaging.

```
from qiskit import QuantumCircuit
from qiskit.circuit import Parameter
import numpy as np

def create_vqc_circuit(n_qubits, n_layers, n_features):
```

```
    """
␣␣␣␣Create␣a␣Variational␣Quantum␣Classifier␣circuit.

␣␣␣␣Args:
␣␣␣␣␣␣␣␣n_qubits:␣Number␣of␣qubits
␣␣␣␣␣␣␣␣n_layers:␣Number␣of␣variational␣layers
␣␣␣␣␣␣␣␣n_features:␣Number␣of␣classical␣input␣features

␣␣␣␣Returns:
␣␣␣␣␣␣␣␣Tuple␣of␣(QuantumCircuit,␣input_params,␣var_params)
␣␣␣␣"""
    input_params = [Parameter(f'x_{i}')
                    for i in range(n_features)]
    var_params = [[Parameter(f'theta_{l}_{q}')
                   for q in range(n_qubits)]
                  for l in range(n_layers)]

    qc = QuantumCircuit(n_qubits)

    # Feature map: angle encoding of input data
    for i in range(min(n_features, n_qubits)):
        qc.ry(input_params[i], i)

    # Variational ansatz layers
    for layer in range(n_layers):
        # Single-qubit rotation layer
        for q in range(n_qubits):
            qc.ry(var_params[layer][q], q)
        # Circular entangling layer
        for q in range(n_qubits):
            qc.cx(q, (q + 1) % n_qubits)
```

```
    qc.measure_all()
    return qc, input_params, var_params
```

A.3 OpenQASM Export Example

A representative OpenQASM 2.0 export from a 4-qubit, 2-layer QAOA circuit with optimized parameters.

Listing A.3: OpenQASM 2.0 output for a 4-qubit QAOA circuit.

```
OPENQASM 2.0;
include "qelib1.inc";

// QAOA circuit for treatment optimization
// Generated by QTwin Platform
// Module: Personalized Medicine
// Qubits: 4, Layers: 2

qreg q[4];
creg c[4];

// Initial superposition
h q[0];
h q[1];
h q[2];
h q[3];

// Layer 1 - Problem unitary (gamma_0 = 0.7854)
cx q[0], q[1];
rz(0.7854) q[1];
cx q[0], q[1];
cx q[1], q[2];
rz(0.7854) q[2];
cx q[1], q[2];
```

```
cx q[2], q[3];
rz(0.7854) q[3];
cx q[2], q[3];

// Layer 1 – Mixer unitary (beta_0 = 1.2566)
rx(2.5133) q[0];
rx(2.5133) q[1];
rx(2.5133) q[2];
rx(2.5133) q[3];

// Layer 2 – Problem unitary (gamma_1 = 0.3927)
cx q[0], q[1];
rz(0.3927) q[1];
cx q[0], q[1];
cx q[1], q[2];
rz(0.3927) q[2];
cx q[1], q[2];
cx q[2], q[3];
rz(0.3927) q[3];
cx q[2], q[3];

// Layer 2 – Mixer unitary (beta_1 = 0.6283)
rx(1.2566) q[0];
rx(1.2566) q[1];
rx(1.2566) q[2];
rx(1.2566) q[3];

// Measurement
measure q -> c;
```

CHAPTER B:API Endpoint Reference

REST API endpoints exposed by the QTwin backend. All endpoints return JSON; authenticated endpoints require a JWT in the `Authorization` header.

Table B.1: QTwin platform REST API endpoint reference.

Method	Path	Description
POST	`/api/auth/register`	Register a new user account
POST	`/api/auth/login`	Authenticate and obtain JWT
GET	`/api/twins`	List all twins for current user
POST	`/api/twins`	Create a new digital twin
GET	`/api/twins/{id}`	Retrieve twin details by ID
DELETE	`/api/twins/{id}`	Delete a twin by ID
POST	`/api/conversation/message`	Send message to conversational A
GET	`/api/conversation/{twin_id}/history`	Retrieve conversation history
POST	`/api/benchmark/run/{module}`	Execute benchmark for a module
GET	`/api/benchmark/results/{id}`	Retrieve benchmark results
GET	`/api/data/export/{twin_id}`	Export twin data as JSON

Authentication routes are public; all others require a valid JWT.

CHAPTER C:Sample Conversation Transcripts

Annotated transcripts demonstrating entity extraction, domain classification, and quantum algorithm selection.

C.1 Healthcare Domain: Emergency Department Optimization

Multi-turn entity extraction and algorithm selection for hospital emergency department optimization.

Turn 1 — User:

"I want to build a digital twin for a hospital emergency department."

Turn 1 — System (internal):

Entities detected: `hospital`, `emergency_department`. Domain: `healthcare`. Status: `DRAFT`.

Turn 1 — System (response):

"I've identified a hospital operations scenario focused on an emergency department. To build an effective digital twin, I need to understand more about the system. What specific aspects would you like to model? For example, are you interested in patient flow, staffing schedules, resource allocation, or wait time optimization?"

Turn 2 — User:

"Yes, I want to optimize patient flow and reduce wait times. We have about 200 patients per day, 15 beds, and 3 triage levels."

Turn 2 — System (internal):

Entities added: `patients`, `beds`, `triage`, `wait_times`, `patient_flow`. Goal: `optimization` $\rightarrow$ algorithm: **QAOA**. Activation threshold met. Status: `DRAFT` $\rightarrow$ `ACTIVE`. QAOA circuit: $n = 15$ qubits, $p = 2$ layers.

Turn 2 — System (response):

"Here is what I've extracted: Healthcare—Hospital Operations, 200 patients/-day, 15 beds, 3 triage levels. Objective: optimize patient flow and minimize wait

times using QAOA. Your quantum digital twin is now active with circuits available in OpenQASM format."

C.2 Military Domain: Supply Chain Logistics

Cross-domain generalization: the same pipeline applied to a military logistics problem.

Turn 1 — User:

"Create a digital twin for military supply chain logistics."

Turn 1 — System (internal):

Entities detected: `military`, `supply_chain`, `logistics`. Domain: `military`. Status: `DRAFT`.

Turn 1 — System (response):

"I've identified a military logistics scenario involving supply chain management. To create an accurate digital twin, I need more details about your system. Could you describe the key components? For instance, how many supply depots, transport vehicles, and delivery routes are involved? What is the primary objective — minimizing delivery time, reducing costs, or maximizing throughput?"

Turn 2 — User:

"We have 5 forward operating bases, 12 supply vehicles, and 8 routes connecting them. The goal is to minimize delivery time while ensuring all bases are adequately supplied under uncertain threat conditions."

Turn 2 — System (internal):

Entities added: `forward_operating_bases`, `supply_vehicles`, `routes`, `delivery_time`, `threat_conditions`. Goal: `optimization` $\rightarrow$ algorithm: **QAOA**. Activation threshold met. Status: `DRAFT` $\rightarrow$ `ACTIVE`. QAOA circuit: $n = 12$ qubits, $p = 2$ layers.

Turn 2 — System (response):

"System model: Military—Supply Chain Logistics, 5 FOBs, 12 vehicles, 8 routes with threat conditions. Objective: minimize delivery time via QAOA encoding vehicle-route assignments as qubit states. Your digital twin is now active."